TECHNICAL UNIVERSITY OF LIBEREC
Faculty of Mechatronics, Informatics
and Interdisciplinary Studies

Model Predictive Control for Demand Response of Thermostatically Controlled Loads

Doctoral thesis

Study programme: N2612 – Electrical Engineering and Informatics
Study branch: 2612V045 – Technical Cybernetics

Author: **Ing. Nikita Zemtsov**
Supervisor: Doc. Dr. Ing. Mgr. Jaroslav Hlava

Liberec 2018

TECHNICKÁ UNIVERZITA V LIBERCI
Fakulta mechatroniky, informatiky
a mezioborových studií

Prediktivní řízení odezvy strany spotřeby využívající termostatické spotřebiče

Disertační práce

Studijní program: N2612 – Elektrotechnika a Informatika
Studijní obor: 2612V045 – Technická kybernetika

Autor práce: **Ing. Nikita Zemtsov**
Vedoucí práce: Doc. Dr. Ing. Mgr. Jaroslav Hlava

Liberec 2018

Declaration

I hereby certify that I have been informed that Act 121/2000, the Copyright Act of the Czech Republic, namely Section 60, Schoolwork, applies to my dissertation in full scope. I acknowledge that the Technical University of Liberec (TUL) does not infringe my copyrights by using my dissertation for TUL's internal purposes.

I am aware of my obligation to inform TUL on having used or licensed to use my dissertation in which event TUL may require compensation of costs incurred in creating the work at up to their actual amount.

I have written my dissertation myself using literature listed therein and consulting it with my supervisor and my tutor.

I hereby also declare that the hard copy of my dissertation is identical with its electronic form as saved at the IS STAG portal.

Date:

Signature:

Abstract

Increasing the share of renewable electricity generation is a characteristic feature of modern energy systems. Renewable electricity generation has important environmental benefits, however, it is also marked by significant stochasticity and its large scale integration into power grid is not possible without new methods for control of electricity consumption, new energy storage technologies and communication infrastructure. Thermostatically controlled loads represent a significant share of total electricity consumption and they are often tightly connected with large thermal storage capacities. For these reasons they can be used for controlling electricity consumption and cost effective energy storage. This motivates the focus of this thesis on advanced control algorithms for thermostatically controlled loads.

Any control requires a suitable control signal. In this thesis, an indirect control signal is used – the role of the control signal is played by variable electricity price. This concept is considered in many pilot projects both in the USA and in the EU. It has certain advantages: the customers can choose the preferred strategy for responding to the needs of the grid, so their comfort is not compromised; also there is no need to install significantly more complex interfaces for direct control of the loads and monitoring of their states. However, the design of suitable control algorithms for responding to variable prices is still a largely open problem. The thesis focuses on two aspects of this problem.

The first part of the thesis considers the control of a single large thermostatically controlled load that responds to the price signal. This load is described by a linear time varying system and a local economic model predictive controller is designed for it. This controller must account for the time varying dynamics of the controlled load. By performing local economic optimization this controller helps to balance supply and demand in the electricity grid. This part of the thesis was created within the framework of H2020 SmartNet project and it considers one of the project pilot demonstrations: heated swimming pool. The time varying character of the

model of this pool is due to the changes of the heat transfer coefficient between water and air depending on the wind speed.

The second part of the thesis focuses on smaller thermostatically controlled loads. They are negligible individually, but they can play an important role if a larger population is aggregated. The structure of the proposed control system is hierarchical. Economic model predictive controller in the upper level responds to varying electricity price and changes the temperature setpoints of the thermostats in the lower level. The objective of the control system is the same as in the first part of the thesis: the cost of the operation of this population is minimized and this helps to keep the balance in the grid. However, the high number of the loads does not allow individual modelling of each load in the model predictive controller and an aggregate model had to be developed and tested. This model is non-linear and economic model predictive controller has to solve mixed integer non-linear optimization problem. The effectiveness of the proposed control strategy was demonstrated by simulation.

Keywords: Smart Grids, Demand Response, Real Time Pricing, Economic model predictive control, Non-linear model predictive control, Modelling of aggregated thermostatically controlled loads, Linear parameter-varying systems

Abstrakt

Charakteristickým rysem moderní energetiky je narůstající podíl výroby elektřiny z obnovitelných zdrojů. To přináší řadu výhod z pohledu kvality životního prostředí. Výroba elektřiny z obnovitelných zdrojů má však výrazně stochastický charakter a integrace většího množství takto vyrobené elektřiny do elektrizační sítě není možná, pokud nebudou vytvořeny nové metody řízení spotřeby elektřiny, nové technologie pro skladování elektrické energie a vyspělá řídicí a komunikační infrastruktura. Na straně spotřeby elektrické energie připadá významný podíl termostaticky řízeným spotřebičům. Ty jsou navíc obvykle těsně propojeny s velkými tepelně akumulačními kapacitami. Jsou proto zvláště vhodné pro řízení spotřeby elektřiny a nákladově efektivní akumulaci energie. Z této motivace vychází zaměření této disertační práce na pokročilé algoritmy pro řízení termostatických spotřebičů.

Jakékoliv řízení nutně předpokládá, že existuje vhodný řídicí signál, kterým můžeme chování řízené soustavy ovlivňovat. V této práci pracujeme s nepřímým řídicím signálem: cenou elektřiny proměnnou v reálném čase. Tento koncept je používán v řadě pilotních projektů v USA i v EU. Z řady hledisek je tento koncept výhodný: zákazníci si mohou sami rozhodnout, jak na proměnnou cenu budou reagovat bez toho, že by jejich komfort byl ohrožen. Rovněž tak není nutné instalovat složitá rozhraní pro přímé ovládání spotřebičů a monitorování jejich stavu. Návrh vhodných algoritmů pro to, jak reagovat na proměnné ceny však zůstává stále do značné míry otevřeným problémem. Tato práce je zaměřena na dva aspekty tohoto problému.

První část práce se zabývá problematikou řízení jednotlivých velkých termostatických spotřebičů, které reaguje na proměnnou cenu elektřiny. Tyto spotřebiče jsou zde popsány obecně jako lineární časově proměnné systémy a jejich řízení je navrženo jako lokální ekonomické prediktivní řízení. Tento ekonomický prediktivní regulátor musí vzít v úvahu časově proměnný charakter řízené soustavy. Tím, že provádí lokální ekonomickou optimalizaci, napomáhá tento regulátor udržet

rovnováhu výroby a spotřeby v elektrizační soustavě. Tato část práce vznikla v rámci projektu H2020 SmartNet a jako případovou studii používá jedno z pilotních experimentálních zařízení tohoto projektu: vyhřívaný plavecký bazén. Časová proměnnost matematického modelu tohoto bazénu pramení ze změn součinitele přestupu tepla mezi vodou a vzduchem v závislosti na rychlosti větru.

Druhá část práce je zaměřena na menší termostatické spotřebiče, které sice mají jednotlivě zanedbatelný příkon, mohou však hrát významnou roli, pokud je jejich větší počet sdružen dohromady. Struktura navrhovaného řídicího systému je hierarchická. Ekonomický prediktivní regulátor na vyšší rovině řízení reaguje na proměnnou cenu elektřiny a mění žádané hodnoty termostatů na nižší rovině. Cíl řízení je stejný jako v první části práce: cena provozu celé skupiny spotřebičů je minimalizována a to napomáhá udržení rovnováhy v síti. Vzhledem k velkému počtu spotřebičů však není možné, aby prediktivní regulátor pracoval s modely všech jednotlivých spotřebičů, ale bylo nutné vyvinout a ověřit sdružený model dynamiky celé skupiny. Tento model je nelineární a ekonomický prediktivní regulátor musí řešit úlohu nelineárního smíšeného celočíselného programování. Efektivita navržené strategie řízení byla prokázána pomocí simulačních experimentů.

Klíčová slova: Inteligentní elektrické sítě, Odezva strany spotřeby, Ceny elektřiny proměnné v reálném čase, Ekonomické prediktivní řízení, Nelineární prediktivní řízení, Modelování skupin termostatických spotřebičů, Lineární v čase proměnné systémy

Contents

List of Abbreviations

AC Air Conditioner. 36

BESS Battery Energy Storage System. 26

CAES Compressed Air Energy Storage. 26

CCVPP Centralized Controlled Virtual Power Plant. 27

CHP Combined Heat and Power. 26

COP Coefficient of Performance. 45, 48, 49, 54

DCC Distribution Dispatching Center. 27

DCVPP Distributed Controlled Virtual Power Plant. 27

DDG Domestic Distributed Generation. 26

DER Distributed Energy Resource. 22, 26–28, 30

DG Distributed Generation. 23, 26

DLC Direct Load Control. 30, 31

DR Demand Response. 22, 30, 31, 42

DSM Demand Side Management. 22, 29, 30, 32, 36, 39, 40, 95

DSO Distribution System Operator. 27, 45

E-MPC Economic Model Predictive Control. 22, 35, 40–44, 53, 56, 94–96

E-NMPC Economic Non-linear Model Predictive Control. 44, 79, 85, 94, 95

EMS Energy Management Systems. 27

ETP Equivalent Thermal Parameter. 17, 36, 37, 40

FACTS Flexible AC Transmissions System. 22

FC Fuel Cell. 26

FDCVPP Fully Distributed Controlled Virtual Power Plant. 28

FWES Flywheel Energy Storage. 26

HPES Hydraulic Pumped Energy Storage. 26

ICT Information Communication Technology. 26, 27

LP Linear Program. 35, 53

LPV Linear Parameter-Varying. 42–46, 49, 53, 94, 95

LTI Linear Time Invariant. 43, 45, 46, 50

MILP Mixed-Integer Linear Program. 53

MPC Model Predictive Control. 22, 33, 35, 36, 40, 42–44, 46, 49, 94

NMPC Non-linear Model Predictive Control. 35, 80

NP Non-linear Program. 35

OCP Optimal Control Problem. 33

PDG Public Distributed Generation. 26

PID Proportional Integral Derivative. 33

QP Convex Quadratic Program. 35

RES Renewable Energy Source. 20, 22, 26, 45

SCADA Supervisory Control and Data Acquisition. 27

SCES Supercapacitor Energy Storage. 26

SG Smart Grid. 22, 30

SMES Super Conductor Magnetic Energy Storage. 26

TCL Thermostatically Controlled Load. 17, 22, 29, 33, 36–46, 56, 59, 65, 79, 80, 94–96

TSO Transmission System Operator. 27, 45

VPP Virtual Power Plant. 22, 26, 27, 29

List of Symbols

Symbol	Description	Unit
A_p	pool area	m^2
A_{bin}	state matrix of the bin state transition model	
A_{hom}	state matrix of the homogeneous model	
A	state matrix of the aggregate model	
B_{bin}	control matrix of the bin state transition model	
C_m	mean thermal capacitance of the TCLs	$kWh/°C$
C_w	specific heat of water	$kWh/(kg{\cdot}°C)$
C_{agg}	output matrix of the aggregate model	
C_{air}	air thermal mass	$kWh/°C$
C_{bin}	output matrix of the bin state transition model	
C_{mass}	thermal mass of the buildings material and other equipment	$kWh/°C$
$C_{smart/thrifty}$	simulated normalized operational cost of the smart or thrifty strategies respectively	
C_{zero}	simulated normalized operational cost of the zero temperature setpoint change strategy	
C	thermal capacitance	$kWh/°C$
D	duty cycle of the TCL	
$E_{glob,H}$	total solar radiation on a horizontal surface	
H_m	total interior mass surface conductance	$kW/°C$
H	hysteresis band of the thermostat	$°C$
N_{bin}	total number of bins per state	
N_{high}	number of bins within high temperature range per state	

Symbol	Description	Unit
N_{low}	number of bins within low temperature range per state	
N_{norm}	number of bins within normal temperature range per state	
N	predictive horizon	
P_m	mean electrical power of the TCLs	kW
P_{nom}	nominal electric power of the heat pump	kW
P_n	normalized electrical power of the population	
P_{sat}	pressure saturation	Pa
P_{stream}	stream pressure	Pa
P_{st}	steady state electrical power of the population	
P	electrical power	kW
Q_{air}	heat gain to the air	kW
Q_{mass}	heat gain to the mass	kW
R_m	mean thermal resistance of the TCLs	$°C/kW$
R	thermal resistance	$°C/kW$
T_0	initial temperature	$°C$
T_p	swimming pool temperature	$°C$
T_{air}	air temperature	$°C$
T_{amb}	ambient temperature	$°C$
$T_{i,low}$	lower temperature boundary of the i-th bin	$°C$
$T_{i,up}$	upper temperature boundary of the i-th bin	$°C$
T_{low}	lower boundary of the working temp. range	$°C$
T_{mass}	mass temperature	$°C$
T_{sp}	temperature setpoint	$°C$
T_{up}	upper boundary of the working temp. range	$°C$
T	temperature controlled by the TCL	$°C$
U_a	total heat loss coefficient	$kW/°C$
V_p	pool volume	m^3
V	state of the heating system	
X_0	initial state vector of the aggregate model	
X	state vector of the aggregate model	
Y	output of the aggregate model	

Symbol	Description	Unit
ΔT_{bin}	temperature range corresponding to one bin	$°C$
ΔT_{low}	difference between the lower boundary of the working temperature range and the temperature setpoint range	$°C$
ΔT_{sp}	temperature setpoint change	$°C$
ΔT_{up}	difference between the upper boundary of the working temperature range and the temperature setpoint	$°C$
α_{evap}	modified evaporation coefficient	
α	heat transfer coefficient	
$\dot{Q}_{cond}$	thermal conduction to the ground	W
$\dot{Q}_{con}$	heat flow rate by convection	W
$\dot{Q}_{evap}$	heat flow rate by evaporation	W
$\dot{Q}_{heat}$	heat gain by the heat pump	W
$\dot{Q}_{in}$	heat gain by heated input water supply	W
$\dot{Q}_{rad}$	heat flow rate by long-wave radiation	W
$\dot{Q}_{sol}$	heat flow rate by short-wave radiation	W
$\dot{m}_{evap}$	mass flow rate out of the pool due to evaporation	kg/s
ρ_w	water density	kg/m^3
σ_{rel}	relative standard deviation	
σ	Stefan-Boltzmann constant	$W/(m^2 \cdot K^4)$
θ	set of parameters defining a TCL unit	
ε_w^*	emissivity coefficient	
k	bin number of the unit	
m_0	initial state of the TCL	
m	state of the TCL	
n_c	number of clusters	
n_i	number of units in i-th cluster	
$n_{OFF/ON,i}$	number of the OFF/ON units belonging to the i-th bin	
n	number of units in the population	
p	normalized electricity price forecast	

Symbol	Description	Unit
r_{sw}	swithing rate	
r	transition rate	
s	operational cost savings (reduction)	%
t_0	current time	sec
t_f	predictive horizon	sec
t_s	sampling time	sec
t_{off}	average "OFF" time of the TCL	sec
t_{on}	average "ON" time of the TCL	sec
t	transition time	sec
$u_{OFF/ON,i}$	number of OFF/ON units considered for manipulation	
u_{opt}	optimal profile of setpoint changes	
u	manipulated variable of the bin state transition model	
v_w	wind speed	m/s
w	weight of the output of the homogeneous model	
x_0	initial state vector	
x	state vector of the bin state transition model	
y	output of the bin state transition model	

List of Figures

List of Tables

1 Future energy systems

Conventionally, the energy systems were operated in a ”supply follows demand” way, which allowed the customer to demand any amount of energy at a constant price. Such strategy has many disadvantages that were first mentioned in the ’80s including [1]:

- inefficient use of fuel in order to always follow the load;
- extra capacity of the distribution and transmission systems in order to operate during peak demand periods;
- isolation of customers from the supply system discourages them from energy conservation and generation.

Current national energy policies tend to replace fossil fuelled power plants with energy production from Renewable Energy Sources (RESs) in order to create more efficient and economic energy system as well as to deal with existing environmental problems [2–6].

In the European Union, the share of renewable energy production has been growing considerably in the past years (see Figure 1.1) [7]. In particular, Germany and Spain make significant efforts in integrating renewable energy sources into their energy systems and aim to cover as much as possible energy production with it [8]. The Nordic countries aim to develop a fossil fuel free energy system by 2035 [9, 10]. For example, Sweden already crossed 50% border and exceeded their 2020 target in 2016 (see Figure 1.2). Energy union, which aims to ensure that Europe has secure, affordable, and climate-friendly energy, is one of the 10 priorities of the European Commission [11].

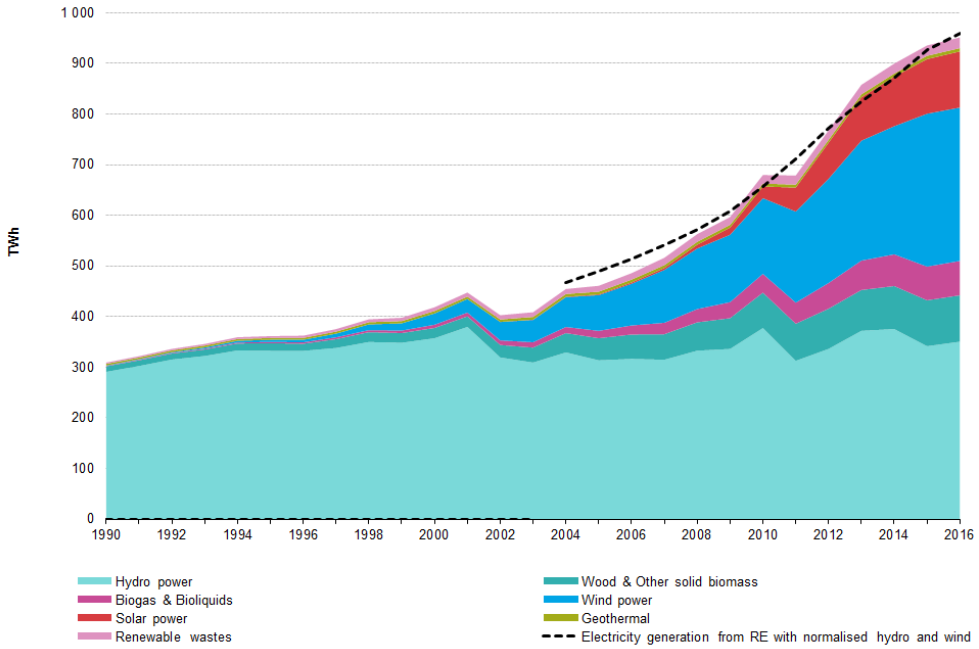

Figure 1.1: Gross electricity generation from renewable sources, EU-28, 1990-2016 (TWh)

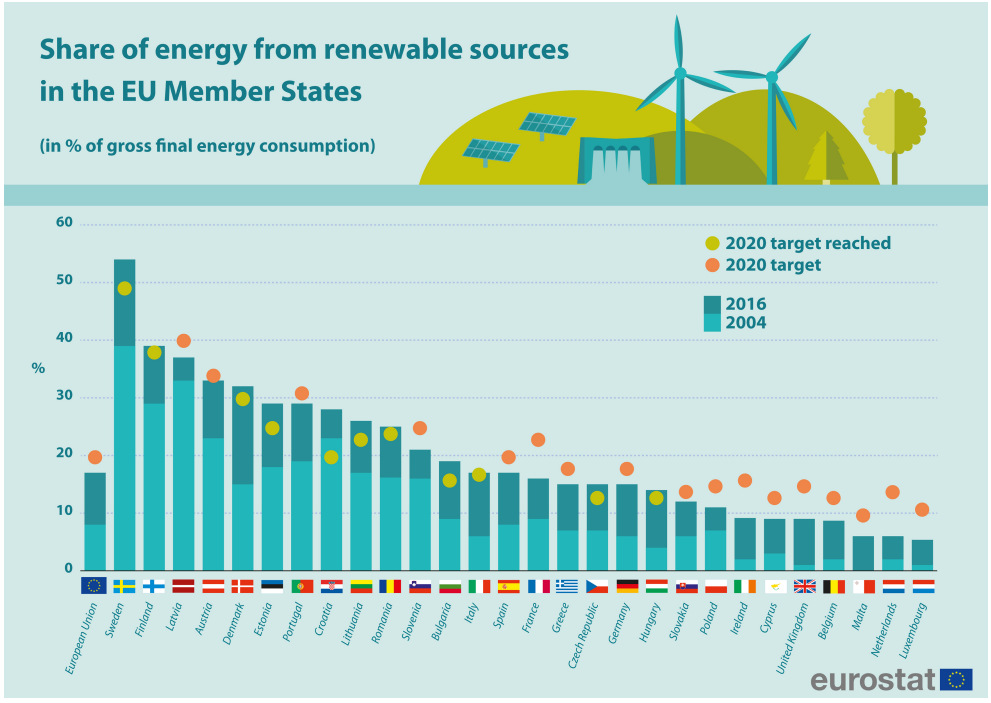

Figure 1.2: Share of energy from renewable sources, 2004 and 2016 (in % of gross final energy consumption)

There are several features specific to utilizing RES related to harvesting, transmitting, storing and consuming renewable energy. Firstly, RES are distributed, e.g. wind turbines, photovoltaic solar panels, and solar thermal units of different sizes that can be located almost anywhere and belong to anyone from government to an individual person. On one hand, it allows to reduce the transmitting capacity of the grid because the energy source can be located closer to the consumers. On the other hand, it requires redesigning the energy system because conventionally most of the energy systems are centralized. Secondly, renewable energy production has intermittent and uncontrollable nature.

The major difficulties in the energy systems with stochastic energy production is to ensure power balance and grid stability [4]. To address these issues the concept of energy system should be modified: new methods for control of electricity consumption side, new energy storage and transmission technologies (e.g. Flexible AC Transmissions Systems (FACTSs) [12]), as well as new communicating infrastructure (e.g. smart communication and metering devices) must be developed.

Smart Grid (SG) aims to improve conventional energy grids to ensure high levels of security, quality, reliability, and availability of electric power [13]. Virtual Power Plant (VPP) is a concept that combines Distributed Energy Resources (DERs), including RESs, to make it appear in market as a single power plant. Together with SG, they help to deal with mentioned above problems and to utilize advanced control and optimization methods in Demand Side Management (DSM).

This chapter is organized as follows. The first section contains a brief introduction to Smart Grid (SG). The second section presents different types of Virtual Power Plant (VPP). The third section discusses the role of Demand Side Management (DSM) and Demand Response (DR) in future energy systems. The fourth section introduces the idea of energy system with variable electricity tariffs. The fifth section gives a brief background of Model Predictive Control (MPC) and Economic Model Predictive Control (E-MPC) as well as their utilization in Smart Grid (SG) and future energy systems. The sixth section discusses the potential of Thermostatically Controlled Load (TCL) in future energy systems, including modelling of TCLs.

1.1 Smart energy grids

Smart grid is a developing concept focused on enhancing and optimization of delivery of electrical energy from suppliers to consumers involving usage of modern information and communication technology. Advanced power electronic devices such as smart meters and energy controllers provide possibility to gather information about producers and consumers of electrical energy, which can be used for this purpose.

Conceptual model of smart grid, proposed by National Institute of Standards and Technology, is presented in Figure 1.3 [14]. Each domain and its sub-domains encompass smart grid actors and applications. Actors include devices, systems, or programs that make decisions and exchange information necessary for performing applications: smart meters, Distributed Generation (DG), and control systems represent examples of devices and systems. Applications, on the other hand, are tasks performed by one or more actors within a domain. The accordance between the domains and the actors is presented in Table 1.1.

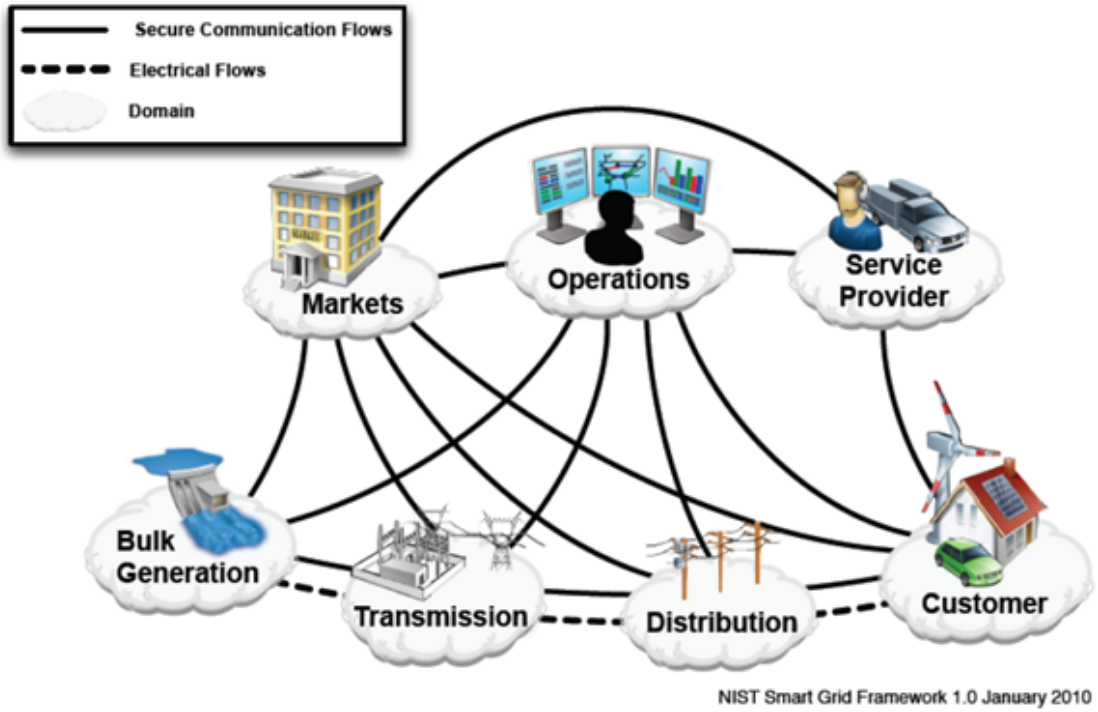

Figure 1.3: Conceptual model of smart grids

Table 1.1: Smart grids domains and actors

Domains	**Actors in the domain**
Customers	The end users of electricity that may also generate, store, and manage the usage of energy. Traditionally, there are three customer types, each with its own domain: residential, commercial, and industrial.
Markets	The operators and participants in electricity markets.
Service providers	The organizations providing services to electrical customers and utilities.
Operations	The managers of the movement of electricity.
Bulk generation	The generators of electricity in bulk quantities, which may also store energy for later distribution.
Transmission	The carriers of bulk electricity over long distances, which may also store and generate electricity.
Distribution	The distributors of electricity to and from customers, which may store and generate electricity.

Smart grids provide the following features which are focused on the goals mentioned above [15]:

- **self-healing**: the grid is able to monitor itself in order to maintain reliability, security, affordability, power quality, and efficiency;
- **motivating and including the consumers**: the individual consumers become active members of the grid that benefits both consumers and overall system reliability;
- **resisting attacks**: there are strict requirements that ensure proper security;
- **providing power quality**: with increasing number of sensitive to power quality loads, the quality of delivered electricity must be improved to meet the requirements;
- **accommodating all generation**: the modern grid will be able to accommodate distributed energy generators (sources). In the ideal case, it should be analogous to plug-and-play in today's computer environment;

- **enabling electricity market**: the electricity market optimizes energy generation (lack of energy can be bought and abundance can be sold); it also provides fairer electricity pricing since the consumers can choose their providers;
- **optimizing assets and improving efficiency**: considering the whole process (generation, transmission and consumption of the electricity) as a single system provides possibility to minimize the costs.

There are several techniques and requirements which provide the features described above [15, 16]. At first the communication system should be standardized and uniform. Hence, it provides possibility to detect and even predict faults in the operation system. In order to restore the faults as fast as possible, the system should meet the following requirements:

- the data and discrete computing should be open and standardized;
- great compatibility to other physical media communications;
- communication devices should be integrated with intelligent devices as an entity.

Secondly, smart grids should help in keeping the balance between production and consumption of the electricity that is a key point in maintaining the constant frequency in the electrical grid. In order to perform it, the advanced metering system should provide the following functions:

- remote control of power quality and voltage;
- available continuous real-time measurement information for consumers;
- support of flexible price for electric power;
- self-control of the electric load based on the real-time price.

It is very important for the smart grids to include advanced power electronics devices such as multifunction solid-state switches, integrated multifunctional devices with logical control, intelligent electronic devices and power distribution devices. All these devices are used to maximize the transmitting ability. In addition to that, the grid should posses intelligent control, self-healing, and advanced transmitting and distributing automation in order to maintain its stability.

1.2 Virtual power plant

As Renewable Energy Sources (RESs) are rapidly penetrating into energy systems, distributed energy generation becomes a major trend in many countries [17]. Virtual Power Plant (VPP) is a new concept dealing with generation and management of energy based on centralized control structure, which connects, controls, and visualizes work of DERs, such as Combined Heat and Power (CHP) units, wind farms, solar parks, and etc. as well as flexible power consumers and batteries [18, 19]. It is defined as "Aggregated control of a number of distributed generation units, grid connected and installed near the loads. The aggregated control can be centralized or decentralized system supported by advanced control algorithms and communication infrastructure, then treated as a single large power plant" that can act as a conventional one and capable of being visible or manageable on an individual basis [17, 19].

There are three main parts of VPP: generation technology, energy storage technologies, and Information Communication Technology (ICT) [17]. DG (generation technology) is divided into Domestic Distributed Generation (DDG) and Public Distributed Generation (PDG) [20]. DDG combines relatively small generation units from residential, commercial, or industrial sectors. DDG can never participate in the power market independently due to low capacity, VPP will allow DDG to do it as an individual participant. On the other hand, PDG already has enough capacity to take its chance in the power market.

Energy storage technologies is a new mean of helping to match varying demand with stochastic and uncontrollable production due to high level of RES. The following energy storage systems are considered for integration in VPP:

- Hydraulic Pumped Energy Storage (HPES),
- Compressed Air Energy Storage (CAES),
- Flywheel Energy Storage (FWES),
- Super Conductor Magnetic Energy Storage (SMES),
- Battery Energy Storage System (BESS),
- Supercapacitor Energy Storage (SCES),
- hydrogen along with Fuel Cell (FC).

ICT is the important requirement for VPP that is used in Energy Management Systems (EMS), Supervisory Control and Data Acquisition (SCADA), and Distribution Dispatching Center (DCC) [17].

The main purpose of VPP is to combine all these components so they operate as a single power plant that can be integrated in the energy system.

From the scope point of view, VPP can be classified as technical VPP and commercial VPP. Technical VPP aggregates DERs from the same geographic location and provides such services as local system management for Distribution System Operator (DSO), Transmission System Operator (TSO) system balancing, and ancillary services. It enables [21]:

- visibility of DER units to the system operator(s);
- contribution of DER units to system management;
- optimal use of the capacity of DER units to provide ancillary services incorporating local network constraints.

Commercial VPP doesn't consider the impact of the distribution network, it is focused on aggregating profile and output to represent the cost and operating characteristics for the DER portfolio. It enables [21]:

- visibility of DER units in energy markets;
- participation of DER units in the energy markets;
- maximization of value from participation of DER units in the energy markets.

From the structure point of view, VPP can be classified as [22]:

- Centralized Controlled Virtual Power Plant (CCVPP) is the simplest structure where all knowledge about the market and the planning of production is separated from the DER (Figure 1.4);
- Distributed Controlled Virtual Power Plant (DCVPP) is a hierarchical structure defining VPPs on different levels. A local VPP supervises and coordinates a limited number of DERs while delegating certain decisions upwards to a higher level VPP (Figure 1.5);

- Fully Distributed Controlled Virtual Power Plant (FDCVPP) is a fully distributed structure where each DER acts as an independent and intelligent agent which participates in and reacts to the state of the power system and market (Figure 1.6).

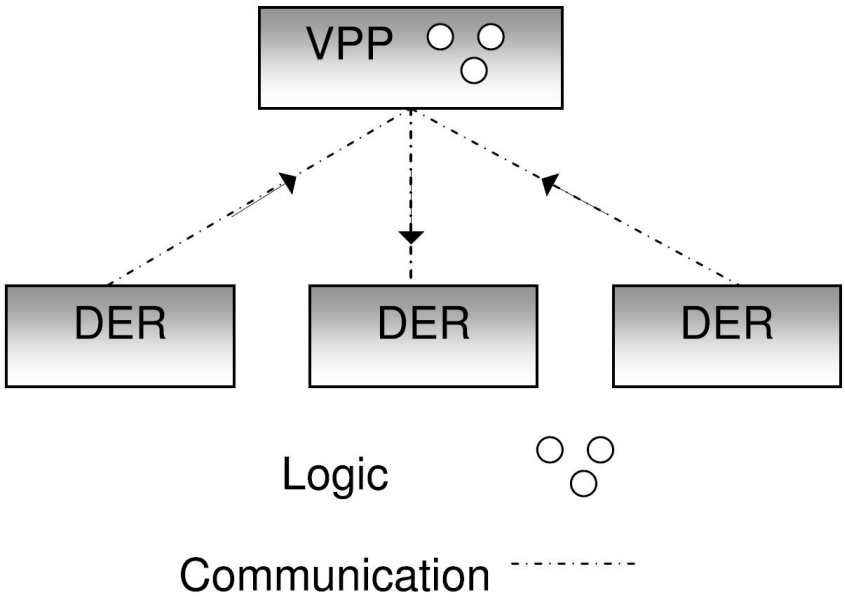

Figure 1.4: CCVPP structure

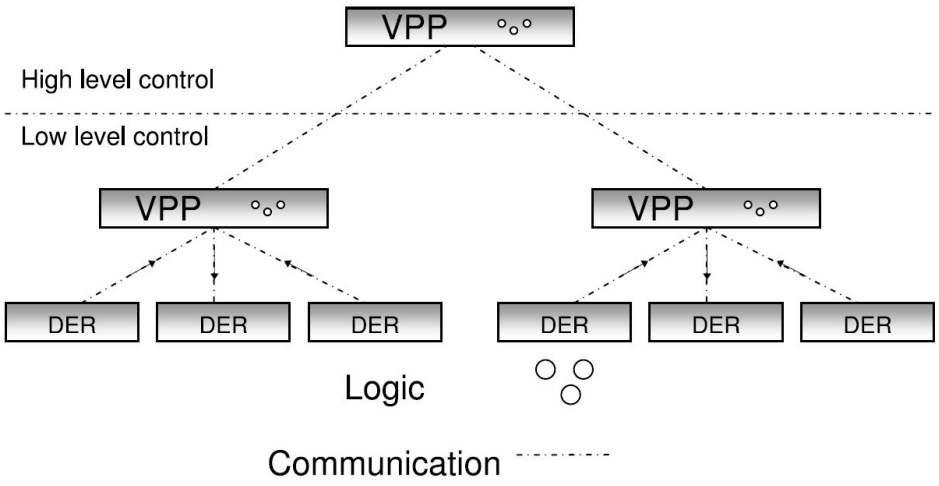

Figure 1.5: DCVPP structure

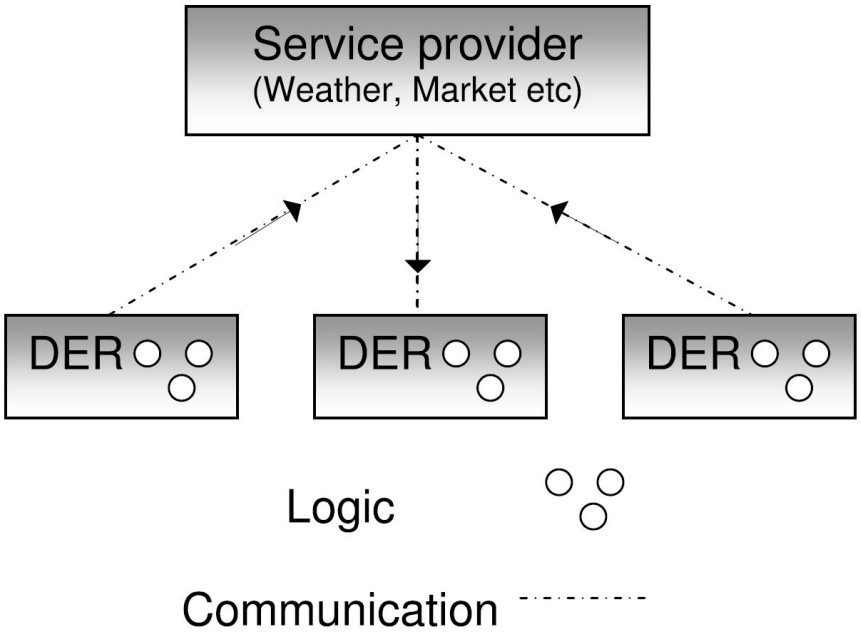

Figure 1.6: FDCVPP structure

Summing it up, introducing VPP will allow more power to be generated locally and shared by participants without needs to transmit it over long distances at high voltage. Consumers will not be passive members of electrical grid anymore. They will be able to influence the power network [22], in other words, they will become prosumers: consumers that are capable of producing electrical energy [23]. Using distributed generators will allow them to decide whether it is more profitable to buy or to produce the electrical energy. Moreover, it will increase the stability of the power network in the regions where blackouts are usual or possible to occur.

It is important to note that all these features imply utilizing advanced control and optimization algorithms in DSM (which can be a part of VPP) for scheduling fossil-fuel electricity production, managing energy storage, predicting the overall energy consumption, and coordinating flexible portion of the loads (e.g. TCLs). Thus, a variety of related problems arise: developing prediction models for the system components (renewable production units, flexible loads, and storage units) as well as models predicting overall production and consumption; defining the control hierarchy and algorithms that would coordinate all the components at different scales.

1.3 Demand side management

Demand Side Management (DSM) aims to increase flexibility and efficiency of already existing power distribution infrastructure, which is conventionally over-designed to cope with maximum expected load peaks [24, 25].

For the past thirty years, DSM or load management programs have been used as an alternative solution for system operation [26, 27]. With increasing penetration of DER and SG technology in power networks, the impact of Demand Response (DR) has become significant. In general, DSM provides the following functions:

- energy saving;
- peak-load shaving;
- load shifting.

There are two control methods applied by DSM [28]. The first method is the indirect load control. The power consumption is controlled from the customer side taking into account the real-time pricing or frequency deviation in power system. The second method is the Direct Load Control (DLC). In this case, the power consumption is controlled directly by a system operator. This method provides more precise adjusting of the consumption, but the customer's needs and preferences might be violated.

The load management programs are divided into economic-based programs and stability-based programs [29]. The economic-based programs are focused on minimizing electricity price spikes during load peak periods. The stability based programs are focused on optimizing power system stability margin without involving additional facilities. As a result, it causes reducing power system operating costs and capacity investment costs.

1.3.1 Demand response

Demand Response (DR) plays an important role in DSM. It is defined as "changes in electric usage by end-use customers from their normal consumption patterns in response to changes in the price of electricity over time, or to incentive payments designed to induce lower electricity use at times of high wholesale market prices or when system reliability is jeopardized" [30, 31]. The main goal is to shift electricity

consumption from on-peak to off-peak periods [32]. In order to motivate customers, DR programs should increase customers' understanding of the benefits deriving from DR and improve their capability to take part in DR programs using control technologies, such as smart thermostats and energy information. There are three types of DR programs [16]:

- **rate-based or price DR programs**: these programs are based on varying of the electricity price in order to motivate customers to adjust their consumption pattern. The price of electricity may be different at pre-set times or may vary dynamically according to the day, week and year and the existing reserve margin. The price would be higher for on-peak periods and lower for off-peak periods. Hence, it is profitable for consumers to move the energy consumption to off-peak periods;

- **incentive or event-based DR programs**: these programs involve customers to provide the possibility to adjust their demand remotely. Aggregate control of remotely controlled loads can be used for reducing energy consumption. For instance, dimming lighting levels or changing the setpoint for heating (cooling) systems;

- **demand reduction bids**: customers participating in this category of programs initiate and send demand reduction bids to the utility or the demand response service provider. The bids would normally include the available demand reduction capacity and the price asked for. This program encourages mainly large customers to provide load reductions at prices for which they are willing to be curtailed, or to identify how much load they would be willing to curtail at the posted price [33].

1.3.2 Energy system with varying electricity price signal

A promising approach to controlling the demand side is price-based control. If this approach is used, consumer price of electricity varies dynamically in the real time. This varying price signal can either follow the prices of the short-term wholesale electricity markets or it can be constructed by the electricity retailer in any other suitable way [34–37].

Although Direct Load Control (DLC) generally provides better ability to control the consumption, the price-based —basically indirect—method has some ad-

vantages: there is no need to develop bi-directional communication interface and share knowledge about the end-user's environment; it is a decentralized structure with common control signal (electricity price) where each customer decides how to respond, so the customer's preferences are not compromised and the system itself is simpler; it clearly motivates customers to participate in DSM by providing economical benefits.

Figure 1.7 contains an example of an energy system with varying electricity price, which is seen as a potential energy system in Denmark [10, 38]. Price Generator is used in the position of consumption controller and generates the optimal electricity price profile to meet the reference consumption taking into account the estimated response.

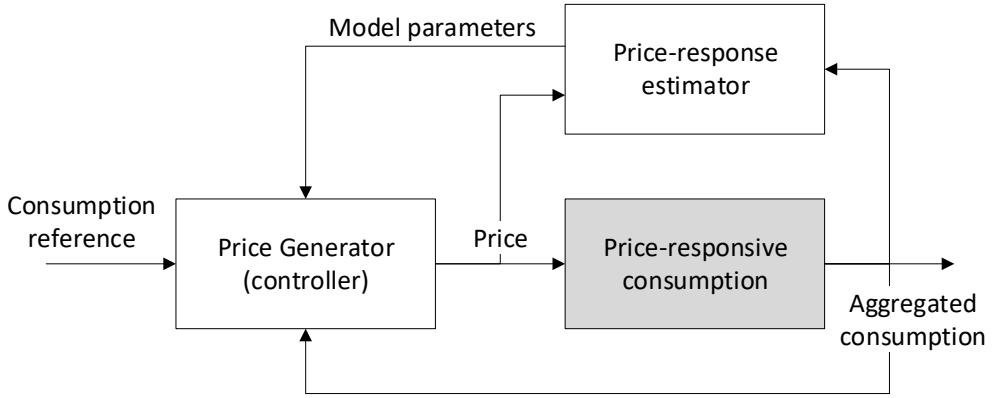

Figure 1.7: Energy system with varying electricity price signal

It is expected that the consumers will adjust their consumption to variable price in order to reduce payments for the electricity, whereas it will positively influence the grid stability (the consumption reference is generated taking into account the grid's needs).

Practical realization of such energy system requires many open questions to be answered. For instance, defining algorithms for generating consumption reference and price generator signals, developing the models for aggregate demand response approximation (price-response estimator), and etc.

In this thesis the main attention is to the flexible consumption side (price-responsive consumption). It is important to propose such optimal control strategies that will motivate the consumers to become members of the presented energy sys-

tem. Ideally, the electricity payments should decrease whereas the customer comfort should not be violated. It is widely accepted in the literature that Model Predictive Control (MPC) is a well-suited method for this class of control problems [39–44].

There are certain types of loads that can be considered as flexible loads. Their common characteristic is that the electrical consumption can be shifted in time without compromising the user comfort. For example, when one is charging an electrical vehicle the exact consumption profile doesn't matter and can be manipulated according to the grid needs as long as the car is fully charged by specified time. Another example is Thermostatically Controlled Loads (TCLs), as long as the controlled temperature remains within comfort boundaries, the consumption profile can be shifted. This thesis focuses on managing TCL due to their ability to perform load shifting and widely-spread usage [28, 45–49].

1.4 Model Predictive Control in Smart grids

MPC is an advanced control technique (more advanced than classical PID controller) that has had a great success in many application in the recent decades. There are several advantages that led to that [50, 51]. Firstly, MPC allows operation near equipment and safety constraints, in the most cases it provides the most efficient or the most profitable regimes. Secondly, the method takes into account internal interaction within the controlled process using a model. In general, it is preferable to use a linear model; however, there are modifications with non-linear models [52, 53]. Thirdly, the basic formulation can easily be extended to multivariable plants with almost no modifications. Moreover, the modern processors allow to solve such optimization problems in real time.

The dynamics models of common energy system components such as electrical vehicles, heating or refrigerating systems, wind farms, solar collectors and heat storage tanks, which are a part of smart grid, are known [54–58]. Therefore, MPC is a very attractive method for coordinating these units in the power network.

1.4.1 MPC basics

Figure 1.8 demonstrates the basic principle of MPC [59, p. 7]. At each iteration the controller solves Optimal Control Problem (OCP) in order to get a sequence of optimum manipulated variables (u). Classical MPC minimizes the distance between

desired output (z) and predicted output (output), which is represented as a weighted least squares objective function [50].

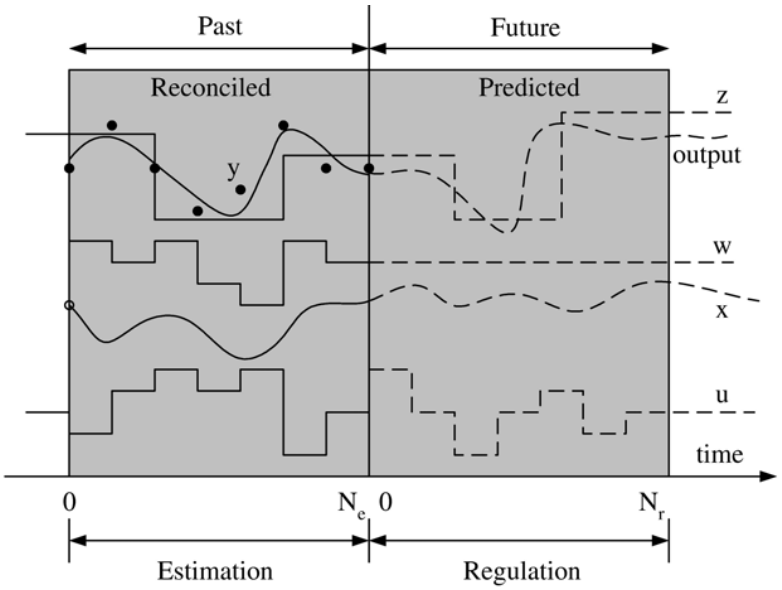

Figure 1.8: Basic principle of MPC

The discussed above tracking control problem implies solving the following optimization problem, which represents the general idea of classical MPC [51, 54]:

$$\min_{u} \phi_{req} = \frac{1}{2} \sum_{k=0}^{N-1} \|y_k - \bar{y}_k\|_Q^2 + \|u_k - \bar{u}_k\|_R^2 \tag{1.1a}$$

$$s.t. \quad x_{k+1} = Ax_k + Bu_k \tag{1.1b}$$

$$y_k = Cx_k + Du_k \tag{1.1c}$$

$$u_{min} \leq u_k \leq u_{max} \tag{1.1d}$$

$$y_{min} \leq y_k \leq y_{max} \tag{1.1e}$$

Here, cost function (1.1a) consists of two terms: the first term is the regulation error between the actual output (y) and the setpoint ($\bar{y}$); the second term penalizes difference between manipulated variable (u) and target manipulated variable ($\bar{u}$). The impact of each term can be adjusted by corresponding weights (Q and R). Mathematical model (1.1b, 1.1c) defines the dynamics of the plant. Inequalities (1.1d, 1.1e) are the input and output constraints respectively.

Many modifications and variations of MPC exist:

- the cost function may include additional term ($\|\Delta u_k\|^2$) penalizing manipulated variable change, in order to avoid undesirable oscillation of the manipulated variable;
- the output constraints might be softened in order to guarantee that the optimization problem always has a feasible solution;
- the plant can be represented by either linear or non-linear model.

In case when an MPC is based on a linear model, the resulting optimization problem is either a Linear Program (LP) or a Convex Quadratic Program (QP). These problems can be solved relatively easy and fast thanks to the algorithms developed in past decades [60, 61].

In case when an MPC is based on a non-linear model, the resulting optimization problem is a Non-linear Program (NP), which requires more effort to solve. An example of a Non-linear Model Predictive Control (NMPC) and solving the corresponding NP are discussed further in this work.

1.4.2 EMPC basics

Economic Model Predictive Control (E-MPC) is a modification of MPC that includes some economical aspects of the process into optimization problem. Such approach is becoming more and more popular in power management, especially in the systems with variable electricity prices, as it provides the most efficient supply and demand plans while observing the plant dynamics and limits [39, 40, 62].

All the basic principles of MPC discussed in Section 1.4.1 apply to Economic Model Predictive Control (E-MPC). The key idea of this modification is that a new economical term of the cost function is introduced:

$$\phi_{eco} = \sum_{k=0}^{N-1} c^T u_k \tag{1.2}$$

Here, c is the price of applying manipulated variable u_k.

If needed, both cost functions (1.1a) and (1.2) can be combined:

$$\phi = \alpha\phi_{reg} + (1-\alpha)\phi_{eco}, \quad \alpha \in [0;1] \tag{1.3}$$

Here, α helps to adjust the trade-off between desired dynamics and economical benefits of the process.

1.5 Potential of TCLs in future energy systems

Thermostatically Controlled Loads (TCLs) is a common class of energy loads that maintain temperature regulation [63]. Thermostat is a device that senses the controlled temperature and manipulates the load [64]. In most residential applications thermostats are hysteresis (ON/OFF) controllers: the load is turned OFF/ON when one of the temperature limits is achieved. There are many different type of TCLs including Air Conditioners (ACs), heat pumps, electrical space heaters, boilers, and refrigerators.

It is widely accepted that TCLs have enormous potential for regulation services provision due to its inherent thermal capacitance, ability of being turned OFF/ON for some period of time without compromising customer's comfort, and widely-spread usage [28, 45–49]. For example, TCLs represent about 20% of total electrical consumption in the United States [65, 66]. Moreover, it has been shown that aggregate control of TCLs is more cost-effective than other energy storage technologies such as flywheels, Li-ion, advanced lead acid, and Zinc Bromide batteries [67]. These facts make TCLs an attractive target for DSM.

1.5.1 Physical modelling of TCLs

Modelling systems with TCLs (e.g. building climate system, commercial refrigerators, swimming pool heating systems, and etc.) is essential for predicting and optimizing the demand response when using MPC.

Thermal dynamics of such systems is often modelled by so-called Equivalent Thermal Parameter (ETP) model, which is presented and used in many other works [28, 39, 66, 68–71]. The model describes the energy balances from the heating/cooling perspective of the TCL and its environment (e.g. a building).

Figure 1.9 contains an example of second-order ETP model of a building heating/cooling system. Here, T_{amb} is the ambient temperature $[^{\circ}C]$; T_{air} is the air temperature $[^{\circ}C]$; T_{mass} is the mass temperature $[^{\circ}C]$; U_a is the total heat loss coefficient $[kW/^{\circ}C]$; H_m is the total interior mass surface conductance $[kW/^{\circ}C]$; C_{air} is the air thermal mass $[kWh/^{\circ}C]$; C_{mass} is the thermal mass of the buildings material and other equipment $[kWh/^{\circ}C]$; Q_{air} is the heat gain to the air $[kW]$, which depends on the state of the TCL; Q_{mass} is the heat gain to the mass $[kW]$.

The following state equations describe the dynamics of air and mass tempera-

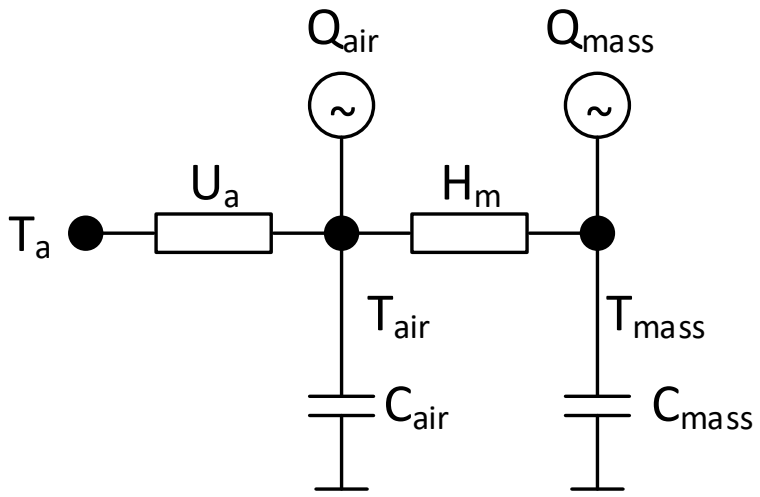

Figure 1.9: Second order ETP model of a building heating/cooling system

tures. Note that the resulting time constant of the mass temperature change is slower than the time constant of the air temperature change:

$$\frac{dT_{air}(t)}{dt} = -\frac{1}{C_{air}}[U_a(T_{amb} - T_{air}) + H_m(T_{mass} - T_{air}) + Q_{air}] \tag{1.4a}$$

$$\frac{dT_{mass}(t)}{dt} = -\frac{1}{C_{mass}}[H_m(T_{air} - T_{mass}) + Q_{mass}] \tag{1.4b}$$

This model can be simplified by assuming that both air and mass temperatures are equal to the temperature controlled by the TCL ($T = T_{air} = T_{mass}$) and that air and mass thermal capacitances are lumped to the total thermal capacitance ($C = C_{air} + C_{mass}$). The resulting first order model is more general and can be used for describing a wider class of TCLs [72–75]:

$$\frac{dT(t)}{dt} = -\frac{1}{CR}[T(t) - T_{amb}(t) - m(t)RP], \tag{1.5}$$

where T is the temperature controlled by the TCL [$^\circ C$]; C is the thermal capacitance [$kWh/^\circ C$] and R is the thermal resistance [$^\circ C/kW$]; P is the electrical power [kW]; T_{amb} is the ambient temperature [$^\circ C$]. Parameter m defines the amount of heating/cooling energy produced by the TCL. As discussed above, in the most residential application, TCLs are controlled according to the hysteretic control rule for

a heating device:

$$m(t^+) = \begin{cases} 0 & \textbf{if} \quad T \geq T_{sp} + H \\ 1 & \textbf{if} \quad T \leq T_{sp} - H \\ m(t) & \textbf{otherwise} \end{cases} \tag{1.6}$$

or for a cooling device:

$$m(t^+) = \begin{cases} -1 & \textbf{if} \quad T \geq T_{sp} + H \\ 0 & \textbf{if} \quad T \leq T_{sp} - H \\ m(t) & \textbf{otherwise} \end{cases} \tag{1.7}$$

$m \in \{0, \pm 1\}$ is the state of the TCL (OFF anf ON respectively), the sign depends on whether the TCL is a cooling (minus) or a heating (plus) device; T_{sp} is the temperature setpoint $[°C]$; H is the hysteresis band of the thermostat $[°C]$.

The temperature controlled by the TCL is kept within the hysteresis dead-band $[T_{sp} - H; T_{sp} + H]$. Figure 1.10 demonstrates the dynamics of a system with heating TCL.

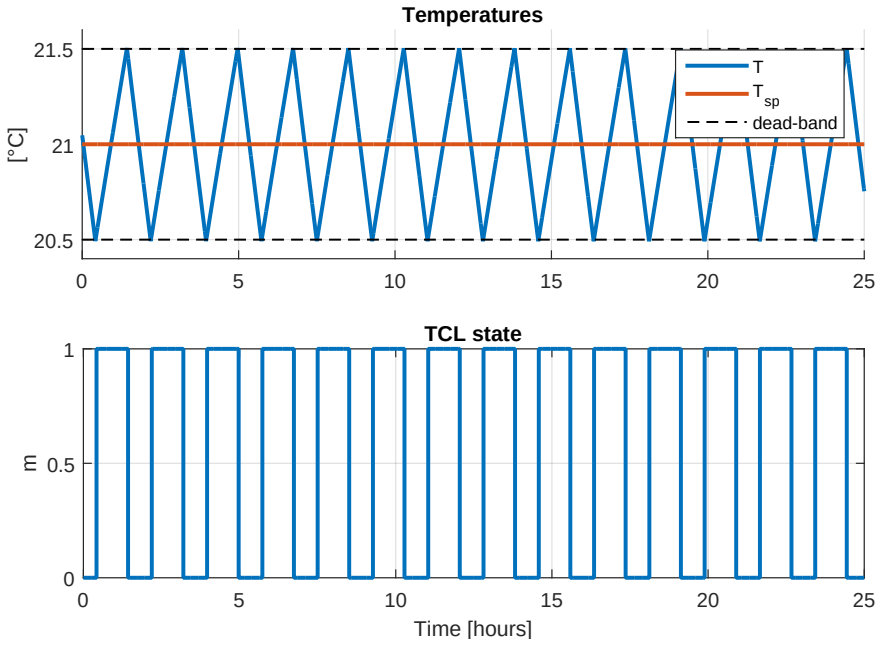

Figure 1.10: Example of temperature evolution in a heating TCL

1.5.2 Thermostatically controlled loads in demand side management

Using TCLs in DSM implies that they can be externally controlled either directly or indirectly. In case of direct control, the system operator has a full control on the loads. This way, of course, provides more precise adjustment of the electricity consumption, but the customer's needs and preferences might be violated: it is more difficult to respect desired temperature boundaries, especially in case of aggregate control. Moreover, it requires an additional interface to manipulate the loads that is usually done by the local thermostat.

Another way is to change the temperature setpoint of the TCLs [55, 76–78] which results in either immediate change of the TCL's state or extending the current state (see Figure 1.11); thus, changing the temperature setpoint allows to shift the ON-OFF cycle of the TCL. Usually, the temperature setpoint is linked to the electricity price [76, 79]. Therefore, the price change indirectly influences the total power consumed by the loads. The advantage of this indirect method is that the customers are able to choose how to react to the electricity price change according to their preferences.

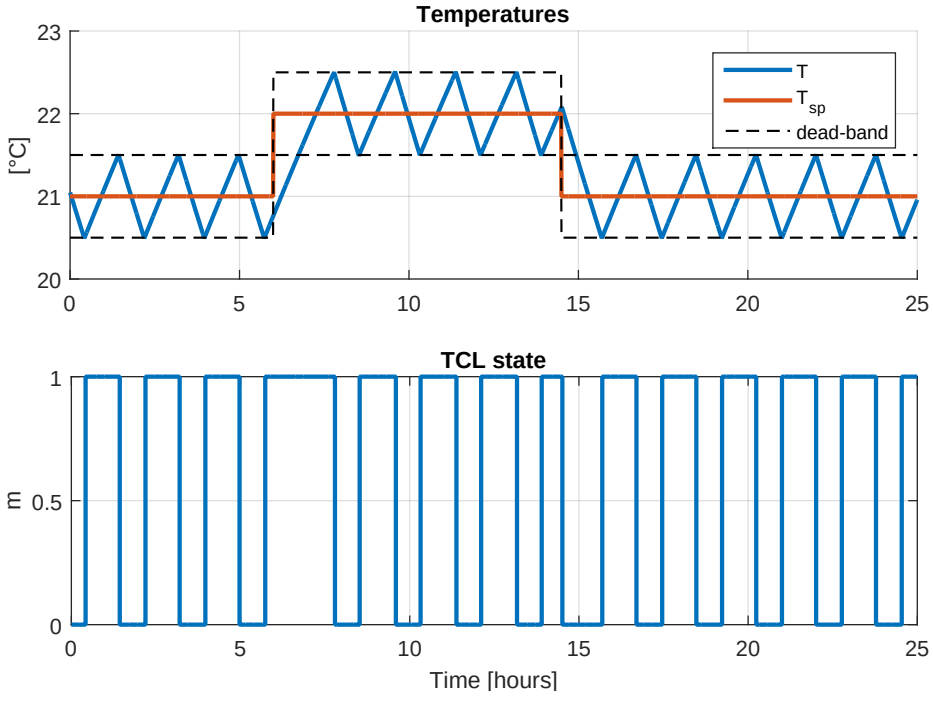

Figure 1.11: Effect of temperature setpoint change of TCL

The price response mechanism that is usually proposed for this class of TCLs is based on linear change of the thermostat setpoint in response to price changes. This mechanism was used in the celebrated Olympic Peninsula project [79] and more recently it has been proposed in a modified form in [80]. Heating setpoint is linearly decreased if the electricity price increases and vice versa. Such static mechanism does not take into account the complex dynamic response of the large groups of TCLs nor can it make use of the prediction of weather or other factors affecting the future consumption of TCLs.

Therefore the recent studies are focused more on using E-MPC [39, 76, 81] for deriving optimal setpoint change profile, so it can make direct use of the dynamic model of the response of the TCLs in order to foresee their responses during the whole prediction horizon (e.g. one day). Utilization of the weather forecast as well as of other predictions is also possible.

1.5.3 Aggregate modelling and control of TCLs

There are many proposed MPC-based control systems for utilizing TCLs in DSM [39–44]. However, in these examples the scope of optimization is limited either to a single building, to relatively small groups of buildings, or to microgrids with quite modest set of power generation and consumption devices. Consequently, the appliances, generators etc. could be described by individual simplified dynamic models (e.g. second-order ETP presented in Section 1.5.1). MPC is then formulated as a relatively simple linear or linear mixed integer program.

Another approach is to focus on a large population of TCLs. Consequently it is no longer possible to model each appliance by its individual model, but suitable aggregate population model must be developed and used instead. Various models describing aggregate demand of a population of TCLs have been presented in the literature. These models can be classified with respect to the control strategy.

The first class of models proposed in [58, 77, 78] implies control strategies based on changing temperature setpoints of the TCLs in the population. Usually the temperature setpoint change is the same for all TCLs. These models are attractive by their simplicity (second order transfer function with complex poles). However, they are based on many simplifying assumptions (constant outdoor temperature, specific probability distribution of TCLs parameters etc.). Consequently, it is not possible to use them in more realistic situations and for the relatively long-term

predictions needed by E-MPC.

The second class of the models implies controlling the TCLs ON/OFF-states directly by generating a switching signal and include probability density model [82, 83], generalized battery model [65,84], and bin state transition model [55,66,85,86].

In probability density model, the duty cycles of TCLs are treated as a random variable, so the model derives an expression for the probability density function of the duty cycles that accounts for the effects of the driving process noise. Such model provide relatively accurate but short-term load predictions of a population of TCLs.

In generalized battery model and its analog called leaky storage model [87], a population of TCLs is considered as an energy storage that losses the stored energy with an intrinsic rate and it is replenished by the variable power consumption. In this model the minimum and maximum energy levels represent the aggregate flexibility of a large population of TCLs and the goal of the control strategy is to keep the stored energy within these limits.

In bin state transition model, the temperature dead-band is divided in equally-spaced (uniform model) or non-equally-spaced (non-uniform model) bins. Each bin state represents the number of TCLs in a particular temperature bin with a particular state (ON or OFF). The model describes distribution and evolution of the TCLs among the bins. The resulting demand is calculated from the number of units in ON state.

The last two models provide highly accurate long-term demand predictions. However, the practical implementation of direct control strategies is more difficult, because it implies direct control of the loads bypassing local thermostats.

2 Objectives of the thesis

This thesis deals with developing advanced control algorithms for utilizing the potential of Thermostatically Controlled Loads (TCLs) in smart energy grid. It is assumed that the energy system employs the concept presented in Section 1.3.2, i.e. the electricity price is changing according to the system needs taking into account current and predicted renewable energy production. The control algorithms design is based on Model Predictive Control (MPC), specifically its economic modification (Economic Model Predictive Control (E-MPC)); this method naturally takes into account the loads dynamics and allows to optimize its behavior over some period of time in the future (predictive horizon).

The focus of the work is on the price-responsive consumer's side, in particular on the optimal control algorithms that can be applied on the consumer's side, whereas the price generation algorithms are out of the thesis scope. The main objective of the control algorithms is to minimize the operational cost of the flexible loads, in particular TCLs, taking into account the current electricity price and future electricity price profile provided by the energy system, environmental conditions (weather forecast), and customer comfort. Such Demand Response (DR) program will motivate consumers to participate because it will reduce their payments for electrical energy. It will also provide regulation services to the grid because the price signal is generated taking into account the grid's needs.

The rest of the thesis is divided into two parts. The first part deals with optimizing energy consumption of a system with a single relatively large TCL, which can be described by a Linear Parameter-Varying (LPV) model. An example of such system is presented in the Danish Pilot, Task 5.3 of the H2020 SmartNet project [88]. A part of this project is to optimize energy consumption of swimming pool heating systems selected for verifying the concept of energy system with varying electricity price. It is expected that environmental conditions will have significant impact on the system dynamics (e.g. ambient temperature, wind speed, and/or occupancy

status). Classical MPC requires a Linear Time Invariant (LTI) model describing plant dynamics, thus possible variation of the model parameters cannot be taken into account, therefore the MPC based on the LPV model was developed.

The objectives related to the first part of the thesis can be summarized as follows:

- formulate an LPV model of a swimming pool heating system for E-MPC controller design;
- modify the E-MPC optimization problem to account variation of the model parameters;
- verify the E-MPC control strategy.

The second part deals with aggregate control of a population of TCLs using E-MPC. These TCLs have smaller thermal capacitance and power consumption, therefore they might be negligible individually. However, these loads can play an important role if a larger population is aggregated. This task doesn't only require developing an appropriate optimal control algorithm, but also an aggregate model describing demand response of the whole population. The structure of the proposed control system is hierarchical. E-MPC in the upper level responds to varying electricity price and changes the temperature setpoints of the thermostats in the lower level.

Section 1.5.3 presents existing aggregate models, however they either assume direct load control or don't provide accurate and long-term approximation of the population demand response. Thus, a new model is needed to be designed in order to meet the following requirements:

- the model should provide accurate and long-term (e.g. 12-24 hours) predictions of electrical energy consumption by the whole population;
- the model should imply indirect load control;
- the complexity of the model should not depend on the number of units in the population.

The proposed model is a non-linear modification of bin state transition that meets these requirements and described further in the thesis.

The objective of the control strategy is the same as in the first part: to minimize the overall operational cost of the population assuming that it belongs to a single owner (e.g. research facility, office building, factory etc.). Since the proposed

model is non-linear, the E-MPC should solve non-linear mixed integer optimization problem.

The objectives related to the second part of the thesis can be summarized as follows:

- design a simulation model for verification of the aggregate model and validation of Economic Non-linear Model Predictive Control (E-NMPC) control strategy;
- develop a non-linear modification of bin state transition model for aggregate modelling of the TCLs population;
- design and verify the E-NMPC control strategy.

The rest of the thesis is organized as follows. Chapter 3 briefly introduces the Danish Pilot and SmartNet project as well as presents the main results: the LPV model of the system; the modification of classical MPC that allows to take into account parameter variation of the model; the control algorithm verification results. Chapter 4 presents the simulation model of the large population of TCLs based on the hybrid model used for validation of the aggregate model and the control strategy. Chapter 5 proposes a novel approach for aggregate modelling of a large population of TCLs. The proposed model is a non-linear modification of bin state transition model. Chapter 6 develops the economic control strategy applying the means of E-MPC based on the proposed aggregate model. The last chapter contains summary of the obtained results and conclusions.

3 E-MPC based on linear parameter-varying model

Some systems with TCLs are better described by Linear Parameter-Varying (LPV) rather than Linear Time Invariant (LTI) model because the model parameters might depend on the environmental conditions. For example, Coefficient of Performance (COP) usually depends on the ambient temperature; thermal conductivity and heat transfer coefficients may depend on the wind speed; and some other parameters may depend on the occupancy status in case of residential applications [89–91].

An example of such system is studied in the Danish Pilot, which is also a part of the SmartNet and the CITIES [92] projects. SmartNet is a big European project that involves 9 European countries and has 22 partners from academia, research organizations and industry [88]. The main goal of the project is to propose new practical solutions to the increasing integration of Renewable Energy Source (RES) in the existing electricity transmission network. The focus is on grid operators at national and local levels (respectively the TSOs and DSOs) and the exchange of information for monitoring and for the acquisition of ancillary services (reserve and balancing, voltage balancing control, congestion management) from subjects located in the distribution segment (flexible load and distributed generation). As a part of the project three Pilots were developed: in Italy, in Denmark, and in Spain.

The aim of the Danish Pilot is to explore the potential of aggregate control of summer houses with swimming pools to be a flexible consumer and store energy harnessed from renewable energy sources. These summer houses consume relatively high amount of energy for the swimming pool temperature and humidity control. At the same time the swimming pools, filled with water, have large thermal mass, which allows to shift and to schedule the heating profile without compromising the occupants comfort in order to optimize the energy consumption. Moreover, booking or occupancy information can be taken into account to prevent unnecessary waste

of energy: performing the temperature control when nobody is using the swimming pool.

Classical MPC requires an LTI model describing plant dynamics. In order to take into account possible variation of the plant model parameters, an MPC based on an LPV model should be developed. This task was divided into the following steps addressed in this chapter:

- formulate an LPV model of the swimming pool heating system for the control strategy verification purpose;
- formulate an optimal control strategy based on the LPV model;
- verify the control algorithm (simulations).

Note that in this chapter the swimming pool heating system is considered as a case study, the obtained results can be applied to other kinds of TCLs with similar properties. The presented results were already published in [93].

3.1 Model of swimming pool heating system

Figure 3.1 contains the structure of the swimming pool heating system. The pump circulates the water in the system. The heat pump and the heat exchanger provide hot water to the system. The heat pump is assumed to be controlled externally.

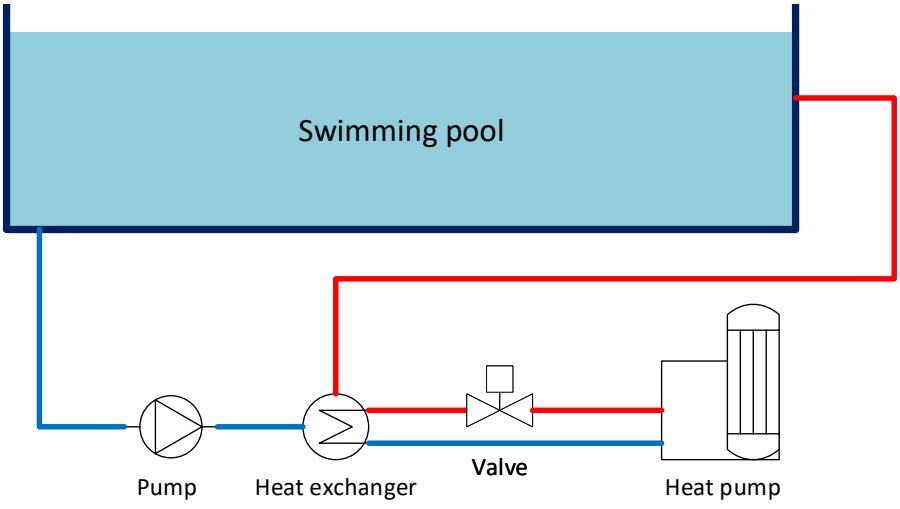

Figure 3.1: Structure of swimming pool heating system

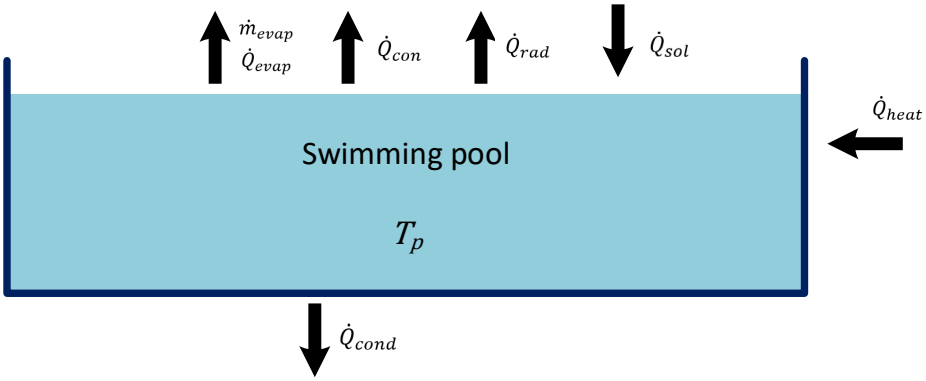

Figure 3.2: Heat and mass flows of the pool

Figure 3.2 contains heat and mass flows of the swimming pool: heat flow rate by evaporation ($\dot{Q}_{evap}$); mass flow rate out of the pool due to evaporation ($\dot{m}_{evap}$); heat flow rate by convection ($\dot{Q}_{con}$); heat flow rate by long-wave radiation ($\dot{Q}_{rad}$); heat flow rate by short-wave radiation ($\dot{Q}_{sol}$); thermal conduction to the ground ($\dot{Q}_{cond}$); heat gain by the heat pump ($\dot{Q}_{heat}$). Long-waves represent radiation exchange with the environment, e.g. walls for indoor pools or the sky for outdoor pools; short-waves represent thermal gain from total solar radiation on a horizontal surface [94].

Note that further in this section the thermal conduction to the ground ($\dot{Q}_{cond}$) is neglected. In case of indoor swimming pool, the pool is usually surrounded by engineering rooms with relatively high ambient temperatures; in case of outdoor swimming pool, it has insignificant influence (<1 %) [94].

According to the first law of thermodynamics:

$$\rho_w \cdot C_w \cdot V_p \cdot \dot{T}_p = \dot{Q}_{in} - \dot{Q}_{evap} - \dot{Q}_{con} - \dot{Q}_{rad} + \dot{Q}_{sol}, \tag{3.1}$$

where T_p is the swimming pool temperature $[^\circ C]$; ρ_w is the water density $[kg/m^3]$; C_w is the specific heat of water $[kWh/(kg \cdot^\circ C)]$; V_p is the pool volume $[m^3]$.

The corresponding heat flows are derived in [89, 94] as follows:

$$\dot{Q}_{evap} = A_p \alpha_{evap} \left(P_{sat}(T_p) - P_{stream}(T_{amb}) \right), \tag{3.2a}$$

$$\alpha_{evap} = 50.58 + 66.9 {v_w}^{0.5}, \tag{3.2b}$$

where A_p is the pool area $[m^2]$; α_{evap} is the modified evaporation coefficient; P_{sat} is the pressure saturation $[Pa]$; P_{stream} is the stream pressure $[Pa]$; v_w is the wind speed $[m/s]$; T_{amb} is the ambient temperature $[^\circ C]$.

$$\dot{Q}_{con} = \alpha A_p \left(T_p - T_{amb}\right), \tag{3.3a}$$

$$\alpha = 3.1 + 4.1 v_w, \tag{3.3b}$$

where α is the heat transfer coefficient.

$$\dot{Q}_{rad} = A_p \varepsilon_w^* \sigma \left({T_p}^4 - {T_{amb}}^4\right), \tag{3.4a}$$

$$\varepsilon_w^* = 0.9, \tag{3.4b}$$

$$\sigma = 5.67 \cdot 10^{-8} \frac{W}{m^2 \cdot K^4}, \tag{3.4c}$$

where ε_w^* is the emissivity coefficient; σ is the Stefan-Boltzmann constant $[W/(m^2 \cdot K^4)]$.

$$\dot{Q}_{sol} = A_p \varepsilon_w^* E_{glob,H}, \tag{3.5}$$

where $E_{glob,H}$ is the total solar radiation on a horizontal surface.

As the dynamics of the heating system (the heat pump, the heat exchanger, and water supply pipes) is significantly faster than thermodynamics of the water mass in the pool, its model can be assumed to be static:

$$\dot{Q}_{heat} = V \cdot P_{nom} \cdot COP \tag{3.6}$$

Here, $V \in \{0, 1\}$ is the state of the heating system, which can be either OFF or ON respectively; P_{nom} is the nominal electric power of the heat pump $[kW]$; COP is the coefficient of performance.

As mentioned earlier, the main purpose of the swimming pool model is to verify the control strategy. The following assumptions were made in order to simplify it:

- evaporation is neglected, thus the volume of the water in the pool is constant;
- all heat losses are lumped to a single heat loss, which depends on the ambient temperature and the wind speed, similar to equations (3.3);
- relationship between COP and T_{amb} is linear [95] within the considered range:

$$COP = 0.0952 \cdot T_{amb} + 3.1. \tag{3.7}$$

The resulting model is defined as follows:

$$\rho_w \cdot C_w \cdot V_p \cdot \dot{T_p} = \alpha A_p \left(T_{amb} - T_p\right) + V \cdot P_{nom} \cdot COP, \tag{3.8a}$$

$$\alpha = \mu + \eta \cdot v_w, \tag{3.8b}$$

where μ and η are the coefficients defining the relationship between the wind speed and the heat transfer coefficient α.

3.2 E-MPC based on LPV model

This section presents economic MPC based on a Linear Parameter-Varying (LPV) model and describes its transformation to a standard linear program. Note that these results were published in 2017 and presented in [93].

Model (3.8) can be generalized as follows:

$$x_{k+1} = A_d(\theta_k)x_k + B_d(\theta_k)u_k + E_d(\theta_k)d_k \tag{3.9a}$$

$$y_k = C_d(\theta_k)x_k \tag{3.9b}$$

Here, y_k is the output vector; x_k is the state vector; u_k is the control vector; d_k is the measured disturbance; A_d, B_d, E_d and C_d are the state matrices; θ_k is the vector of parameters influencing the state matrices.

3.2.1 Optimization problem

The objective of the economic MPC is to minimize operational cost of the system taking into account input and output constraints [39]:

$$\min_{u} \quad \sum_{k=0}^{N-1} c_k u_k + \rho_v v_{k+1} \tag{3.10a}$$

$$s.t. \quad x_{k+1} = A_d(\theta_k)x_k + B_d(\theta_k)u_k + E_d(\theta_k)d_k \tag{3.10b}$$

$$y_k = C_d(\theta_k)x_k \tag{3.10c}$$

$$y_{min,k} - v_k \leq y_k \leq y_{max,k} + v_k \tag{3.10d}$$

$$u_{min,k} \leq u_k \leq u_{max,k} \tag{3.10e}$$

Here, N is the prediction horizon; c_k is the cost coefficients (e.g. electricity price); v_k is the slack variables relaxing the output constraints with corresponding penalty cost ρ_v; $y_{min,k}$ and $y_{max,k}$ are the output constraints; $u_{min,k}$ and $u_{max,k}$ are the input constraints.

3.2.2 Corresponding linear program

Problem (3.10) can be converted to a standard linear optimization problem of the following form:

$$\min_{x} \quad f^T x \tag{3.11a}$$

$$s.t. \quad A_{ineq} x \leq b_{ineq} \tag{3.11b}$$

$$x_{min} \leq x \leq x_{max} \tag{3.11c}$$

Here, f is the vector of cost coefficients; x is the vector of variables to be determined; A_{ineq} and b_{ineq} define the inequality constraints; x_{min} and x_{max} are the minimum and maximum boundaries of x respectively.

The transformation from optimal problem (3.10) to optimal problem (3.11) is presented below. Table 3.1 contains corresponding notations. The transformation is based on similar transformation for the case of the LTI model presented in [51,96]

Table 3.1: MPC for LPV model notations

Parameter	Description
$U = [u_0\ u_1\ ...\ u_{N-1}]^T$	Vector of future inputs
$Y = [y_1\ y_2\ ...\ y_N]^T$	Vector of predicted outputs
$U_{min} = [u_{min,0}\ ...\ u_{min,N-1}]^T$	Vector of min. input constraints
$U_{max} = [u_{max,0}\ ...\ u_{max,N-1}]^T$	Vector of max. input constraints
$Y_{min} = [y_{min,1}\ ...\ y_{min,N}]^T$	Vector of min. output constraints
$Y_{max} = [y_{max,1}\ ...\ y_{max,N}]^T$	Vector of max. output constraints
$D = [d_0\ d_1\ ...\ d_{N-1}]^T$	Vector of measured disturbances
$\Theta = [\theta_0\ \theta_2\ ...\ \theta_N]^T$	Vector of parameters
$C = [c_0\ c_1\ ...\ c_{N-1}]^T$	Vector of cost coefficients
$V = [v_0\ v_1\ ...\ v_{N-1}]^T$	Vector of slack variables
$P = [\rho_v\ \rho_v\ ...\ \rho_v]^T$	Vector of penalty cost coefficients

Equations (3.12) and (3.13) demonstrate calculation of state and output vectors predictions with given initial states x_0, future control inputs U, and measured

disturbances D. Where $A_k = A_d(\theta_k)$, $B_k = B_d(\theta_k)$, $E_k = E_d(\theta_k)$ and $C_k = C_d(\theta_k)$.

$$x_1 = A_0 x_0 + B_0 u_0 + E_0 d_0 \tag{3.12a}$$

$$\begin{aligned} x_2 &= A_1 x_1 + B_1 u_1 + E_1 d_1 \\ &= A_1(A_0 x_0 + B_0 u_0 + E_0 d_0) + B_1 u_1 + E_1 d_1 \\ &= A_1 A_0 x_0 + A_1 B_0 u_0 + B_1 u_1 + A_1 E_0 d_0 + E_1 d_1 \end{aligned} \tag{3.12b}$$

$$\begin{aligned} x_3 &= A_2 x_2 + B_2 u_2 + E_2 d_2 \\ &= A_2(A_1 A_0 x_0 + A_1 B_0 u_0 + B_1 u_1 + A_1 E_0 d_0 + E_1 d_1) + \\ &+ B_2 u_2 + E_2 d_2 \\ &= A_2 A_1 A_0 x_0 + A_2 A_1 B_0 u_0 + A_2 B_1 u_1 + B_2 u_2 + \\ &+ A_2 A_1 E_0 d_0 + A_2 E_1 d_1 + E_2 d_2 \end{aligned} \tag{3.12c}$$

$$\begin{aligned} &\dots \\ x_k = &\left(\prod_{i=0}^{k-1} A_i\right) x_0 + \sum_{i=0}^{k-1} \left(\prod_{j=k-1}^{i+1} A_j\right) B_i u_i + \\ &+ \sum_{i=0}^{k-1} \left(\prod_{j=k-1}^{i+1} A_j\right) E_i d_i \end{aligned} \tag{3.12d}$$

$$\begin{aligned} y_k = &\; C_k \left(\prod_{i=0}^{k-1} A_i\right) x_0 + C_k \sum_{i=0}^{k-1} \left(\prod_{j=k-1}^{i+1} A_j\right) B_i u_i + \\ &+ C_k \sum_{i=0}^{k-1} \left(\prod_{j=k-1}^{i+1} A_j\right) E_i d_i \end{aligned} \tag{3.13}$$

$$\begin{aligned} \underbrace{\begin{bmatrix} y_1 \\ y_2 \\ \dots \\ y_N \end{bmatrix}}_{Y} = &\underbrace{\begin{bmatrix} O_1 \\ O_2 \\ \dots \\ O_N \end{bmatrix}}_{\Phi} x_0 + \underbrace{\begin{bmatrix} H_{u,1,0} & 0 & \dots & 0 \\ H_{u,2,0} & H_{u,2,1} & \dots & 0 \\ \dots & \dots & \dots & \dots \\ H_{u,N,0} & H_{u,N,1} & \dots & H_{u,N,N-1} \end{bmatrix}}_{\Gamma_u} \underbrace{\begin{bmatrix} u_0 \\ u_1 \\ \dots \\ u_{N-1} \end{bmatrix}}_{U} \\ &+ \underbrace{\begin{bmatrix} H_{d,1,0} & 0 & \dots & 0 \\ H_{d,2,0} & H_{d,2,1} & \dots & 0 \\ \dots & \dots & \dots & \dots \\ H_{d,N,0} & H_{d,N,1} & \dots & H_{d,N,N-1} \end{bmatrix}}_{\Gamma_d} \underbrace{\begin{bmatrix} d_0 \\ d_1 \\ \dots \\ d_{N-1} \end{bmatrix}}_{D} \end{aligned} \tag{3.14}$$

Output vector predictions (3.13) can be rewritten in a shorter form:

$$y_k = O_k x_0 + \sum_{i=0}^{k-1} H_{u,k,i} u_i + \sum_{i=0}^{k-1} H_{d,k,i} d_i \tag{3.15}$$

Here O_k is the extended observability matrix:

$$O_k = C_k \left(\prod_{i=0}^{k-1} A_i \right) \tag{3.16}$$

Here H_u and H_d are the Markov parameters with respect to manipulated variable and measured disturbance:

$$H_{u,k,i} = C_k \left(\prod_{j=k-1}^{i+1} A_j \right) B_i \tag{3.17a}$$

$$H_{d,k,i} = C_k \left(\prod_{j=k-1}^{i+1} A_j \right) E_i \tag{3.17b}$$

The predicted output vector Y is calculated using (3.15):

$$Y = \Phi x_0 + \Gamma_u U + \Gamma_d D \tag{3.18}$$

see equation (3.14) for detailed structures of matrices Φ, Γ_u, and Γ_d.

The input constraints are:

$$U_{min} \leq U \leq U_{max} \tag{3.19}$$

The output constraints are:

$$Y_{min} - V \leq Y \leq Y_{max} + V \tag{3.20}$$

Using (3.18), (3.20) can be rewritten as:

$$Y_{min} - V \leq \Phi x_0 + \Gamma_u U + \Gamma_d D \leq Y_{max} + V \tag{3.21a}$$

$$\Gamma_u U - V \leq Y_{max} - \Phi x_0 - \Gamma_d D \tag{3.21b}$$

$$-\Gamma_u U - V \leq -Y_{min} + \Phi x_0 + \Gamma_d D \tag{3.21c}$$

Finally, the parameters of linear optimization problem (3.11) can be found as follows:

$$x = \begin{bmatrix} U \\ V \end{bmatrix} \tag{3.22a}$$

$$f = \begin{bmatrix} C \\ P \end{bmatrix} \tag{3.22b}$$

$$A_{ineq} = \begin{bmatrix} \Gamma_u & -I \\ -\Gamma_u & -I \\ 0 & -I \end{bmatrix} \tag{3.22c}$$

$$b_{ineq} = \begin{bmatrix} Y_{max} - \Phi x_0 - \Gamma_d D \\ -Y_{min} + \Phi x_0 + \Gamma_d D \\ 0 \end{bmatrix} \tag{3.22d}$$

$$x_{min} = \begin{bmatrix} U_{min} \\ -\infty \end{bmatrix} \tag{3.22e}$$

$$x_{max} = \begin{bmatrix} U_{max} \\ +\infty \end{bmatrix} \tag{3.22f}$$

In this section the E-MPC based on an LPV model and its transformation into an LP optimization problem is presented. Note that in some systems, including the swimming pool heating system considered in Section 3.1, the manipulated variables can only have two states (”OFF”/”ON”). The proposed technique can still be applied for E-MPC design by adding the following constrain: $U \in \{0, 1\}$. Then (3.11) becomes a Mixed-Integer Linear Program (MILP) optimization problem.

3.3 Simulation results

This section contains simulation results that verify the proposed E-MPC based on the LPV model. The control strategy is able to take into account the influence of the environmental conditions (wind speed and ambient temperature) on the swimming pool water mass thermodynamics. Also the occupancy status is taken into account by adjusting the temperature constraints: when the swimming pool is not used, the minimum swimming pool temperature is lowered (16 $°C$) in order to reduce the energy consumption; when the swimming pool is occupied, the minimum swimming pool temperature is equal to comfort temperature (22 $°C$). Since the controller has information about the occupancy status, it can start heating the swimming pool in advance; therefore, when the swimming pool is assumed to be occupied, its temperature is already comfortable.

Table 3.2: Simulation parameters for swimming pool heating system

	Value	Units	
V_p	27	m^3	pool volume
A_p	18	m^2	pool area
P_{nom}	1	kW	nominal electric power of the heat pump
COP	5		Coefficient of Performance at $20°C$
t_s	1	$hour$	controller sampling time
t	216	$hours$	simulation time
N	48	$hours$	predictive horizon
ρ_v	10^4		softening constraints coefficient

Table 3.2 contains simulation and system parameters: t_s is the sampling time, t is the simulation time.

Figure 3.3 demonstrates the obtained simulation results. The figure consists of three parts: the first part contains water temperature of the swimming pool and the minimum comfort constraint; the second part contains normalized price signal and the optimal profile of heat pump state; the third part contains weather forecast (outdoor temperature T_{amb} and wind speed v_w).

The first graph demonstrates that the system consumes the least amount of energy possible: the controlled temperature is kept as close as possible to the lower limit, thus the main objective of the optimal control strategy is met. The slight violation of the comfort constraint (at 55 hours of simulation time) is due to slow heating dynamics: the controller started heating 48 hours (predictive horizon) in advance, but the heating system couldn't provide enough power (the heating system was in ON state all the time until the lower temperature limit change).

The second graph demonstrates that the system operates in economic regime, which also corresponds to the main objective of the control strategy. The heating system is ON, which means that it consumes electrical energy, during the periods of time with lowest electricity prices.

The third graph contains information about weather conditions that have significant impact on the swimming pool heating dynamics as described earlier.

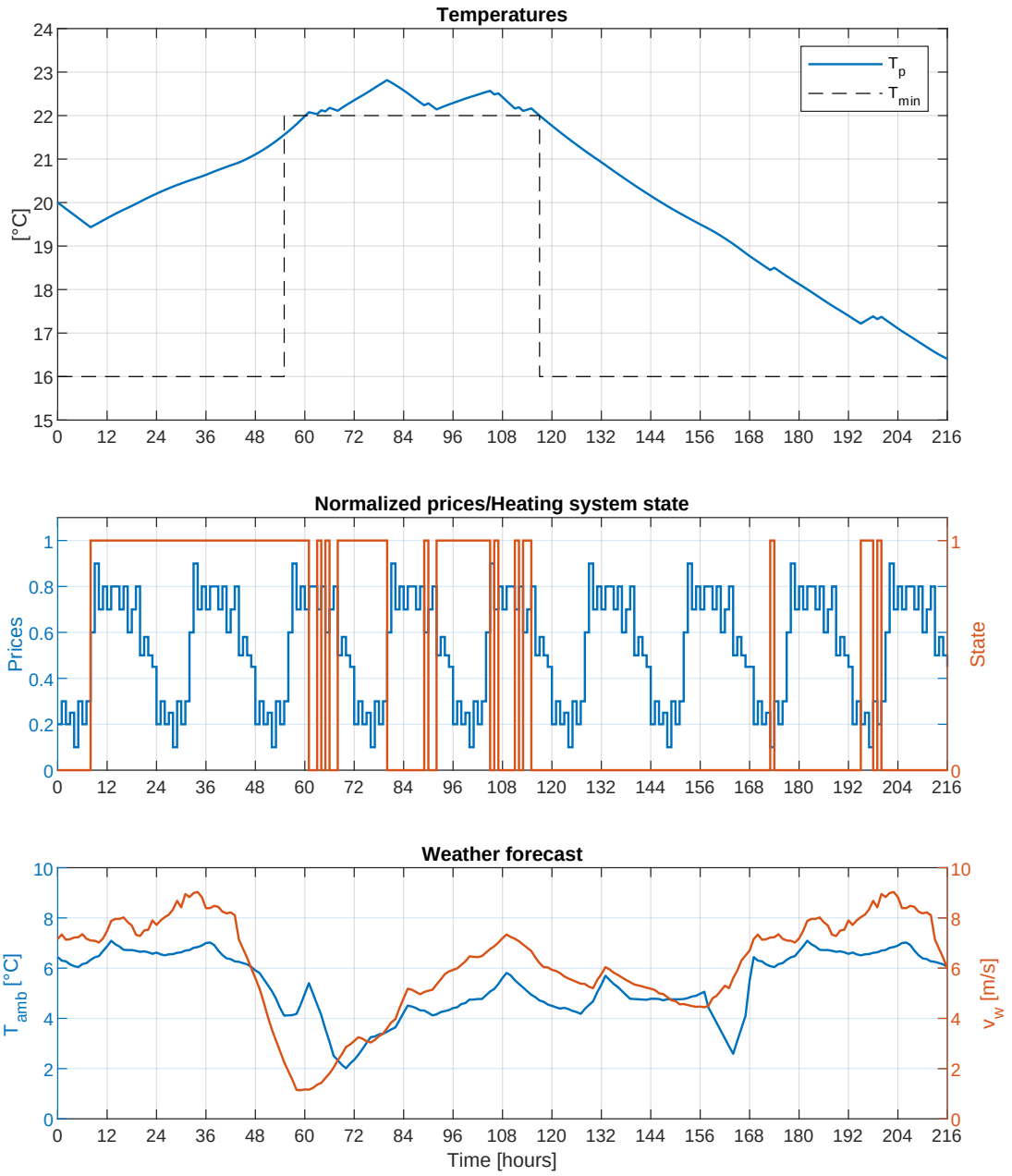

Figure 3.3: Simulation results: swimming pool heating system

4 Simulation model of TCLs population

As discussed previously, one of the main objectives of the thesis is to develop an economically optimal control system for a population of Thermostatically Controlled Loads (TCLs) in energy system with variable and predictable electricity price. The simulation model is developed to verify the control system and control algorithm. The main requirement for the simulation model is to provide accurate and realistic dynamics of the population, which is achieved by simulating each unit individually. A population of electrical space heaters is considered as a case study.

This chapter is organized as follows. The first section describes the model of an individual electrical space heater based on a modified model presented in Subsection 1.5.1. The second section describe the simulation model of the whole population. The third section presents simulation results and analyze the influence of the population parameters on the demand response.

4.1 Model of an individual system with an electrical space heater

An electrical space heater is a Thermostatically Controlled Load (TCL) with hysteresis control law: the load is turned ON when the controlled temperature is below the lower hysteresis boundary and turned OFF when the controlled temperature is above the higher hysteresis boundary. When turned ON, the unit consumes electrical power, whereas in OFF state the consumption is equal to zero.

It is assumed that the temperature setpoint can be externally changed in order to conform with the control system. This feature provides an interface for the higher level E-MPC to indirectly influence the state of the unit.

The resulting model is a modified model presented in Subsection 1.5.1:

$$\frac{dT(t)}{dt} = -\frac{1}{CR}[T(t) - T_{amb}(t) - m(t)RP], \tag{4.1a}$$

$$m(t^+) = \begin{cases} 0 & \textbf{if} \quad T \geq T_{sp} + \Delta T_{sp} + H \\ 1 & \textbf{if} \quad T \leq T_{sp} + \Delta T_{sp} - H \\ m(t) & \textbf{otherwise} \end{cases} \tag{4.1b}$$

Here, T is the temperature controlled by the TCL $[°C]$; C is the thermal capacitance $[kWh/°C]$ and R the is thermal resistance $[°C/kW]$ of the heated area (e.g. room); P is the electrical power $[kW]$; T_{amb} is the ambient temperature $[°C]$; $m \in \{0, 1\}$ is the state of the TCL (OFF anf ON respectively); T_{sp} is the temperature setpoint $[°C]$; ΔT_{sp} is the temperature setpoint change $[°C]$; H is the hysteresis band of the thermostat $[°C]$.

Separated T_{sp} and ΔT_{sp} signals allow to have a single manipulated variable (ΔT_{sp}) to control all the units in the population, whereas each unit can have an individual T_{sp} specified by the customer.

4.2 Model of population of electrical space heaters

The simulation model provides demand response of the whole population to the temperature setpoint change (ΔT_{sp}) and the ambient temperature (T_{amb}). The population consist of n heating systems with electrical space heaters, each unit of the population is described by an individual set of parameters $\theta_i = [C_i,\ R_i,\ P_i,\ T_{sp,i},\ H,\ T_{0,i},\ m_{0,i}]$ and simulated according to (4.1). Therefore the model is highly accurate, but the complexity of the model depends on the number of units in the population, that is why this model is not suitable for model based control system design.

Figure 4.1 contains the corresponding Simulink model. The wide lines are vectors of size equal to the number of units in the population. All blocks perform element-wise operations, thus elements with particular index are the signals corresponding to the particular unit from the population with the same index. Such structure of the model provides possibility to simulate a population of any size.

The "Thermostats" block applies equation (4.1b) for each element of T, the vector of the temperatures controlled by the population units, and generates m, the vector of the states of the population units. This block also generates state vector X, which is used in control algorithm and described further in the thesis.

The thermal capacitances (C_i), the thermal resistances (R_i), and the electrical powers (P_i) of units are log-normally distributed with the corresponding means

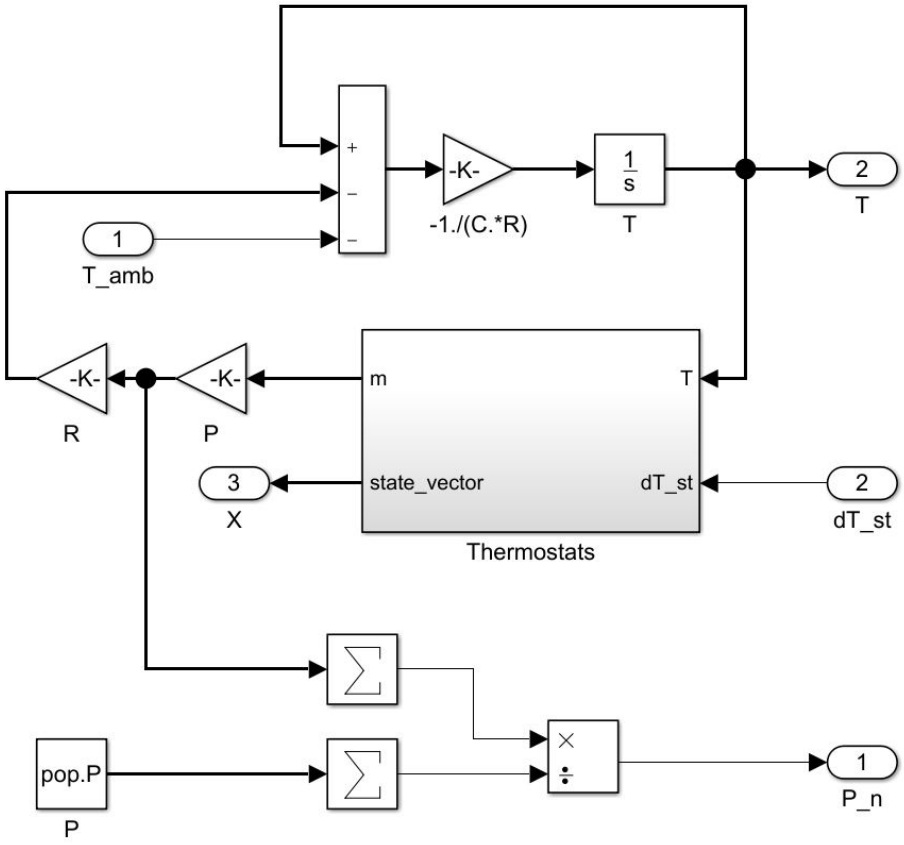

Figure 4.1: Simulink model of TCLs population

(C_m, R_m, and P_m) and relative standard deviation (σ_{rel}). Log-normal distribution guaranties that these parameters never take negative value, which corresponds to the realistic scenario. It is shown in [97] that the type of distribution doesn't have a significant impact on the demand response.

The hysteresis band of the thermostats (H) is the same for all units; the temperature setpoints ($T_{sp,i}$) are evenly distributed within $[T_{low} + H,\ T_{up} - H]$, here $[T_{low},\ T_{up}]$ corresponds to the working temperature range of the population; the initial temperatures ($T_{0,i}$) are randomly chosen from $[T_{sp,i} - H,\ T_{sp,i} + H]$.

The output of the model, the aggregate normalized demand of the whole population, is given by the following ratio:

$$P_n(t) = \frac{\sum_1^n m_i(t) P_i}{\sum_1^n P_i} \tag{4.2}$$

The initial state of the TCLs ($m_{0,i}$) are chosen taking into account the duty cycles of the loads: the probability of each unit to be turned "ON" in the beginning

of simulation is equal to its duty cycle D_i. Thus the output of the model in the beginning of simulation is equal to the steady state electrical power of the population (P_{st}):

$$P_{st} = \frac{\sum_1^n D_i P_i}{\sum_1^n P_i} \tag{4.3}$$

Here, D is the duty cycle of the TCL and calculated as follows:

$$D_i = \frac{t_{on,i}}{t_{on,i} + t_{off,i}} \tag{4.4a}$$

$$t_{on,i} = -R_i C_i \ln\left(\frac{T_{sp,i} - H - T_{amb} - P_i R_i}{T_{sp,i} + H - T_{amb} - P_i R_i}\right) \tag{4.4b}$$

$$t_{off,i} = -R_i C_i \ln\left(\frac{T_{sp,i} + H - T_{amb}}{T_{sp,i} - H - T_{amb}}\right) \tag{4.4c}$$

Equations (4.4b) and (4.4c) are derived in [74].

4.3 Simulation results

This section presents analysis of the influence of temperature setpoint change on electricity consumption of a single unit and the population of TCLs. Additionally, the influence of the heterogeneity level on the electricity consumption is presented.

Table 4.1 contains values of the population parameters used for simulation and derived from typical building stock in the Czech Republic [98]. The ambient temperature (T_{amb}) is constant.

Table 4.1: Population parameters

Par.	Value	Units	Description
R_m	3.4	$°C/kW$	mean thermal resistance of the TCLs
C_m	7	$kWh/°C$	mean thermal capacitance of the TCLs
P_m	13.4	kW	mean electrical power of the TCLs
σ_{rel}	0.05 - 0.5		relative standard deviation
H	0.5	$°C$	hysteresis band of the thermostat
T_{low}	20	$°C$	lower boundary of the working temp. range
T_{up}	24	$°C$	upper boundary of the working temp. range
T_{amb}	-5	$°C$	ambient temperature

Figure 4.2 contains simulation results for the case of a single unit ($n = 1$). Evolution of the temperature controlled by the TCL (T) is a periodic process. The normalized electrical power of the population (P_n) basically demonstrates whether the load is ON or OFF. Changing the temperature setpoint (T_{sp}) indirectly influence the state of the TCL (m): it can either extend/shorten the current state (shift the load cycle) or force immediate change of the state (reverse the load cycle). In the figure, increasing the temperature setpoint change (ΔT_{sp}) leads to extending the ON state and decreasing the temperature setpoint change (ΔT_{sp}) leads to changing the ON state to the OFF state. Similarly, decreasing the temperature setpoint change (ΔT_{sp}) when the unit is OFF will lead to extending the OFF state; increasing the temperature setpoint change (ΔT_{sp}) when the unit is ON will lead to shortening or changing the ON state.

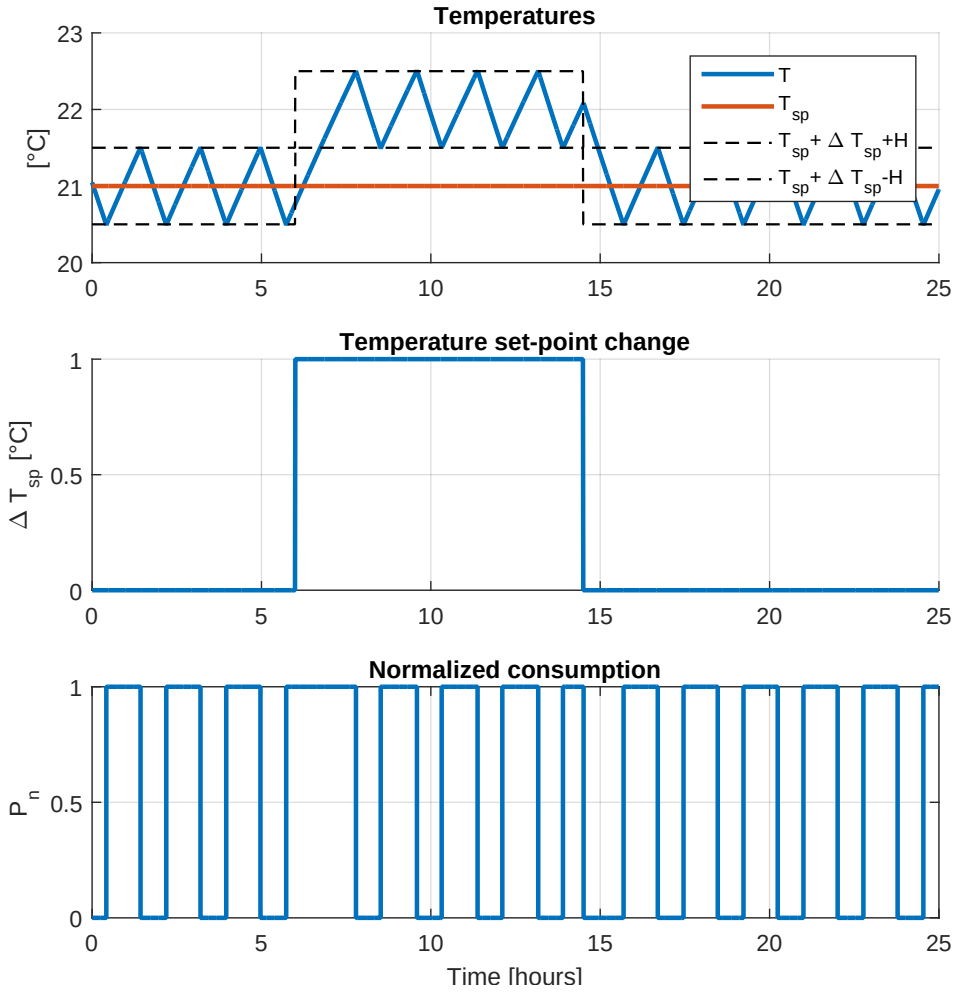

Figure 4.2: Single unit: temperature setpoint change test

Figure 4.3 contains simulation results for the case of a relatively large population of TCLs (n = 10 000). The population can either be balanced (constant consumption) or imbalanced (changing consumption). When the population is balanced the temperature controlled by the TCLs ($T_{,i}$) are distributed such that ratio between ON and OFF units is a constant. This is possible due to heterogeneity of the population and relatively high number of units. Increasing/decreasing the temperature setpoint change (ΔT_{sp}) leads to changing the ON/OFF cycles of the units as described above: at 5-th hour of the simulation time some of the units immediately changed their state from OFF to ON, consequently the consumption immediately increased; the following oscillations can be explained by the fact that the ON/OFF cycles of the units shifted. The opposite situation occurred at 15-th hour: the consumption immediately decreased due to decrease of the temperature setpoint change (ΔT_{sp}).

Figures 4.3 - 4.6 demonstrate that the dynamics of demand response to the temperature setpoint change (ΔT_{sp}) significantly depends on the relative standard deviation (σ_{rel}), which represents the level of heterogeneity of the population. Lower σ_{rel} corresponds to lower variability of the parameters and therefore leads to more oscillatory transitions: the units with smaller deviation of the parameters are more synchronized. In the extreme case (when all the units are identical) the population will behave similar to the case of a single unit (Figure 4.2). Higher σ_{rel} corresponds to higher variability of the parameters, the population with higher σ_{rel} lose coherence faster, therefore leads to less oscillatory and faster transitions.

Figure 4.7 demonstrates that the dynamics of demand response is non-linear. The experiment is similar to Figure 4.5, but the temperature setpoint change (ΔT_{sp}) is two times higher. When ΔT_{sp} is high enough (more or equal to the hysteresis band of the thermostats (H)) all units turn ON (or OFF in case of decreasing ΔT_{sp}) and remain in this state for some time (depending on value of ΔT_{sp}).

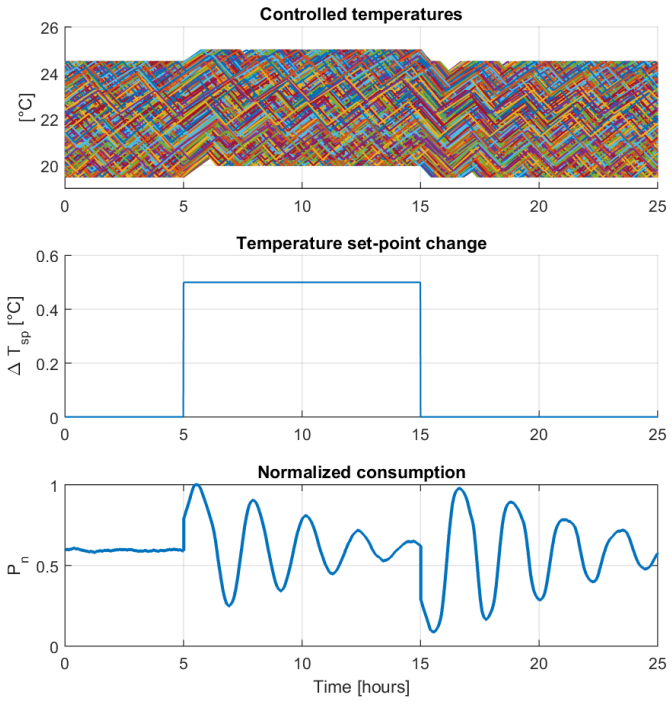

Figure 4.3: Population: temperature setpoint change test, $\sigma_{rel} = 0.05$

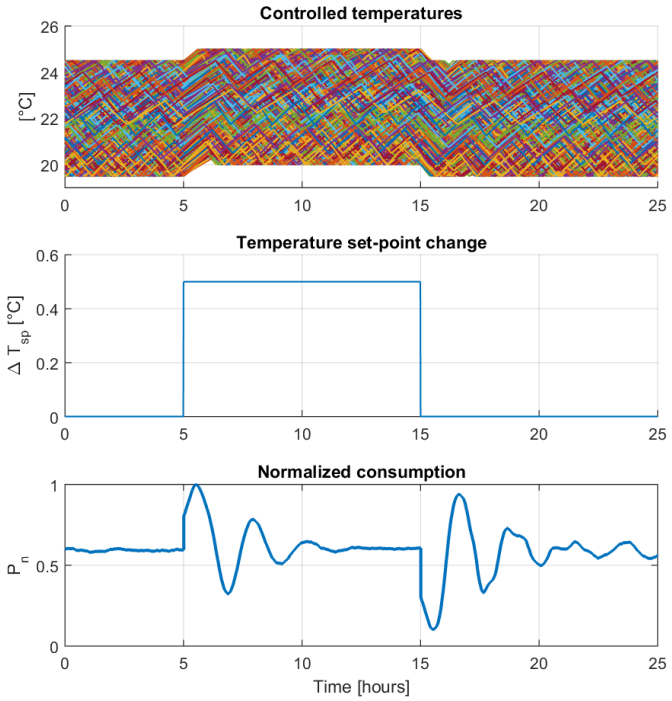

Figure 4.4: Population: temperature setpoint change test, $\sigma_{rel} = 0.1$

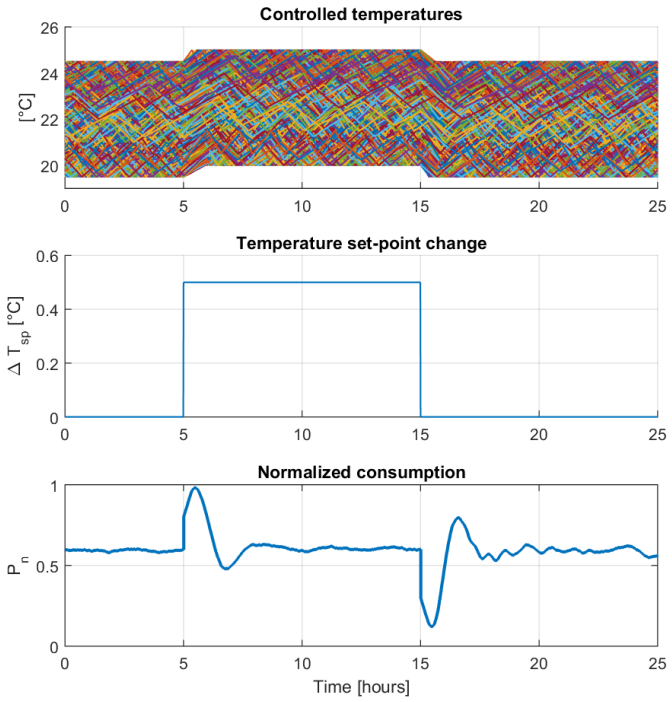

Figure 4.5: Population: temperature setpoint change test, $\sigma_{rel} = 0.2$

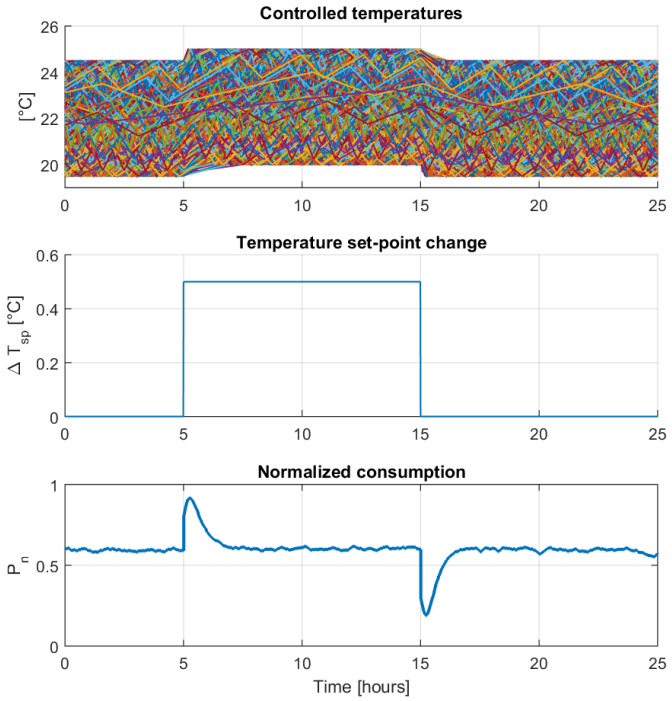

Figure 4.6: Population: temperature setpoint change test, $\sigma_{rel} = 0.5$

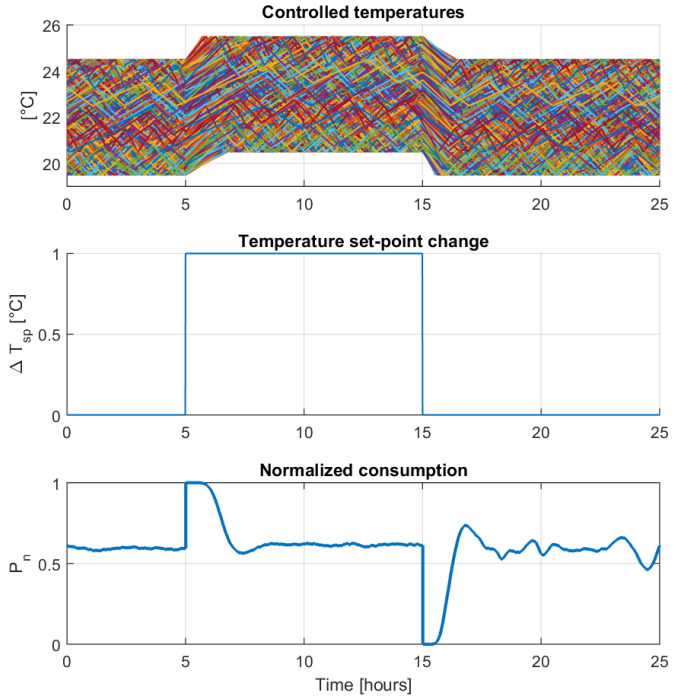

Figure 4.7: Population: temperature setpoint change test, $\sigma_{rel} = 0.2$

5 Aggregate model of the population

The simulation model presented in Chapter 4 is computationally too intensive to be utilized for model-based control of a large population of TCLs. As discussed in Subsection 1.5.3, the existing aggregate models cannot provide relatively accurate demand response of the population of TCLs to a temperature setpoint change.

The aggregate model presented in this chapter is based on the bin state transition model presented in [85, 86, 99]. The original model describes evolution of the units states and implies direct control of the population: the input signal of the model allows to manipulate the loads states; such approach have some disadvantages discussed in Subsection 1.3.1.

The proposed aggregate model is a non-linear modification of the bin state transition model which allows to control the population by changing the temperature setpoint (indirectly influencing the load states).

This chapter is organized as follows. The first section contains description of bin state transition model. The second section introduces the non-linear modification of bin state transition model for homogeneous population. The third section extends the modified model to heterogeneous population applying clustering technique. The forth section contains simulation results demonstrating that the model can accurately capture the demand response of a population of TCLs and robust to the level of heterogeneity.

5.1 Bin state transition model

The original bin state transition model is used for approximating demand response of a large population of TCLs assuming that their states can be directly controlled. In the original formulation it is assumed that the population is homogeneous: the loads are defined by identical set of parameters $\theta = [C,\ R,\ P,\ T_{sp},\ H]$. The operating temperature range $[T_{low}\ T_{up}]$ is evenly divided into $2N_{bin}$ state bins, see Figure 5.1.

The idea of the model is to describe distribution and natural transition of the unis over these bins. Each bin is characterized by the corresponding state, temperature range, and transitions rate to the next bin. The solid lines demonstrate transition of the unis under normal operational conditions: when the loads are turned OFF the controlled temperature decreases and vice versa; when the controlled temperature reaches one of the temperature limits $[T_{low}\ T_{up}]$ the corresponding loads change their state according to the hysteresis control law. Direct manipulation of the loads states is shown by the dashed lines. More detailed description of bin state transition model can be found in [85, 86, 99].

Although Sanandaji et al. claim in [85] that the non-uniform structure provides better prediction and better deals with heterogeneity, however the proposed modification requires conformity between ON and OFF bins, therefore the uniform structure is considered.

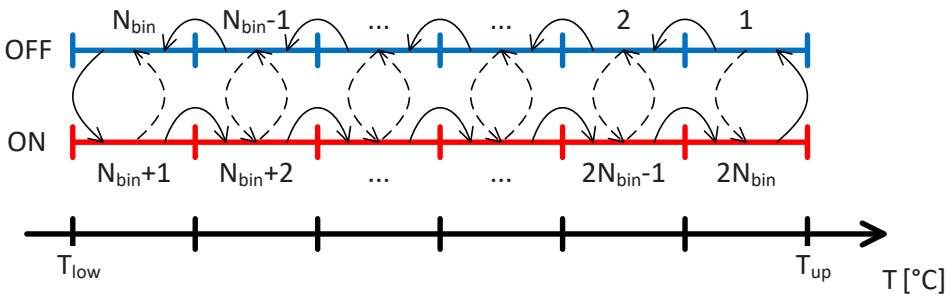

Figure 5.1: Uniform bin state transition model

The model is given in state-space form as:

$$\dot{x}(t) = A_{bin}x(t) + B_{bin}u(t) \tag{5.1a}$$

$$y(t) = C_{bin}x(t) \tag{5.1b}$$

Here $A_{bin} \in \mathbb{R}^{2N_{bin}\times 2N_{bin}}$ is the state matrix of the bin state transition model, $B_{bin} \in \mathbb{R}^{2N_{bin}\times 2N_{bin}}$ is the control matrix of the bin state transition model, $C_{bin} \in \mathbb{R}^{1\times 2N_{bin}}$ is the output matrix of the bin state transition model, $x \in \mathbb{R}^{2N_{bin}\times 1}$ is the state vector of the bin state transition model, $u \in \mathbb{R}^{1\times 2N_{bin}}$ is the manipulated variable of the bin state transition model, y is the output of the bin state transition model, which is normalized power consumption of the population. The following

derivation of the state matrices structures and parameters is presented in [85] in greater details.

The state vector x defines the current distribution of the population over the bins:

$$x = \begin{bmatrix} n_{OFF,1} \\ n_{OFF,2} \\ n_{OFF,3} \\ \dots \\ n_{OFF,N_{bin}} \\ n_{ON,N_{bin}+1} \\ \dots \\ n_{ON,2N_{bin}} \end{bmatrix} \tag{5.2}$$

Here, $n_{OFF/ON,i}$ is the number of the OFF or ON units respectively belonging to the i-th bin, $i \in [1...2N_{bin}]$.

The state matrix A_{bin} defines transition of the units over the bins and has the following structure:

$$A_{bin} = \begin{bmatrix} -r_1 & 0 & & \cdots & & 0 & r_{2N_{bin}} \\ r_1 & \ddots & \ddots & & \cdots & & 0 \\ 0 & \ddots & -r_{N_{bin}-1} & 0 & & & \\ & \ddots & r_{N_{bin}-1} & -r_{N_{bin}} & 0 & & \vdots \\ \vdots & & 0 & r_{N_{bin}} & -r_{N_{bin}+1} & \ddots & \\ & & & \ddots & \ddots & \ddots & 0 \\ 0 & & \cdots & & 0 & r_{2N_{bin}-1} & -r_{2N_{bin}} \end{bmatrix} \tag{5.3}$$

The matrix consists of the transition rates r_i which are the inverse of the times t_i it takes for a unit defined by the set of parameters θ to cool/heat the controlled temperature within the corresponding (i-th) bin temperature range. In other words, the time it takes for the units to transfer from the i-th bin to the $i+1$ bin.

$$r_i = \frac{1}{t_i} \tag{5.4}$$

The times for the **OFF-bins** ($i \in [1...N_{bin}]$) are calculated as:

$$t_i = -RC\ln\left(\frac{T_{i,up} - T_{amb}}{T_{i,low} - T_{amb}}\right) \tag{5.5a}$$

$$T_{i,low} = T_{up} - (i-1)\Delta T_{bin} \tag{5.5b}$$

$$T_{i,up} = T_{up} - i \cdot \Delta T_{bin} \tag{5.5c}$$

The times for the **ON-bins** ($i \in [N_{bin}+1 \; ... \; 2N_{bin}]$) are calculated as:

$$t_i = -RC\ln\left(\frac{T_{i,low} - T_{amb} - PR}{T_{i,up} - T_{amb} - PR}\right) \tag{5.6a}$$

$$T_{i,low} = T_{low} - (i - N_{bin} - 1)\Delta T_{bin} \tag{5.6b}$$

$$T_{i,up} = T_{low} - (i - N_{bin})\Delta T_{bin} \tag{5.6c}$$

Here, $[T_{i,low} \; T_{i,up}]$ defines the temperature range of the i-th bin, T_{amb} is the ambient temperature, ΔT_{bin} is the temperature range corresponding to one bin:

$$\Delta T_{bin} = \frac{T_{up} - T_{low}}{N_{bin}} \tag{5.7}$$

The control vector u has a similar to the state vector structure:

$$u = \begin{bmatrix} u_{OFF,1} \\ u_{OFF,2} \\ u_{OFF,3} \\ ... \\ u_{OFF,N_{bin}} \\ u_{ON,N_{bin}+1} \\ ... \\ u_{ON,2N_{bin}} \end{bmatrix} \tag{5.8}$$

Here, $u_{OFF/ON,i}$ is the number of OFF/ON units considered for manipulation.

The control matrix B_{bin} contains the fraction of the units belonging to one bin that are transported to the corresponding bin (with the same temperature range) of the opposite state as shown in Figure 5.1 by the dashed lines and has the following structure:

$$B_{bin} = \begin{bmatrix} -1 & 0 & \cdots & 0 & 0 & \cdots & 0 & 1 \\ 0 & -1 & \cdots & 0 & 0 & \cdots & 1 & 0 \\ \vdots & \vdots & \ddots & & & & \vdots & \vdots \\ 0 & 0 & & -1 & 1 & & 0 & 0 \\ 0 & 0 & & 1 & -1 & & 0 & 0 \\ \vdots & \vdots & & & & \ddots & \vdots & \vdots \\ 0 & 1 & \cdots & 0 & 0 & \cdots & -1 & 0 \\ 1 & 0 & \cdots & 0 & 0 & \cdots & 0 & -1 \end{bmatrix} \tag{5.9}$$

The output matrix C_{bin} is defined as follows:

$$C_{bin} = \frac{1}{n}\left[\underbrace{0\;0\;...\;0}_{N_{bin}}\;\underbrace{1\;1\;...\;1}_{N_{bin}}\right] \tag{5.10}$$

5.2 Homogeneous model

The proposed non-linear modification of bin state transition model, unlike the standard approach, approximates the demand response of the population to temperature set-point change. The advantages of controlling the setpoint rather than loads states were discussed earlier in this work. Firstly the homogeneous model is developed, then it is extended to heterogeneous model.

The aggregate homogeneous model implies extended operating temperature range which does not only include the dead-band of the units (defined by the hysteresis width), but also some low- and high-temperature margins as shown in Figure 5.2. This modification allows to influence the units states indirectly, by changing the temperature setpoint. Note that the temperature axis is shifted by T_{sp} in order to demonstrate the influence of the setpoint change on the model structure. Consequently, the operating range of the modified model defines the acceptable temperature setpoint change. Note that the results with non-linear aggregate model were published in 2018 an presented in [100].

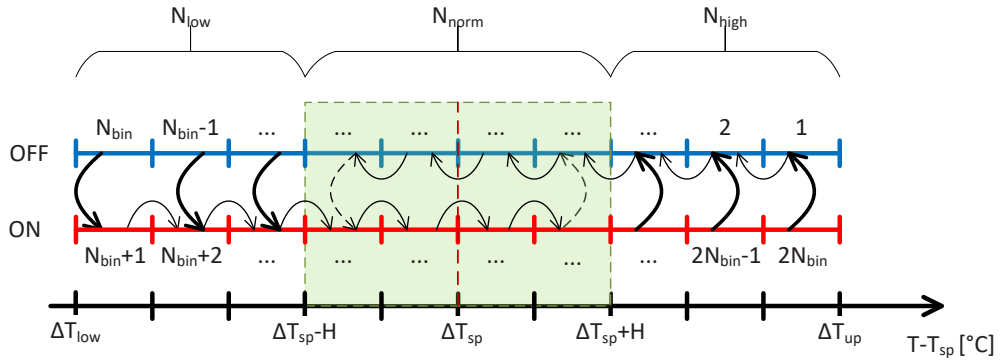

Figure 5.2: Homogeneous aggregate model

The operating range $[\Delta T_{low},\ \Delta T_{up}]$ is divided into three parts: low, normal, and high temperatures. The normal temperature range $[\Delta T_{sp} - H,\ \Delta T_{sp} + H]$ (marked by green colour) contains N_{norm} OFF and N_{norm} ON bins. The units corresponding to these bins behave according to the original bin state transition model: the solid thin lines correspond to heating or cooling process depending on the units states according to (4.1a), the dashed thin lines correspond to changing the state when a unit reachs one of the hysteresis boundaries according to (4.1b).

The low temperature range $[\Delta T_{low},\ \Delta T_{sp} - H]$ contains N_{low} OFF and N_{low} ON bins. The units corresponding to the low OFF bins behave differently: they should immediately change their states which means to be transferred to the corresponding ON bins (shown by thick solid lines). Such situation occurs after the setpoint has been increased and some heaters are instantly switched ON by the thermostats with accordance to (4.1b).

The high temperature range $[\Delta T_{sp} + H,\ T_{low}]$ contains N_{high} OFF and N_{high} ON bins and implies the opposite situation: the temperature setpoint has been decreased and some heaters are instantly switched OFF.

Homogeneous model (5.11) is given in a state-space form, however, the state matrix A_{hom} is no longer static: its structure depends on the temperature setpoint change. In addition the model takes into account the ambient temperature according to equations (5.5) and (5.6). The control matrix B_{bin} and manipulated variable u are omitted because the model does not impliy direct manipulation of the units states.

$$\dot{x}(t) = A_{hom}(\Delta T_{sp}(t), T_{amb}(t))x(t) \tag{5.11a}$$

$$y(t) = C_{bin}x(t) \tag{5.11b}$$

The modification introduces a new transition rate called forced switching rate (shown by the thick solid lines), which is the same for all bins and should meet the following requirement:

$$r_{sw} \gg \max(r_i),\ i \in [1...2N_{bin}] \tag{5.12}$$

Structure of the state matrix depends on the number of bins in the low and high temperature ranges. Elements corresponding to the **natural transition** (thin solid lines, $i \in [1\ ...\ N_{high} + N_{norm} - 1,\ N_{bin} + 1\ ...\ N_{bin} + N_{low} + N_{norm}]$):

$$A_{hom,i,i} = -r_i \tag{5.13a}$$

$$A_{hom,i+1,i} = r_i \tag{5.13b}$$

Switching (thin dashed lines, $i \in \{N_{high} + N_{norm},\ N_{bin} + N_{low} + N_{norm}\}$:

$$A_{hom,i,i} = -r_i \tag{5.14a}$$

$$A_{hom,2N_{bin}+1-i,i} = r_i \tag{5.14b}$$

Forced switching (thick solid lines, $i \in [N_{high} + N_{norm} + 1 \ ... \ N_{bin}, \ N_{bin} + N_{low} + N_{norm} + 1 \ ... \ 2N_{bin}]$:

$$A_{hom,i,i} = -r_{sw} \tag{5.15a}$$

$$A_{hom,2N_{bin}+1-i,i} = r_{sw} \tag{5.15b}$$

The number of bins corresponding to the normal temperature ($2N_{norm}$) range does not depend on the temperature setpoint change:

$$N_{norm} = \frac{2H}{\Delta T_{bin}} \tag{5.16}$$

Whereas the number of bins corresponding to the low/high temperature ranges ($2N_{low}$ and $2N_{high}$ respectively) depends on the temperature setpoint change:

$$N_{low} = \frac{\Delta T_{low} - \Delta T_{sp} + H}{N_{bin}} \tag{5.17a}$$

$$N_{high} = \frac{\Delta T_{sp} + H - \Delta T_{up}}{N_{bin}} \tag{5.17b}$$

5.3 Heterogeneous model

In real population there are no identical units, each of them is defined by the unique set of parameters $\theta^{(i)}$, $i \in [1...n]$. The heterogeneous model deals with this variation of the parameters applying the k-means clustering method [55, 66, 101]. The population of n units is divided into into n_c clusters, each cluster is associated with the corresponding set of parameters θ_i and the number of units belonging to this cluster n_i, such that $n = \text{sum}(n_i)$, $i \in [1...n_c]$.

The heterogeneous model is a combination of n_c homogeneous models defined in the previous section:

$$\dot{X}(t) = A(\Delta T_{sp}(t), T_{amb}(t))X(t) \tag{5.18a}$$

$$Y(t) = C_{agg}X(t) \tag{5.18b}$$

Here, $A \in \mathbb{R}^{2n_cN_{bin} \times 2n_cN_{bin}}$ is the state matrix of the aggregate model, $C_{aggi} \in \mathbb{R}^{1 \times 2n_cN_{bin}}$ is the output matrix of the aggregate model, $X_i \in \mathbb{R}^{2n_cN_{bin} \times 1}$ is the state vector of the aggregate model, Y_i is the output of the aggregate model, which is approximation of the normalized aggregate response of the heterogeneous population (4.2).

The state vector X is given as:

$$X = \begin{bmatrix} x_1 \\ x_2 \\ \cdots \\ x_{n_c} \end{bmatrix} \tag{5.19}$$

The state matrix A is given as:

$$A = \begin{bmatrix} A_{hom,1} & 0_{2N_{bin}} & \cdots & 0_{2N_{bin}} \\ 0_{2N_{bin}} & A_{hom,2} & \cdots & 0_{2N_{bin}} \\ \cdots & \cdots & \cdots & \cdots \\ 0_{2N_{bin}} & 0_{2N_{bin}} & \cdots & A_{hom,n_c} \end{bmatrix} \tag{5.20}$$

The output matrix C_{agg} weighs the outputs of the homogeneous models in order to normalize the output of the aggregate model to the maximum power consumption:

$$C_{agg} = \begin{bmatrix} w_1 C_{bin,1} & w_2 C_{bin,2} & \cdots & w_{n_c} C_{bin,n_c} \end{bmatrix} \tag{5.21}$$

$$w_i = \sum_{j \in \text{cluster } i} P_j / \sum_{j \in 1}^{n} P_j \tag{5.22}$$

Here, $A_{hom,i}$, x_i, and $C_{bin,i}$ are the corresponding to the i-th cluster parameters of homogeneous model, w_i is the weight of the output of the homogeneous model of the i-th cluster, $0_{2N_{bin}}$ is the zero matrix of the corresponding dimension, $\text{sum}(x_i) = n_i$, $i \in [1...n_c]$.

5.4 Simulation results

In this section the performance of the aggregate model (agg) presented in Section 5.3 was compared to the simulation model (sim) presented in Section 4.2. Additionally, the influence of the model parameters (N_{bin} and n_c) and the population heterogeneity defined by the relative standard deviation of the loads parameters (σ_{rel}) on the approximation quality was studied.

The population consists of n electrical space heaters; the parameters are log-normally distributed with the corresponding means C_m, R_m, P_m and standard deviation σ_{rel}; hysteresis width H_i is the same for all units; temperature setpoints $T_{sp,i}$ and initial values of the controlled temperatures $T_{0,i}$ are evenly distributed over

$[T_{low} + H,\ T_{up} - H]$, $i \in [1...n]$. The temperature setpoint change ΔT_{sp} may vary within $[\Delta T_{low}\ \Delta T_{up}]$, which is related to the customer comfort boundaries. Table 5.1 contains values of these parameters used for simulation (typical building stock in the Czech Republic [98]), the parameters are the same as in Chapter 4.

Table 5.1: Simulation parameters for aggregate model verification

Par.	Value	Units	Description
R_m	3.4	°C/kW	Mean thermal resistance
C_m	7	kWh/°C	Mean thermal capacitance
P_m	13.4	kW	Mean thermal power
σ_{rel}	0.05 - 0.5		Relative standard deviation
H	0.5	°C	Hysteresis width
T_{low}	19.5	°C	Lower limit of the working temp. range
T_{up}	24.5	°C	Upper limit of the working temp. range
ΔT_{low}	-2.5	°C	Lower limit on temp. setpoint change
ΔT_{up}	2.5	°C	Upper limit on temp. setpoint change
n	10000		Number of units in the population

The first results demonstrate that the aggregate model is able to deal with heterogeneity. The test scenario is following: at 1 hour all units are instructed to increase the temperature setpoint by 0.5°C ($\Delta T_{sp} = 0.5$). The test was repeated for different values of σ_{rel}. Figures 5.3-5.6 contain the obtained simulation results. Since the complexity of the model depends significantly on the number of clusters (n_c) and the number of bins (N_{bin}), these values were chosen as a trade-off between complexity and accuracy of the aggregate model. Note, that higher variance of the population parameters or higher σ_{rel} requires higher number of clusters and less sensitive to the number of bins and vice versa.

The second results present the influence of the number of clusters and the number of bins on the aggregate model performance using the same test scenario. Figures 5.7 and 5.8 contain the corresponding results and demonstrate that the both parameters affect the accuracy: increasing any of these parameters leads to better approximation of the demand response.

The third results show how the aggregate model captures the demand response to a sequence of setpoint changes. This is the most important property of the model that is used for model-based control system design. Figure 5.9 contains the obtained

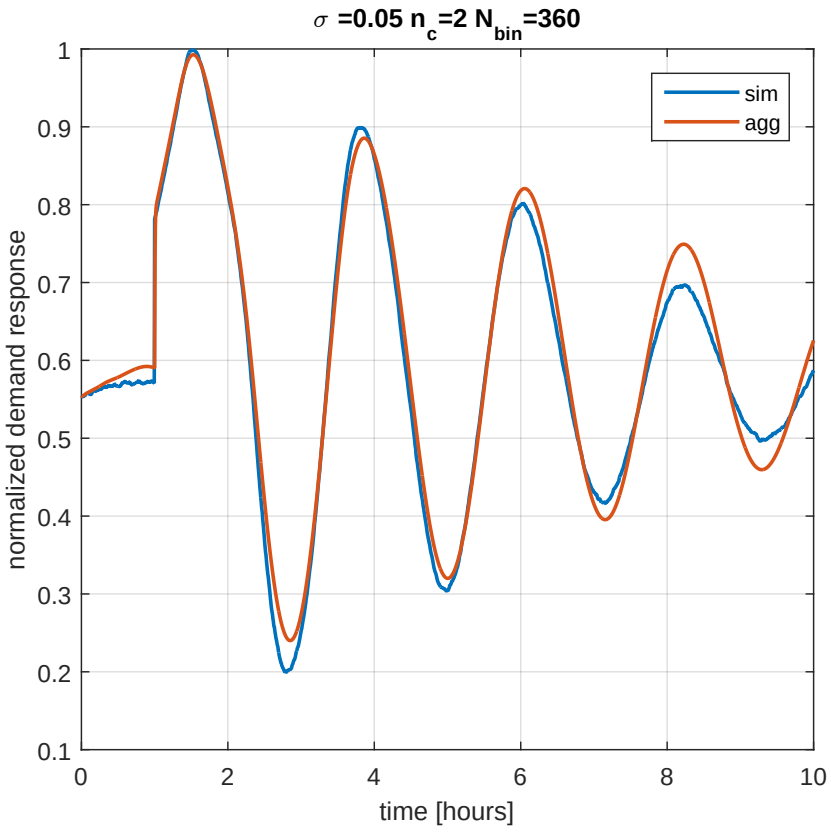

Figure 5.3: Simulation results: $\sigma_{rel} = 0.05$, $n_c = 2$, $N_{bin} = 360$

simulation results. $n_c = 4$ and $N_{bin} = 80$ is the empirically found trade-off between the complexity and the accuracy of the model.

In the last, it is shown how the aggregate model reflects the ambient temperature change. This property allows us to take into account weather forecast in model-based control system design. Figure 5.10 contains the obtained simulation results.

The complexity of the model depends on the number of bins (N_{bin}), which is also mentioned in other works, e.g. [65]. Nevertheless, the further results demonstrate that for this particular problem it is possible to form a mixed integer optimization problem and solve it in real time.

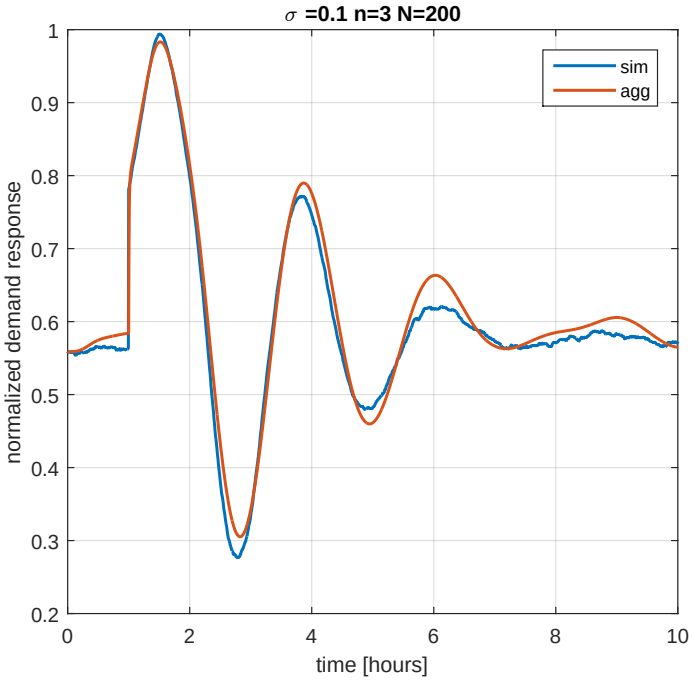

Figure 5.4: Simulation results: $\sigma_{rel} = 0.1$, $n_c = 3$, $N_{bin} = 200$

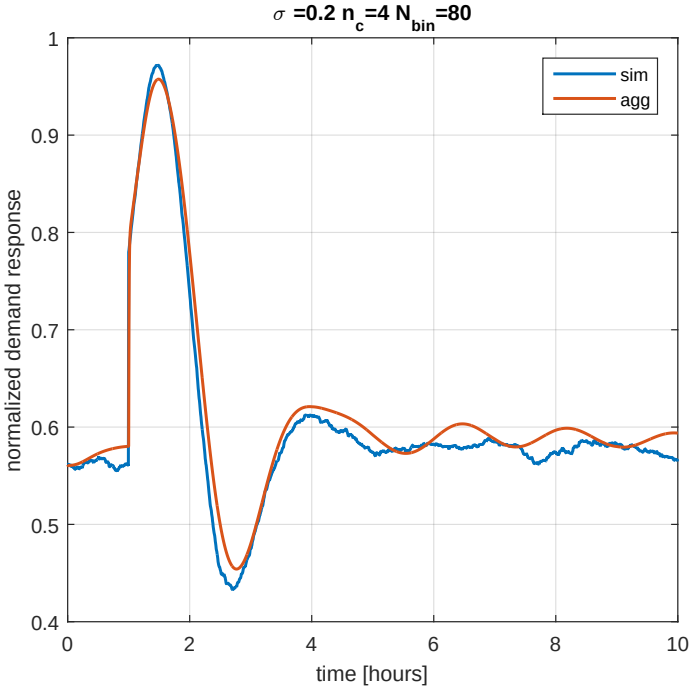

Figure 5.5: Simulation results: $\sigma_{rel} = 0.2$, $n_c = 4$, $N_{bin} = 80$

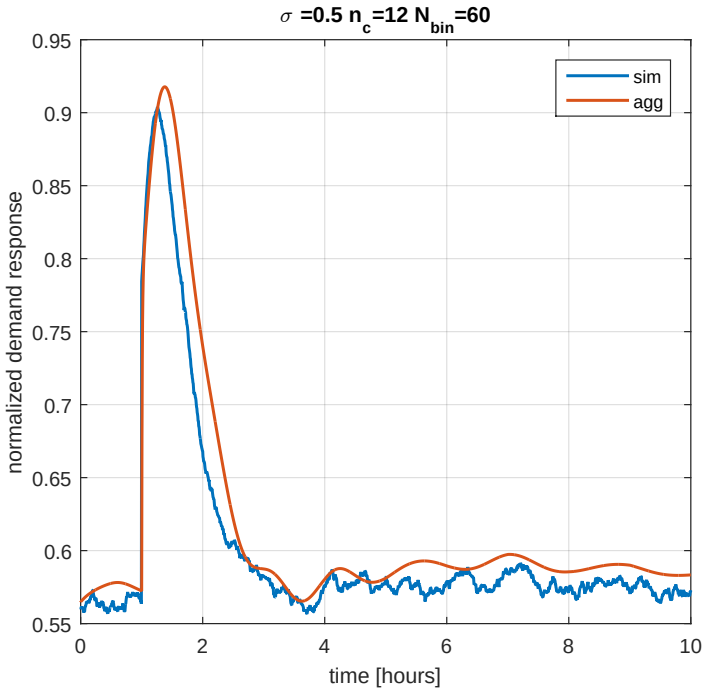

Figure 5.6: Simulation results: $\sigma_{rel} = 0.5$, $n_c = 12$, $N_{bin} = 60$

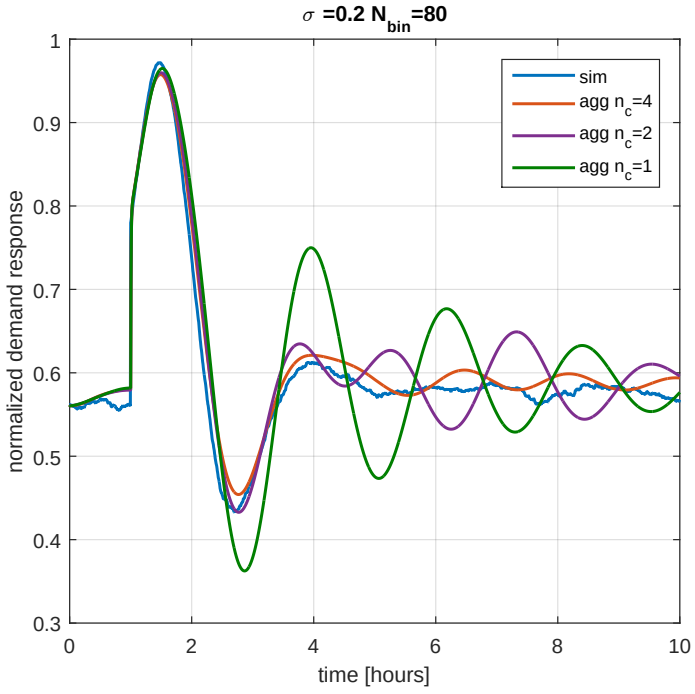

Figure 5.7: Simulation results: influence of n_c

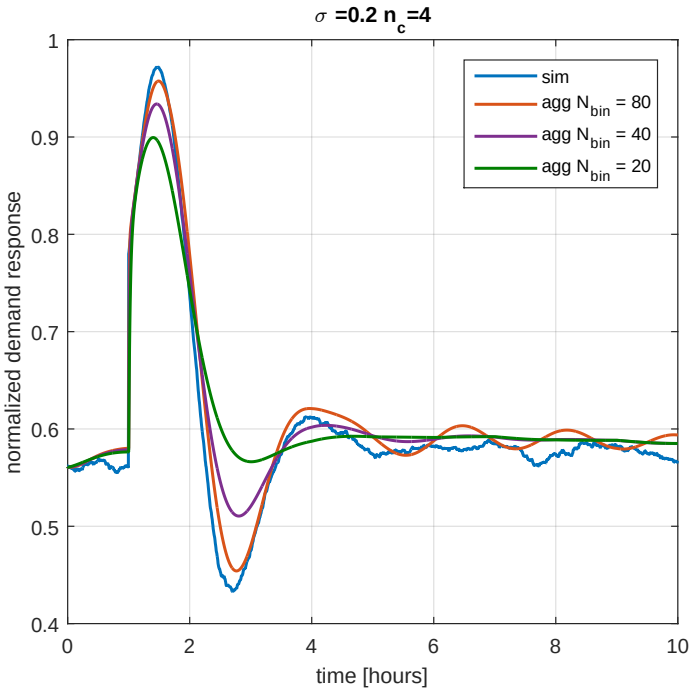

Figure 5.8: Simulation results: influence of N_{bin}

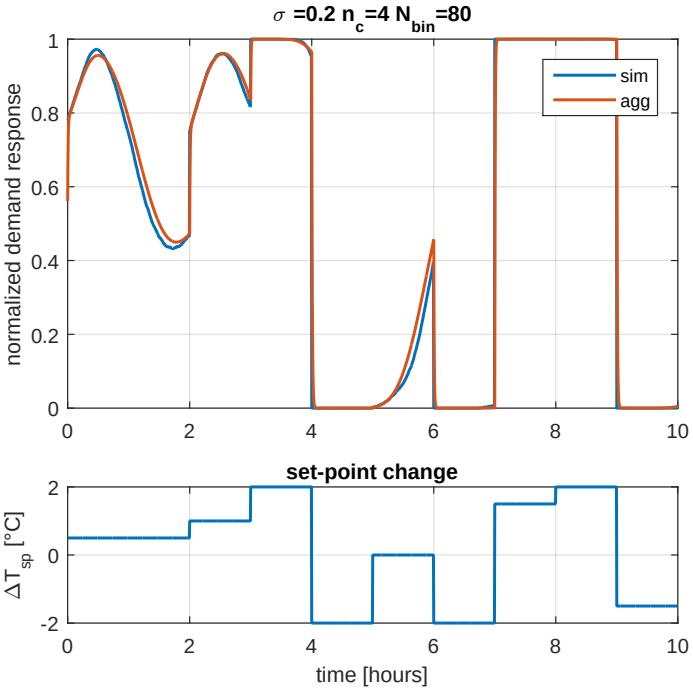

Figure 5.9: Approximated response to the sequence of setpoint changes

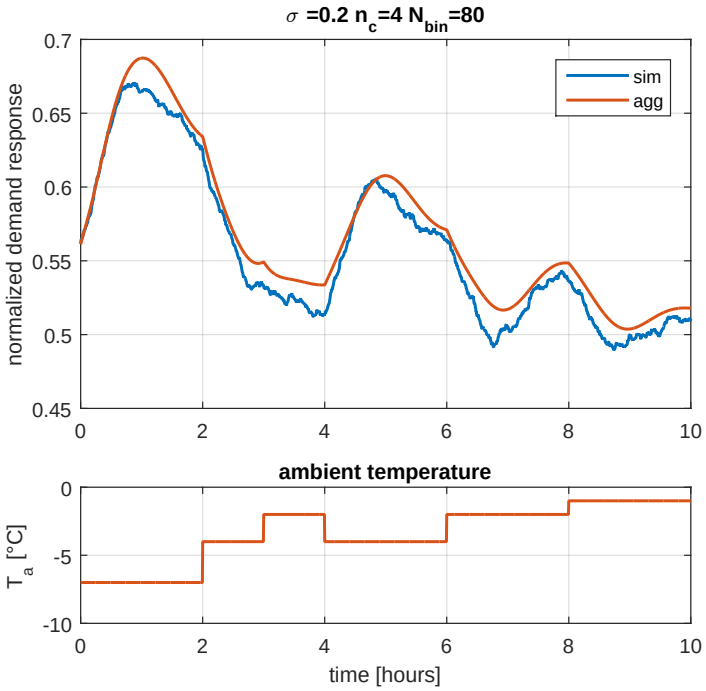

Figure 5.10: Approximated response to the sequence of ambient temperatures

6 E-NMPC for the population of TCLs

This chapter develops a price-responsive control strategy for the population of TCLs using the aggregate model developed in Chapter 5. Figure 6.1 contains structure of the control system. The controller design is based on the idea of E-NMPC [53, 102, 103]. It is assumed that electricity price regularly changes and the electricity price forecast is available at least one day ahead. The main objective of the controller is to minimize operational cost of the whole population by shifting the electricity consumption of the population to the low-price periods.

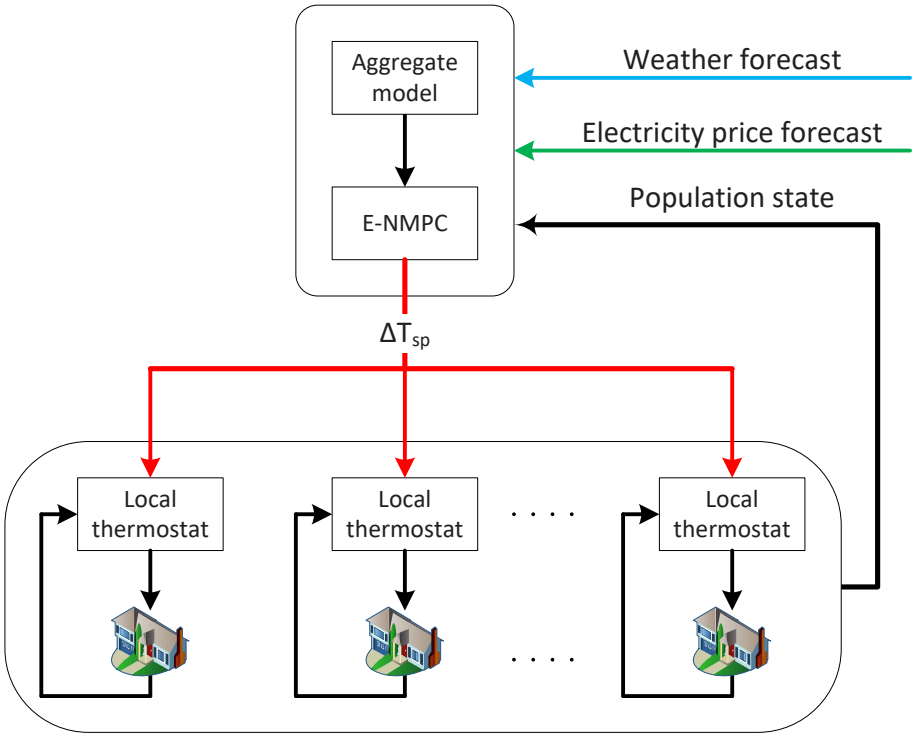

Figure 6.1: E-NMPC control system structure

The TCLs ON/OFF states (which are directly linked to the electrical energy consumption) are manipulated indirectly by changing temperature setpoints of the units. The optimal temperature setpoint change signal generated by the controller is constrained taking into account the customers comfort boundaries. Information about the population (current values of the controlled temperature, the units states, and total electrical power consumption) is used as a feedback signal.

This chapter is organized as follows. The first section formulates the optimal control problem. The second section presents the numerical algorithm for solving the control problem in real time. The third section contains the simulation results demonstrating the economical benefits of applying the proposed control system.

Note that the results presented in this chapter were published in 2018 and presented in [100].

6.1 Optimal control problem formulation

The control problem (6.1) is formulated as a constrained continuous-time optimization problem, because the developed non-linear aggregate model in Chapter 5 is also presented in continuous-time domain. Moreover, Non-linear Model Predictive Control (NMPC) is often formulated as a continuous-time optimization problem [53, 102, 103].

$$\min_{\Delta T_{sp}} \psi = \int_{t_0}^{t_f} p(t)Y(t)dt \tag{6.1a}$$

$$s.t. \quad \dot{X}(t) = A(\Delta T_{sp}(t), T_{amb}(t))X(t) \tag{6.1b}$$

$$Y(t) = C_{agg}X(t) \tag{6.1c}$$

$$X(t_0) = X_0 \tag{6.1d}$$

$$\Delta T_{low} \leq \Delta T_{sp}(t) \leq \Delta T_{up} \tag{6.1e}$$

$$\frac{T_{sp}(t)}{\Delta T_{bin}} \in \mathbb{Z} \tag{6.1f}$$

$$t \in [t_0\ t_f] \tag{6.1g}$$

Here, t_0 is the current time; t_f is the predictive horizon; p is the normalized electricity price forecast; Y is the predicted normalized electrical consumption by the whole population; ΔT_{low}, ΔT_{up} correspond to the comfort constraints; X_0 is the initial state vector of the aggregate model.

Algorithm 1 Calculation of initial state vector

function CalcStateVector($[T_1, T_2, \cdots, T_n]$, $[m_1, m_2, \cdots, m_n]$, $[\theta_1, \theta_2, \cdots, \theta_{n_c}]$)
  define X_0 **as an empty array**
  for $j = 1 : 1 : n_c$ **do**
    $x_j = 0^{1 \times 2N_{bin}}$
    for $i \in$ cluster j **do**
      $k = \text{GetBinNumber}(\theta_j, T_i, m_i)$ ▷ bin number of the unit
      $x_{j,k} = x_{j,k} + 1$ ▷ k-th entry of x_j
    end for
    $X_0 = \begin{bmatrix} X_0 \\ x_{j,k} \end{bmatrix}$
  end for
  return X_0
end function
function GetBinNum(θ, T, m)
  $k = \text{floor}\left(\frac{T - T_{sp}}{\Delta T_{bin}}\right)$ ▷ round towards zero
  if m = 1 **then**
    k = $2N_{bin}$-1+k
  end if
  return k
end function

Cost function (6.1a) represents predicted normalized operational cost of the population for given ΔT_{sp} profile. Aggregate model described by (6.1b) and (6.1c) is the model defined in Section 5.3 used for calculating the normalized demand predictions.

It is assumed that the controller has information about current controlled temperatures and states of each electrical space heater, thus X_0 can be calculated using Algorithm 1.

The proposed aggregate model implies that the temperature setpoint change can only take a finite number of values defined by (5.7). This limitation also makes sense from practical point of view: usually the temperature setpoint can be changed with a fixed step-size (ΔT_{bin}). This requirement corresponds to condition (6.1f).

6.2 Numerical solution of optimal control problem

6.2.1 Continuous-discrete-time optimal control problem

The solution of optimization problem (6.1) is infinite-dimensional. Therefore, it is needed to be converted into a finite-dimensional continuous-discrete-time problem by approximating the input and disturbance profiles by corresponding piece-wise constant profiles:

$$\Delta T_{sp,k} = \Delta T_{sp}(t)\ t_k \leq t \leq t_{k+1} \tag{6.2a}$$

$$T_{amb,k} = T_{amb}(t)\ t_k \leq t \leq t_{k+1} \tag{6.2b}$$

$$p_k = p(t)\ t_k \leq t \leq t_{k+1} \tag{6.2c}$$

Consequently the resulting continuous-discrete-time optimization problem is given as:

$$\min_{\Delta T_{sp}} \psi = \sum_{k=1}^{N} \int_{t_k}^{t_{k+1}} p_k Y(t) dt \tag{6.3a}$$

$$s.t. \quad \dot{X}_i(t) = A(\Delta T_{sp,k}, T_{amb,k}) X(t) \tag{6.3b}$$

$$Y(t) = C_{agg} X(t) \tag{6.3c}$$

$$X(t_0) = X_0 \tag{6.3d}$$

$$\Delta T_{low} \leq \Delta T_{sp,k} \leq \Delta T_{up} \tag{6.3e}$$

$$\frac{\Delta T_{sp,k}}{\Delta T_{bin}} \in \mathbb{Z} \tag{6.3f}$$

$$t \in [t_0\ t_f] \tag{6.3g}$$

$$k \in [0\ N] \tag{6.3h}$$

The predictive horizon $[t_0\ t_f]$ is divided into N steps with sampling time t_s.

The solution of problem (6.3) is the optimal profile of temperature setpoint changes:

$$u_{opt}(t_0) = [u_0,\ u_1,\ ...,\ u_{N-1}]^T,\ u_{opt}(t_0) \in \mathbb{R}^{N \times 1} \tag{6.4}$$

At each step the first entry of the profile is implemented on the process and kept during the following sampling time.

6.2.2 Adjoint sensitivity computation

Gradient ($\nabla_{\Delta T_{sp}}\psi$) evaluation is necessary to solve optimization problem (6.3). The adjoint method for sensitivity computation is particularly efficient, when number of parameters is large, e.g. predictive and optimal control [52, 104–106].

Control problem (6.3) can be converted into discrete-time optimal control problem in the following form:

$$\min_{u} \psi = \sum_{k=1}^{N} G_k(x_k, u_k) + h(x_N) \tag{6.5a}$$

$$s.t. \quad x_{k+1} = F_k(x_k, u_k) \tag{6.5b}$$

$$u_{min} \leq u_k \leq u_{max} \tag{6.5c}$$

$$k \in [0\ N] \tag{6.5d}$$

Here the manipulated variable is the temperature setpoint change:

$$u_k = \Delta T_{sp,k} \tag{6.6}$$

state vector is the state vector of the aggregate model:

$$x_k = X(t_k) \tag{6.7}$$

G_k and F_k are computed by:

$$G_k(x_k, u_k) = \left\{ \int_{t_k}^{t_{k+1}} g(x(t), u_k)dt : \dot{x} = f(x(t), u_k), x(t_k) = x_k \right\} \tag{6.8a}$$

$$F_k(x_k, u_k) = x_k + \int_{t_k}^{t_{k+1}} f(x(t), u_k)dt \tag{6.8b}$$

$$F_k(x_k, u_k) = \{x_{k+1} = x(t_{k+1} : \dot{x} = f(x(t), u_k), x(t_k) = x_k\} \tag{6.8c}$$

Here $g(x(t), u_k)$ and $f(x(t), u_k)$ represent the cost function (6.3a) and aggregate model (6.3b) respectively:

$$g(X(t), \Delta T_{sp,k}) = p_k C_{agg} X(t) \tag{6.9a}$$

$$f(X(t), \Delta T_{sp,k}) = A(\Delta T_{sp,k}, T_{amb,k})X(t) \tag{6.9b}$$

$$h(x_N) = 0 \tag{6.9c}$$

Computation of ($\nabla_{\Delta T_{sp}}\psi$) requires the following gradients: $\frac{\partial F_k}{\partial x_k}$, $\frac{\partial F_k}{\partial u_k}$, $\frac{\partial G_k}{\partial x_k}$, and $\frac{\partial G_k}{\partial u_k}$. The sensitivities equations of (6.3a)-(6.3d):

$$\dot{S}_{x_k}(t) = \frac{\partial f}{\partial x}(x(t), u_k)S_{x_k}(t) \qquad S_{x_k}(t_k) = I \tag{6.10a}$$

$$\dot{S}_{u_k}(t) = \frac{\partial f}{\partial x}(x(t), u_k)S_{u_k}(t) + \frac{\partial f}{\partial u}(x(t), u_k) \qquad S_{u_k}(t_k) = 0 \tag{6.10b}$$

Algorithm 2 Gradient computation

```
function CompGrad(x_0, {u_k}_{k=0}^{N-1})
    for k = 0 : 1 : N − 1 do
        compute x_{k+1} = F_k(x_k, u_k), G_k(x_k, u_k), and {A_k, B_k, q_k, r_k}
    end for
    for k = N − 1 : −1 : 1 do
        ∇_{u_k} ψ = r_k + B_k λ_{k+1}
        λ_k = q_k + A_k λ_{k+1}
    end for
    ∇_{u_0} ψ = r_0 + B_0 λ_1
    return ∇_u ψ;
end function
```

with $S_{x_k}(t) = \left\{ \frac{\partial x}{\partial x_k}(t) : x(t_k) = x_k \right\}$ and $S_{u_k}(t) = \left\{ \frac{\partial x}{\partial u_k}(t) : x(t_k) = x_k \right\}$ can be used to calculate these gradients:

$$A_k = \frac{\partial F_k}{\partial x_k}(x_k, u_k) = S_{x_k}(t_{k+1}) \tag{6.11a}$$

$$B_k = \frac{\partial F_k}{\partial u_k}(x_k, u_k) = S_{u_k}(t_{k+1}) \tag{6.11b}$$

$$q_k^T = \frac{\partial G_k}{\partial x_k}(x_k, u_k) = \int_{t_k}^{t_{k+1}} \frac{\partial g}{\partial x}(x(t), u_k) S_{x_k}(t) dt \tag{6.11c}$$

$$r_k^T = \frac{\partial G_k}{\partial u_k}(x_k, u_k) = \int_{t_k}^{t_{k+1}} \frac{\partial g}{\partial x}(x(t), u_k) S_{u_k}(t) + \frac{\partial g}{\partial u}(x(t), u_k) dt \tag{6.11d}$$

Gradient ($\nabla_u \psi$) can be computed using Algorithm 2. Note that for computation of $F_k(x_k, u_k)$, $G_k(x_k, u_k)$, and $\{A_k,\ B_k,\ q_k,\ r_k\}$ some numerical method, e.g. forward Euler method, should be used.

6.2.3 Solver of the optimization problem

The solver for the mixed integer non-linear optimization problem (6.3) presented in this section takes into account some physical limitations of the units of the population. For instance, it ensures that the provided solution is a set of feasible setpoints.

The solver is based on the gradient descent method (see Algorithm 3). It uses the current distribution of the heaters over the state bins (x_0) and the optimal manipulated variables defined at the previous step ($u_{opt}(t_{-1}),\ t_{-1} = t_0 - t_s$) as an

Algorithm 3 Solver

1: **function** SolveMINLP(x_0, $u_{opt}(t_{-1})$)
2: **define** $u_{opt}(t_0)$
3: **repeat**
4: **calculate** $\nabla_{u_{opt}(t_0)}\psi$
5: $\nabla_{u_{opt}(t_0),norm}\psi = \left(\frac{\nabla_{u_{opt}(t_0)}\psi}{\max(\text{abs}(\nabla_{u_{opt}(t_0)}\psi))}\right)$
6: $\Delta u = -\text{round}\left(\nabla_{u_{opt}(t_0),norm}\psi\right)\Delta T_{bin}$
7: $\Delta u(u_{opt}(t_0) + \Delta u < u_{min}) = 0$
8: $\Delta u(u_{opt}(t_0) + \Delta u > u_{max}) = 0$
9: $u_{opt}(t_0) = u_{opt}(t_0) + \Delta u$
10: **until** $\text{sum}(\Delta u)! = 0$
11: **return** $u_{opt}(t_0)$;
12: **end function**

initial guess (line 2). The previous solution contains initial guess for all elements of the current solution except the last one, which is replaced by 0.

Calculation of the gradient (line 4) is presented in Section 6.2.2.

The descent direction (lines 5, 6) is a normalized to the maximum gradient multiplied by the minimum temperature setpoint change (ΔT_{bin}).

The constraints are taken into account such that if the following changing the manipulated variable leads to violating the constraints (lines 7 and 8); the step size for this particular element is set equal to 0.

The algorithm stops (line 10) when all entries of Δu are equal to 0. It means that further minimization requires reducing the step size (ΔT_{bin}), which is not supported by the algorithm (it may lead to unimplementable solution), or that the solution has reached the constraints.

6.3 Simulation results

Two different scenarios were simulated in order to verify the aggregate model and E-NMPC algorithm. First, 24 hours scenario was simulated: the algorithm aims to minimize the operational cost of the whole population for the given electricity price and ambient temperature profiles. The same parameters of the population (Table 5.1) were used as in Chapter 5. Table 6.1 contains parameters of the aggregate model and the controller. Figure 6.2 contains the obtained simulation results: higher

Table 6.1: Aggregate model and controller parameters

Par.	Value	Units	Description
σ_{rel}	0.2		Relative standard deviation
ΔT_{low}	-2	°C	Lower limit on temperature setpoint change
ΔT_{up}	2	°C	Upper limit on temperature setpoint change
n_c	4		Number of clusters
N_{bin}	80		Number of bins
t_s	1	hour	Sampling time of the controller
N	12		Predictive horizon
ΔT_{bin}	0.5	°C	Minimum increment of setpoint change

electricity price corresponds to the lower energy consumption and vice versa; the setpoint change tends to the lower limit which corresponds to the economically optimal operating regime. Moreover, the algorithm overheats the population during low-price periods in order to reduce the consumption during high-price periods.

Secondly, two energy saving strategies and zero temperature setpoint change strategy ($\Delta T_{sp} = 0$, which basically means that there is no external influence on the population) were compared in order to demonstrate the performance of the designed E-NMPC control system. The first strategy is the smart energy saving (smart) which implies that the optimal temperature setpoint change is provided by the E-NMPC. The second is the thrifty energy saving (thrifty) which implies that the temperature setpoint change is set equal to the lower limit ($\Delta T_{sp} = \Delta T_{low}$). This strategy demands less power to perform the temperature control compared to the zero temperature setpoint change strategy, however it doesn't take into account the price and weather forecasts as well as the population dynamics unlike the smart strategy.

Figures 6.3-6.6 contain the comparison results for different ΔT_{low} and ΔT_{up}: the normalized operational cost of the smart and thrifty strategies are always less than the operational cost of the zero temperature setpoint change strategy. Moreover, after sometime the operational cost of the smart strategy is always less than the operational cost of the thrifty strategy. Whereas the temperature deviation of the smart strategy is closer to zero which means that the customer comfort is less compromised.

There are two main factors influencing the reduction of the population oper-

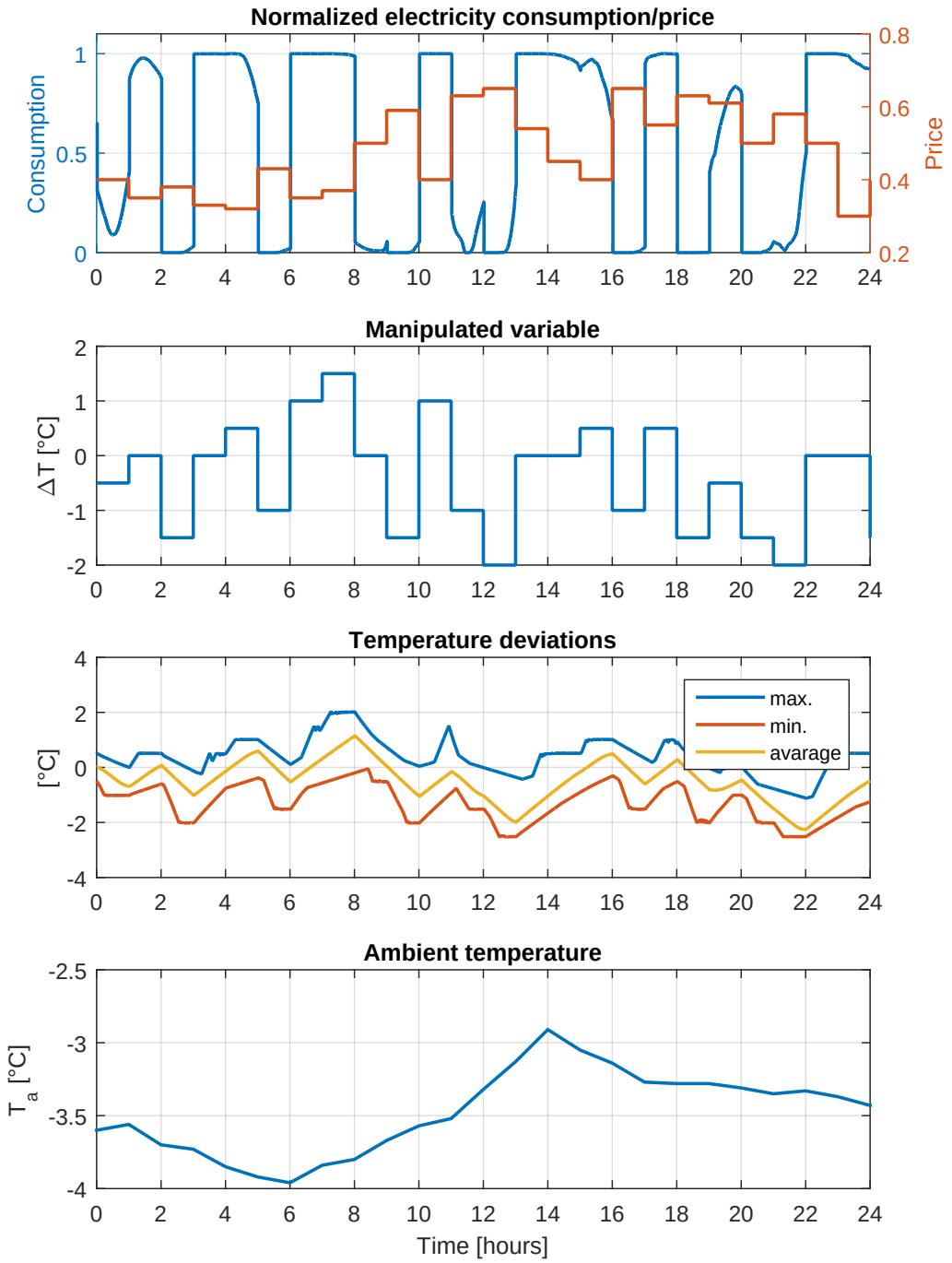

Figure 6.2: Simulation results: performance test

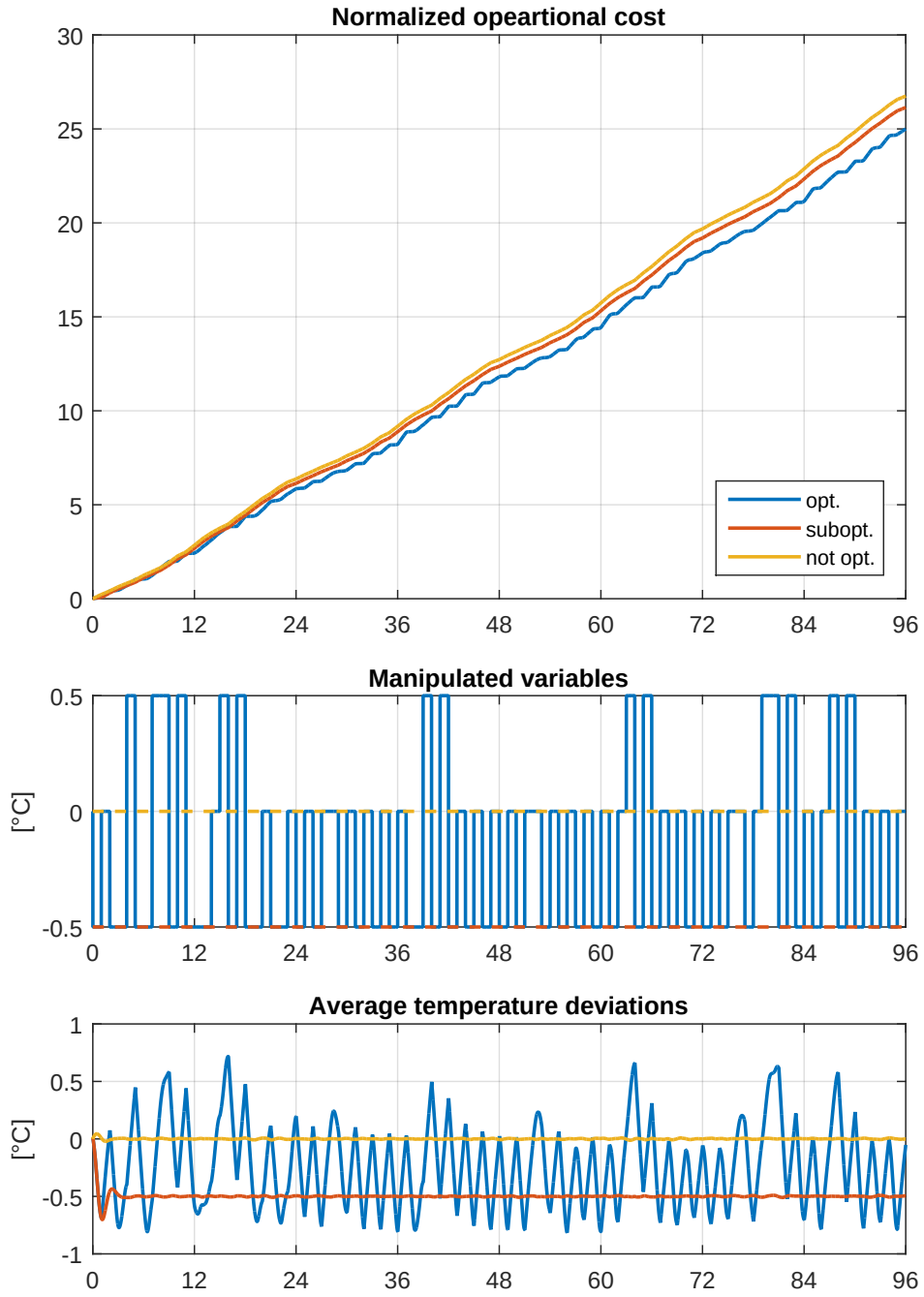

Figure 6.3: Comparison of the energy saving strategies: $\Delta T_{low} = -0.5,\ \Delta T_{up} = 0.5$

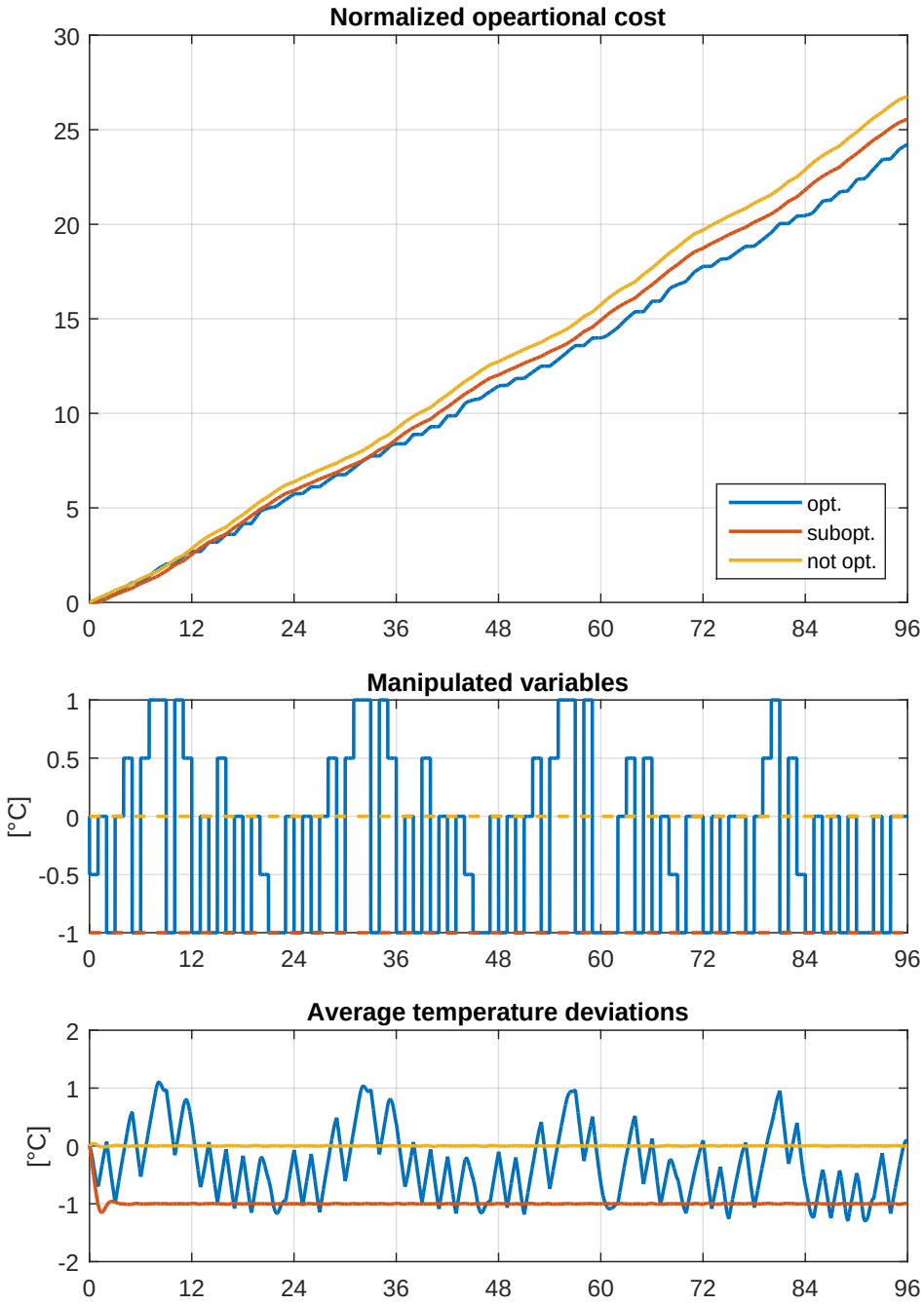

Figure 6.4: Comparison of the energy saving strategies: $\Delta T_{low} = -1,\ \Delta T_{up} = 1$

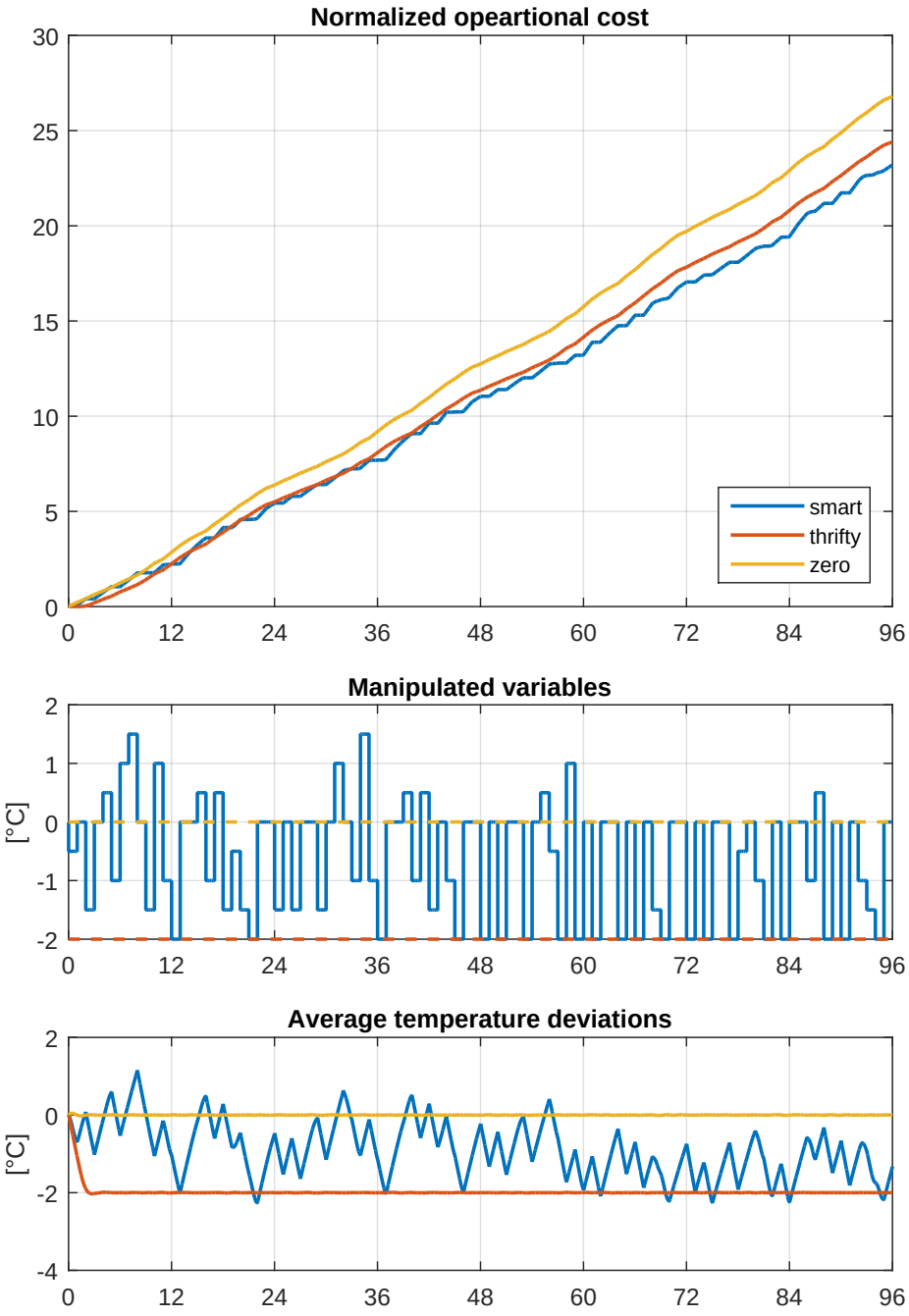

Figure 6.5: Comparison of the energy saving strategies: $\Delta T_{low} = -2,\ \Delta T_{up} = 2$

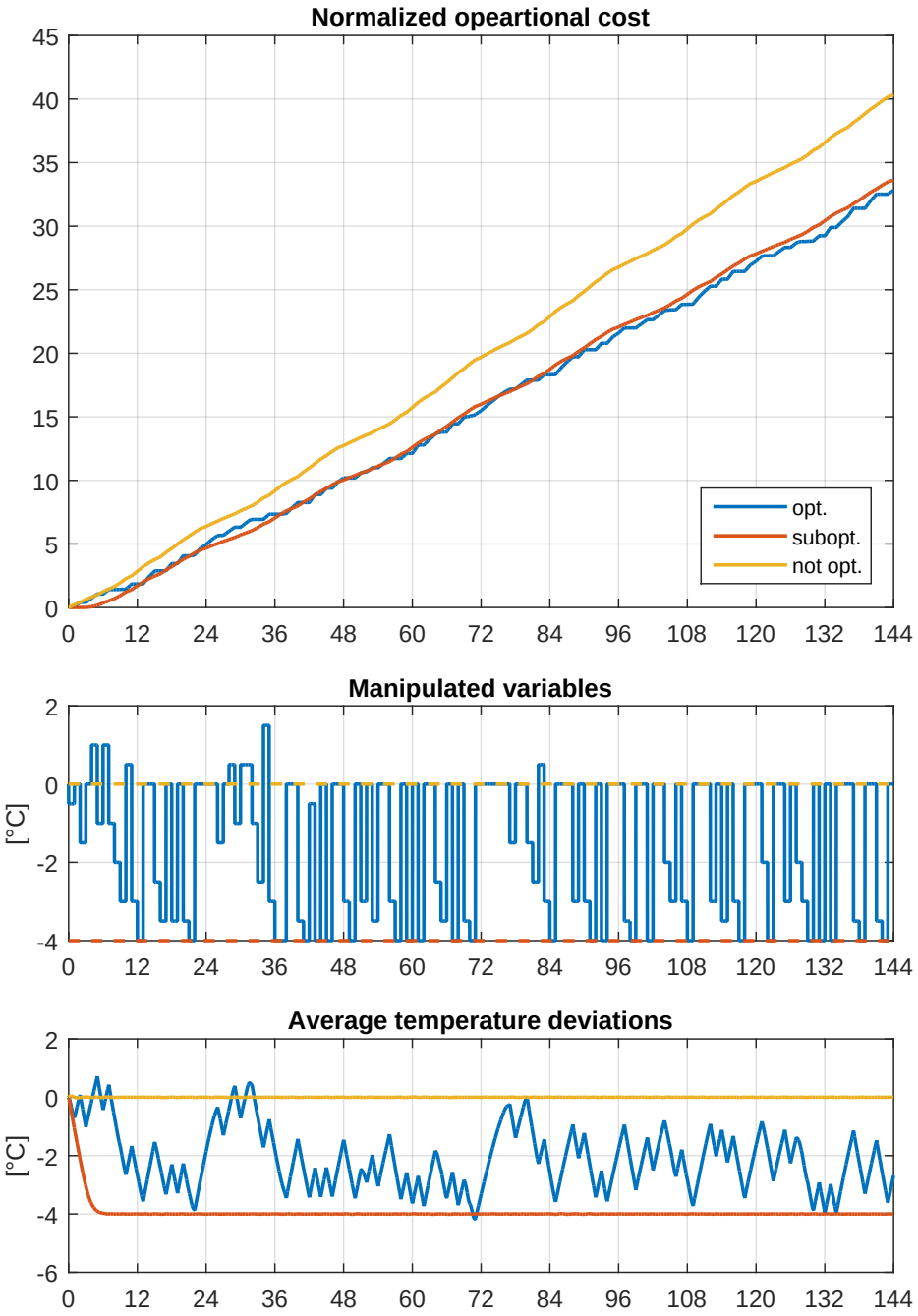

Figure 6.6: Comparison of the energy saving strategies: $\Delta T_{low} = -4,\ \Delta T_{up} = 4$

Table 6.2: Operational cost reduction

$[\Delta T_{low}\ \Delta T_{up}]$	smart	thrifty
[−0.5°C 0.5°C]	6.5%	2%
[−1°C 1°C]	9.5%	4.5%
[−2°C 2°C]	13.5%	9%
[−4°C 4°C]	19%	16.5%

ational cost: fluctuation of the electricity prices and acceptable range of setpoint changes. The electricity price forecast depends on the current and predicted renewable energy production, whereas the customer comfort limits can be changed. Table 6.2 illustrates relationship between the variation of this limits and the operational cost reductions (percentage), which is calculated as follows:

$$s = \frac{C_{zero} - C_{smart/thrifty}}{C_{zero}} \cdot 100\% \tag{6.12}$$

here, $C_{smart/thrifty}$ is the simulated normalized operational cost of the smart or thrifty strategies respectively; C_{zero} is the simulated normalized operational cost of the zero temperature setpoint change strategy.

Although the smart strategy is always economically more efficient, increasing the temperature setpoint change limits reduces the difference between smart and thrifty strategies. However, these limits should not exceed some reasonable value (e.g. ±2°C) because they are directly connected to the customer comfort.

The computation time mainly depends on the initial guess of the solution. Using the solution from the previous step helps to speed up the process. The simulations were run in MATLAB 2015a using a PC with the following parameters: Intel Core i5-3570 3.4 GHz CPU; 8GB RAM. Figure 6.7 contains the computation times of obtaining the optimal temperature setpoint change at each sampling time for simulations presented in Figure 6.5. The average computation time is around 30 seconds which is fast enough compared to the sampling time of 1 hour.

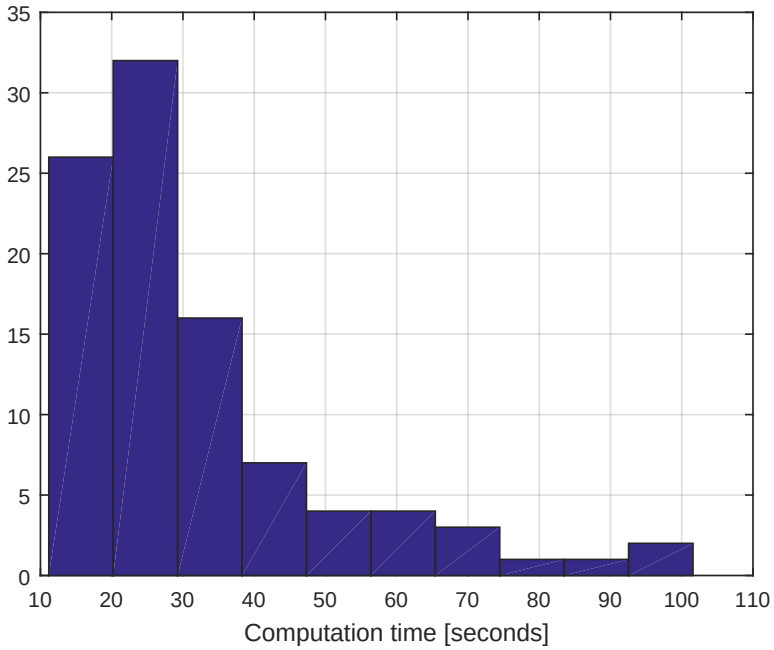

Figure 6.7: Computation times

Summary and conclusions

This thesis presents a study about utilizing high potential of Thermostatically Controlled Loads (TCLs) for providing regulation reserve in Smart Energy Grids using advanced control techniques. There are two main questions addressed in the work. First, developing a Model Predictive Control (MPC) based on a Linear Parameter-Varying (LPV) model for optimizing energy consumption of a system with TCL. Second, indirect control of a large population of systems with TCLs in energy grid with variable electricity price. According to the concept of energy system with variable electricity price, the proposed economic control strategies are assumed to be applied on the customer side, so-called price responsive consumers. The main objective of the control strategies is to minimize operational cost of either a single unit or the whole population, taking into account forecasted electricity price change which consequently stabilizes the energy system.

The rest of this chapter summarizes the obtained results and demonstrates that the defined objectives were met:

- related to developing MPC based on LPV model (Chapter 3):
  - formulate an LPV model of the considered system;
  - modify the Economic Model Predictive Control (E-MPC) optimization problem to account variation of the model parameters;
  - verify the E-MPC control strategy.
- related to the aggregate control of a population of TCLs:
  - design a simulation model for verification of the aggregate model and validation of Economic Non-linear Model Predictive Control (E-NMPC) control strategy (Chapter 4);
  - develop a non-linear modification of bin state transition model for aggregate modelling of the TCLs population (Chapter 5);

– design and verify the E-NMPC control strategy (Chapter 6).

Chapter 1 presents overview of the future energy systems with renewable energy production share up to 100%. Demand Side Management (DSM) is an essential part of such energy systems that allows to utilize some of the electrical loads, including TCLs, for balancing electrical energy production and consumption. TCLs is one of the most common type of electrical loads and therefore have very high potential for regulation service provision. Energy system with variable electricity price is a kind of system that is very likely to be used in the future. Electricity price signal enables indirect load control. There are a few key advantages of indirect load control compared to direct load control. Firstly, the customers' comfort and preferences are less compromised because they can choose the exact strategy of responding to the price changes. Secondly, it provides a generic interface suitable for any kind of load, thus there is no need in any additional devices for monitoring and controlling the loads.

Chapter 3 presents detailed description of E-MPC based on an LPV model. The control objective is to minimize operational cost of a system with TCL. The method requires the variables influencing the model parameters to be known for prediction horizon at each sampling time. Thus, it is able to predict the influence of the parameters variation on the system dynamics.

A simplified model of swimming pool heating system was considered as a case study. The model is LPV due to influence of wind speed and ambient temperature. The simulation results demonstrate that the presented method can handle the parameters variation model and that the energy consumption is shifted to the low-price periods, which corresponds to the economically optimal regime.

Chapter 4 presents the simulation model of a population of TCLs that is used for verification of the aggregate model and the economic control strategy. High accuracy of the model is achieved by simulating each unit individually. The model provides possibility to simulate a population of any size with various types of loads parameters distribution.

Chapter 5 contains description of the proposed aggregate model that is a non-linear modification of bin state transition model and aimed to be used in model-based control system design. The original model provides accurate aggregate response of a population of TCLs to switching signal, which directly instructs the loads to change their states. The proposed non-linear modification provides accurate aggregate response of the population of TCLs to temperature setpoint change signal,

which indirectly influences the states of the loads. In the first case, control strategy generating the switching signal should ensure that the customer comfort is not compromised besides optimizing the aggregate consumption. Whereas, the proposed approach lets the local thermostats to deal with the customers comfort, which can be easily managed by limiting the temperature setpoint change, thus reducing the complexity of the control system. Additionally, the model takes into account the influence of the ambient temperature on the loads dynamics.

The proposed aggregate model was developed in two stages: the first stage deals with the model of homogeneous population, then it is extended to heterogeneous population applying clustering technique. There are several key advantages of the proposed aggregate model that are important for model-based control system design. Firstly, the model is relatively accurate compared to the other models providing aggregate response to the temperature setpoint change. High accuracy is achieved by reusing the idea of original bin state transition model, which implicitly tracks the state of each load in the population. Secondly, the model deals with different levels of heterogeneity of the population, which is verified through simulations. Thirdly, the complexity of the model does not depend on the number of units in the population because it does not influence the structure or order of the model. In general, the order of the model is proportional to the number bins and clusters. The optimal values for these parameters vary with different levels of heterogeneity of the population in contrary way: higher heterogeneity leads to higher number of clusters and lower number of bins and vice versa; thus, the level of heterogeneity also does not influence the complexity of the model. Lastly, the model provides long-term demand forecast (e.g. one day), which is a reasonable predictive horizon for a model-based control strategy, because the price signal is expected to be changing every hour and be broadcasted one day ahead.

Chapter 6 presents the proposed price-responsive control strategy aiming to coordinate a population of TCLs. It is assumed that the electricity price is changing every hour, electricity price and weather forecasts are available for the following 24 hours, and that the population belongs to a single owner. The control strategy is based on the means of E-MPC. The main objective is to minimize the operational cost of the whole population, which consequently helps to provide ancillary services to the energy system. The controller employs the developed aggregate model for predicting demand response of the population. Taking into account the dynamics of the population allows to better schedule the temperature setpoints for the loads

compared to the earlier proposed strategies where the temperature setpoint is defined as a linear function of the electricity price. Since the model is non-linear, the optimization problem is non-linear as well and solved using gradient and adjoint sensitivity analysis methods. One of the main requirements is to respect the customer comfort, which is met by limiting the temperature setpoint change.

Simulation results demonstrate effectiveness of the proposed control strategy. Firstly, it allows to reduce the operational cost of the whole population up to 20%. The reduction depends on the specified temperature setpoint change limits; in other words, it allows the customer to find a compromise between reducing the electricity payments and compromising their comfort. Secondly, the proposed optimal regime is more efficient than setting the temperature setpoint equal to the lower limit: the operational cost is lower, the customer comfort is less compromised. Thirdly, the computation time analysis demonstrates that on average the optimal problem is solved during 30-40 seconds (on a regular PC), whereas the sampling time is 1 hour. Thus the algorithm can run in real time, moreover there is a margin that allows to increase the population size and/or run the algorithms on a machine with less computational power (e.g. on microcontroller unit or programmable logical controller).

References

[1] F. C. Schweppe, R. D. Tabors, J. L. Kirtley, H. R. Outhred, F. H. Pickel, and A. J. Cox, "Homeostatic utility control," *IEEE Transactions on Power Apparatus and Systems*, no. 3, pp. 1151–1163, 1980.

[2] A. Grubler, M. Jefferson, A. McDonald, S. Messner, N. Nakicenovic, H.-H. Rogner, and L. Schrattenholzer, "Global energy perspectives to 2050 and beyond," 1995.

[3] N. Nakićenović, A. Grübler, and A. McDonald, *Global energy perspectives*. Cambridge University Press, 1998.

[4] I. Dincer, "Renewable energy and sustainable development: a crucial review," *Renewable and Sustainable Energy Reviews*, vol. 4, no. 2, pp. 157–175, 2000.

[5] T. Boden, G. Marland, and R. Andres, "Global, regional, and national co2 emissions," 2009.

[6] S. C. Doney, V. J. Fabry, R. A. Feely, and J. A. Kleypas, "Ocean acidification: the other co2 problem," 2009.

[7] "Renewable energy statistics," http://ec.europa.eu/eurostat/statistics-explained/index.php/Renewable_energy_statistics, accessed: 2018-02-18.

[8] F. Blaabjerg, F. Iov, T. Kerekes, R. Teodorescu, and K. Ma, "Power electronics-key technology for renewable energy systems," in *Power Electronics, Drive Systems and Technologies Conference (PEDSTC), 2011 2nd*. IEEE, 2011, pp. 445–466.

[9] A. Clausen, G. Ghatikar *et al.*, "Load management of data centers as regulation capacity in denmark," in *Green Computing Conference (IGCC), 2014 International*. IEEE, 2014, pp. 1–10.

[10] P. Meibom, K. B. Hilger, H. Madsen, and D. Vinther, "Energy comes together in denmark: The key to a future fossil-free danish power system," *IEEE power and energy magazine*, vol. 11, no. 5, pp. 46–55, 2013.

[11] "Energy," https://europa.eu/european-union/topics/energy_en, accessed: 2018-02-18.

[12] Q. Yu, "Applications of flexible ac transmissions system (facts) technology in smartgrid and its emc impact," in *Electromagnetic Compatibility (EMC), 2014 IEEE International Symposium on*. IEEE, 2014, pp. 392–397.

[13] F. P. Sioshansi, *Smart grid: integrating renewable, distributed and efficient energy*. Academic Press, 2011.

[14] G. Locke and P. D. Gallagher, "Nist framework and roadmap for smart grid interoperability standards, release 1.0," *National Institute of Standards and Technology*, vol. 33, 2010.

[15] Z. Li and T. Yao, "Renewable energy basing on smart grid," in *Wireless Communications Networking and Mobile Computing (WiCOM), 2010 6th International Conference on*. IEEE, 2010, pp. 1–4.

[16] P. Siano, "Demand response and smart grids—a survey," *Renewable and Sustainable Energy Reviews*, vol. 30, pp. 461–478, 2014.

[17] H. Saboori, M. Mohammadi, and R. Taghe, "Virtual power plant (vpp), definition, concept, components and types," in *Power and Energy Engineering Conference (APPEEC), 2011 Asia-Pacific*. IEEE, 2011, pp. 1–4.

[18] P. Landsbergen, "Feasibility, beneficiality, and institutional compatibility of a micro-chp virtual power plant in the netherlands," 2009.

[19] D. Pudjianto, C. Ramsay, and G. Strbac, "Virtual power plant and system integration of distributed energy resources," *IET Renewable Power Generation*, vol. 1, no. 1, pp. 10–16, 2007.

[20] E. Mashhour and S. Moghaddas-Tafreshi, "The opportunities for future virtual power plant in the power market, a view point," in *Clean Electrical Power, 2009 International Conference on*. IEEE, 2009, pp. 448–452.

[21] M. Braun, "Virtual power plants in real applications," *Sixth Research Framework Programme of the European Union for the FENIX project (SES6–518272)*, 2009.

[22] L. B. Nikonowicz and J. Milewski, "Virtual power plants-general review: structure, application and optimization," *Journal of Power Technologies*, vol. 92, no. 3, p. 135, 2012.

[23] Z. Stepančič, A. Krpič, A. Kos, K. Koželj, D. Bobek, A. Savanović, and D. Gabrijelčič, "Prosumer flexibility management in smart grids," in *2018 41st International Convention on Information and Communication Technology, Electronics and Microelectronics (MIPRO)*, May 2018, pp. 0432–0437.

[24] D. S. Callaway and I. A. Hiskens, "Achieving controllability of electric loads," *Proceedings of the IEEE*, vol. 99, no. 1, pp. 184–199, 2011.

[25] K. Schisler, T. Sick, and K. Brief, "The role of demand response in ancillary services markets," in *Transmission and Distribution Conference and Exposition, 2008. T&D. IEEE/PES*. IEEE, 2008, pp. 1–3.

[26] J. Zhong, C. Kang, and K. Liu, "Demand side management in china," in *Power and Energy Society General Meeting, 2010 IEEE*. IEEE, 2010, pp. 1–4.

[27] P. Palensky and D. Dietrich, "Demand side management: Demand response, intelligent energy systems, and smart loads," *IEEE transactions on industrial informatics*, vol. 7, no. 3, pp. 381–388, 2011.

[28] N. Lu, "An evaluation of the hvac load potential for providing load balancing service," *IEEE Transactions on Smart Grid*, vol. 3, no. 3, pp. 1263–1270, 2012.

[29] N. Hajibandeh, M. Ehsan, S. Soleymani, M. Shafie-khah, and J. P. Catalão, "The mutual impact of demand response programs and renewable energies: A survey," *Energies*, vol. 10, no. 9, p. 1353, 2017.

[30] M. H. Albadi and E. F. El-Saadany, "A summary of demand response in electricity markets," *Electric power systems research*, vol. 78, no. 11, pp. 1989–1996, 2008.

[31] F. E. R. Commission *et al.*, "Demand response and advanced metering," Staff Report.[online]. Available: http://www. ferc. gov, Tech. Rep., 2015.

[32] O. A. Sianaki and M. A. Masoum, "A fuzzy topsis approach for home energy management in smart grid with considering householders' preferences," in *Innovative Smart Grid Technologies (ISGT), 2013 IEEE PES*. IEEE, 2013, pp. 1–6.

[33] S. Mohagheghi, J. Stoupis, Z. Wang, Z. Li, and H. Kazemzadeh, "Demand response architecture: Integration into the distribution management system," in *Smart Grid Communications (SmartGridComm), 2010 First IEEE International Conference on*. IEEE, 2010, pp. 501–506.

[34] F. L. Alvarado, "Controlling power systems with price signals," *Decision Support Systems*, vol. 40, no. 3-4, pp. 495–504, 2005.

[35] S. P. Holland and E. T. Mansur, "The short-run effects of time-varying prices in competitive electricity markets," *The Energy Journal*, pp. 127–155, 2006.

[36] A. Jokić, M. Lazar, and P. P. van den Bosch, "Real-time control of power systems using nodal prices," *International Journal of Electrical Power & Energy Systems*, vol. 31, no. 9, pp. 522–530, 2009.

[37] A. J. Roscoe and G. Ault, "Supporting high penetrations of renewable generation via implementation of real-time electricity pricing and demand response," *IET Renewable Power Generation*, vol. 4, no. 4, pp. 369–382, 2010.

[38] O. Corradi, H. Ochsenfeld, H. Madsen, and P. Pinson, "Controlling electricity consumption by forecasting its response to varying prices," *IEEE Transactions on Power Systems*, vol. 28, no. 1, pp. 421–429, 2013.

[39] R. Halvgaard, N. K. Poulsen, H. Madsen, and J. B. Jørgensen, "Economic model predictive control for building climate control in a smart grid," in *Innovative Smart Grid Technologies (ISGT), 2012 IEEE PES*. IEEE, 2012, pp. 1–6.

[40] T. G. Hovgaard, L. F. Larsen, and J. B. Jørgensen, "Flexible and cost efficient power consumption using economic mpc a supermarket refrigeration benchmark," in *Decision and Control and European Control Conference (CDC-ECC), 2011 50th IEEE Conference on*. IEEE, 2011, pp. 848–854.

[41] S. Wang and X. Jin, "Model-based optimal control of vav air-conditioning system using genetic algorithm," *Building and Environment*, vol. 35, no. 6, pp. 471–487, 2000.

[42] Y. Ma, A. Kelman, A. Daly, and F. Borrelli, "Predictive control for energy efficient buildings with thermal storage: Modeling, stimulation, and experiments," *IEEE Control Systems*, vol. 32, no. 1, pp. 44–64, 2012.

[43] M. Maasoumy, B. M. Sanandaji, A. Sangiovanni-Vincentelli, and K. Poolla, "Model predictive control of regulation services from commercial buildings to the smart grid," in *American Control Conference (ACC), 2014*. IEEE, 2014, pp. 2226–2233.

[44] Y. Ma, F. Borrelli, B. Hencey, B. Coffey, S. Bengea, and P. Haves, "Model predictive control for the operation of building cooling systems," *IEEE Transactions on control systems technology*, vol. 20, no. 3, pp. 796–803, 2012.

[45] J. L. Mathieu, S. Koch, and D. S. Callaway, "State estimation and control of electric loads to manage real-time energy imbalance," *IEEE Transactions on Power Systems*, vol. 28, no. 1, pp. 430–440, 2013.

[46] S. Bashash and H. K. Fathy, "Modeling and control of aggregate air conditioning loads for robust renewable power management," *IEEE Transactions on Control Systems Technology*, vol. 21, no. 4, pp. 1318–1327, 2013.

[47] Y. Lin, P. Barooah, and S. P. Meyn, "Low-frequency power-grid ancillary services from commercial building hvac systems," in *Smart Grid Communications (SmartGridComm), 2013 IEEE International Conference on*. IEEE, 2013, pp. 169–174.

[48] F. Oldewurtel, D. Sturzenegger, G. Andersson, M. Morari, and R. S. Smith, "Towards a standardized building assessment for demand response," in *Decision and Control (CDC), 2013 IEEE 52nd Annual Conference on*. IEEE, 2013, pp. 7083–7088.

[49] S. P. Meyn, P. Barooah, A. Bušić, Y. Chen, and J. Ehren, "Ancillary service to the grid using intelligent deferrable loads," *IEEE Transactions on Automatic Control*, vol. 60, no. 11, pp. 2847–2862, 2015.

[50] P. Tatjewski, *Advanced control of industrial processes: structures and algorithms*. Springer Science & Business Media, 2007.

[51] J. M. Maciejowski, *Predictive control: with constraints*. Pearson education, 2002.

[52] J. B. Jorgensen, "Adjoint sensitivity results for predictive control, state-and parameter-estimation with nonlinear models," in *Control Conference (ECC), 2007 European*. IEEE, 2007, pp. 3649–3656.

[53] L. N. Petersen, J. B. Jorgensen, and J. B. Rawlings, "Economic optimization of spray dryer operation using nonlinear model predictive control with state estimation," *IFAC-PapersOnLine*, vol. 48, no. 8, pp. 507–513, 2015.

[54] R. Halvgaard, J. B. Jørgensen, N. K. Poulsen, and H. Madsen, "Model predictive control for smart energy systems," 2014.

[55] W. Zhang, J. Lian, C.-Y. Chang, and K. Kalsi, "Aggregated modeling and control of air conditioning loads for demand response," *IEEE transactions on power systems*, vol. 28, no. 4, pp. 4655–4664, 2013.

[56] G. K. Larsen, N. D. van Foreest, and J. M. Scherpen, "Distributed control of the power supply-demand balance," *IEEE Transactions on Smart Grid*, vol. 4, no. 2, pp. 828–836, 2013.

[57] S. Rahnama, J. Stoustrup, and H. Rasmussen, "Model predictive control for integration of industrial consumers to the smart grid under a direct control policy," in *Control Applications (CCA), 2013 IEEE International Conference on*. IEEE, 2013, pp. 515–520.

[58] C. Perfumo, J. H. Braslavsky, and J. K. Ward, "Model-based estimation of energy savings in load control events for thermostatically controlled loads," *IEEE Transactions on Smart Grid*, vol. 5, no. 3, pp. 1410–1420, 2014.

[59] D. Boiroux, "Model predictive control algorithms for pen and pump insulin administration," Ph.D. dissertation, Technical University of Denmark, 2012.

[60] R. E. Bixby, "A brief history of linear and mixed-integer programming computation," *Documenta Mathematica*, pp. 107–121, 2012.

[61] J. B. Jørgensen, *Moving horizon estimation and control*. Citeseer, 2005.

[62] T. G. Hovgaard, K. Edlund, and J. B. Jørgensen, "The potential of economic mpc for power management," in *Decision and Control (CDC), 2010 49th IEEE Conference on*. IEEE, 2010, pp. 7533–7538.

[63] J. Taneja, D. Culler, and P. Dutta, "Towards cooperative grids: Sensor/actuator networks for renewables integration," in *Smart Grid Communications (SmartGridComm), 2010 First IEEE International Conference on*. IEEE, 2010, pp. 531–536.

[64] J. E. Brumbaugh, *Audel HVAC Fundamentals: Volume 1: Heating Systems, Furnaces and Boilers*. John Wiley & Sons, 2004, vol. 17.

[65] H. Hao, B. M. Sanandaji, K. Poolla, and T. L. Vincent, "Aggregate flexibility of thermostatically controlled loads," *IEEE Transactions on Power Systems*, vol. 30, no. 1, pp. 189–198, 2015.

[66] W. Zhang, K. Kalsi, J. Fuller, M. Elizondo, and D. Chassin, "Aggregate model for heterogeneous thermostatically controlled loads with demand response," in *Power and Energy Society General Meeting, 2012 IEEE*. IEEE, 2012, pp. 1–8.

[67] H. Hao, B. M. Sanandaji, K. Poolla, and T. L. Vincent, "Potentials and economics of residential thermal loads providing regulation reserve," *Energy Policy*, vol. 79, pp. 115–126, 2015.

[68] N. Wilson, B. Wagner, and W. Colborne, "Equivalent thermal parameters for an occupied gas-heated house," *ASHRAE Trans.;(United States)*, vol. 91, no. CONF-850606-, 1985.

[69] R. C. Sonderegger, "Dynamic models of house heating based on equivalent thermal parameters," 1978.

[70] H. Madsen and J. Holst, "Estimation of continuous-time models for the heat dynamics of a building," *Energy and buildings*, vol. 22, no. 1, pp. 67–79, 1995.

[71] N. Friling, M. J. Jiménez, H. Bloem, and H. Madsen, "Modelling the heat dynamics of building integrated and ventilated photovoltaic modules," *Energy and Buildings*, vol. 41, no. 10, pp. 1051–1057, 2009.

[72] J. H. Braslavsky, C. Perfumo, and J. K. Ward, "Model-based feedback control of distributed air-conditioning loads for fast demand-side ancillary services," in *Decision and Control (CDC), 2013 IEEE 52nd Annual Conference on*. IEEE, 2013, pp. 6274–6279.

[73] C. Perfumo, J. Braslavsky, J. K. Ward, and E. Kofman, "An analytical characterisation of cold-load pickup oscillations in thermostatically controlled loads," in *Control Conference (AUCC), 2013 3rd Australian*. IEEE, 2013, pp. 195–200.

[74] N. Mahdavi, J. H. Braslavsky, and C. Perfumo, "Mapping the effect of ambient temperature on the power demand of populations of air conditioners," *IEEE Transactions on Smart Grid*, 2016.

[75] N. Mahdavi, C. Perfumo, and J. H. Braslavsky, "Bayesian parameter estimation for direct load control of populations of air conditioners," *IFAC Proceedings Volumes*, vol. 47, no. 3, pp. 9924–9929, 2014.

[76] R. Halvgaard, N. K. Poulsen, H. Madsen, and J. B. Jorgensen, "Thermal storage power balancing with model predictive control," in *Control Conference (ECC), 2013 European*. IEEE, 2013, pp. 2567–2572.

[77] S. N. Backhaus, N. Sinitsyn, S. Kundu, and I. Hiskens, "Modeling and control of thermostatically controlled loads," Los Alamos National Laboratory (LANL), Tech. Rep., 2011.

[78] C. Perfumo, E. Kofman, J. H. Braslavsky, and J. K. Ward, "Load management: Model-based control of aggregate power for populations of thermostatically controlled loads," *Energy Conversion and Management*, vol. 55, pp. 36–48, 2012.

[79] D. J. Hammerstrom, R. Ambrosio, T. A. Carlon, J. G. DeSteese, G. R. Horst, R. Kajfasz, L. L. Kiesling, P. Michie, R. G. Pratt, M. Yao *et al.*, "Pacific northwest gridwise™ testbed demonstration projects; part i. olympic peninsula project," Pacific Northwest National Laboratory (PNNL), Richland, WA (US), Tech. Rep., 2008.

[80] J. H. Yoon, R. Baldick, and A. Novoselac, "Dynamic demand response controller based on real-time retail price for residential buildings," *IEEE Transactions on Smart Grid*, vol. 5, no. 1, pp. 121–129, 2014.

[81] W. C. Clarke, C. Manzie, and M. J. Brear, "An economic mpc approach to microgrid control," in *Control Conference (AuCC), 2016 Australian.* IEEE, 2016, pp. 276–281.

[82] A. Noureddine, A. Alouani, and S. Patil, "On the probability density function of an air conditioner duty cycle," in *American Control Conference, 1991.* IEEE, 1991, pp. 2089–2093.

[83] L. C. Totu, "Large scale demand response of thermostatic loads," Ph.D. dissertation, Ph. D. dissertation, Faculty of Engineering and Science, Aalborg University, 2015.

[84] H. Hao, B. M. Sanandaji, K. Poolla, and T. L. Vincent, "A generalized battery model of a collection of thermostatically controlled loads for providing ancillary service," in *Communication, Control, and Computing (Allerton), 2013 51st Annual Allerton Conference on.* IEEE, 2013, pp. 551–558.

[85] B. M. Sanandaji, H. Hao, and K. Poolla, "Fast regulation service provision via aggregation of thermostatically controlled loads," in *System Sciences (HICSS), 2014 47th Hawaii International Conference on.* IEEE, 2014, pp. 2388–2397.

[86] S. Koch, J. L. Mathieu, and D. S. Callaway, "Modeling and control of aggregated heterogeneous thermostatically controlled loads for ancillary services," in *Proc. PSCC*, 2011, pp. 1–7.

[87] V. Trovato, S. H. Tindemans, and G. Strbac, "Leaky storage model for optimal multi-service allocation of thermostatic loads," *IET Generation, Transmission & Distribution*, vol. 10, no. 3, pp. 585–593, 2016.

[88] "Smartnet project," http://smartnet-project.eu/the-project/, accessed: 2018-07-28.

[89] J. Czarnecki and CSIRO, *Swimming Pool Heating by Solar Energy*, ser. CSIRO Division of Mechanical Engineering. Technical report no. TR 19. CSIRO Division of Mechanical Engineering, 1978.

[90] S.-E. Pohl, "Use of air conditioning heat rejection for swimming pool heating," Ph.D. dissertation, University of Wisconsin–Madison, 1999.

[91] "Coefficient of performance," http://industrialheatpumps.nl/en/how_it_works/cop_heat_pump/, accessed: 2018-08-25.

[92] "Citites - centre for it–intelligent energy systems in cities," http://smart-cities-centre.org/, accessed: 2018-07-28.

[93] N. Zemtsov, J. Hlava, G. Frantsuzova, H. Madsen, R. G. Junker, and J. B. Jørgensen, "Economic mpc based on lpv model for thermostatically controlled loads," in *Control and Communications (SIBCON), 2017 International Siberian Conference on.* IEEE, 2017, pp. 1–5.

[94] T. Auer, "Assessment of an indoor or outdoor swimming pool," *TRANSSOLAR Energietechnik GmbH, Strategies for energy efficient design and thermal comfort in buildings*, 1996.

[95] "How low can nordic heat pumps go?" https://www.nordicghp.com/2017/01/heat-pump-effective-temperature-range/, accessed: 2018-10-28.

[96] J. B. Jørgensen, J. K. Huusom, and J. B. Rawlings, "Finite horizon mpc for systems in innovation form," in *Decision and Control and European Control Conference (CDC-ECC), 2011 50th IEEE Conference on.* IEEE, 2011, pp. 1896–1903.

[97] C. N. Perfumo *et al.*, "Dynamic modelling and control of heterogeneous populations of thermostatically controlled loads," 2013.

[98] J. Antonín, "Průzkum fondu budov a možností úspor energie," *Rešerše stávajících studií a vỳpočtové ověření pro rezidenční budovy. Šance pro budovy, prosinec*, 2013.

[99] S. Bashash and H. K. Fathy, "Modeling and control insights into demand-side energy management through setpoint control of thermostatic loads," in *American Control Conference (ACC), 2011.* IEEE, 2011, pp. 4546–4553.

[100] N. Zemtsov, J. Hlava, G. Frantsuzova, H. Madsen, and J. B. Jørgensen, "Economic nonlinear mpc for a population of thermostatically controlled loads,"

Computer Science-Research and Development, vol. 33, no. 1-2, pp. 157–167, 2018.

[101] S. Lloyd, "Least squares quantization in pcm," *IEEE transactions on information theory*, vol. 28, no. 2, pp. 129–137, 1982.

[102] L. N. Petersen and J. B. Jorgensen, "Real-time economic optimization for a fermentation process using model predictive control," in *Control Conference (ECC), 2014 European*. IEEE, 2014, pp. 1831–1836.

[103] L. N. Petersen, N. K. Poulsen, H. H. Niemann, C. Utzen, and J. B. Jørgensen, "Economic optimization of spray dryer operation using nonlinear model predictive control," in *Decision and Control (CDC), 2014 IEEE 53rd Annual Conference on*. IEEE, 2014, pp. 6794–6800.

[104] M. R. Kristensen, J. B. Jørgensen, P. G. Thomsen, and S. B. Jørgensen, "An esdirk method with sensitivity analysis capabilities," *Computers & chemical engineering*, vol. 28, no. 12, pp. 2695–2707, 2004.

[105] J. B. Jørgensen, "A runge-kutta based software package for nonlinear model predictive control," in *International Workshop on Assessment and Future Directions of NMPC*, 2008.

[106] M. R. Kristensen, J. B. Jørgensen, P. G. Thomsen, and S. B. Jørgensen, "Efficient sensitivity computation for nonlinear model predictive control," *IFAC Proceedings Volumes*, vol. 37, no. 13, pp. 567–572, 2004.

List of Publications

[1] Jaroslav Hlava and Nikita Zemtsov. Aggregated control of electrical heaters for ancillary services provision. In *System Theory, Control and Computing (ICSTCC), 2015 19th International Conference on*, pages 508–513. IEEE, 2015.

[2] Jaroslav Hlava and Nikita Zemtsov. Secondary control with thermostatically controlled loads using mpc based on extended bin state transition model. In *Methods and Models in Automation and Robotics (MMAR), 2016 21st International Conference on*, pages 619–624. IEEE, 2016.

[3] Jaroslav Hlava, Nikita Zemtsov, and Galina Frantsuzova. Application of pid controller based on the localization method for ancillary service provision. In *Control and Communications (SIBCON), 2016 International Siberian Conference on*, pages 1–6. IEEE, 2016.

[4] Nikita Zemtsov and Galina Frantsuzova. Using thermostatically controlled loads for the secondary control provision based on the modal method. In *Actual Problems of Electronics Instrument Engineering (APEIE), 2016 13th International Scientific-Technical Conference on*, volume 3, pages 135–139. IEEE, 2016.

[5] Nikita Zemtsov and Jaroslav Hlava. Direct control of a large population of electrical space heaters based on bin state transition model. In *Control and Automation (MED), 2016 24th Mediterranean Conference on*, pages 310–315. IEEE, 2016.

[6] Nikita Zemtsov, Jaroslav Hlava, and Galina Frantsuzova. Using the robust pid controller to manage the population of thermostatically controlled loads. In *Industrial Engineering, Applications and Manufacturing (ICIEAM), 2017 International Conference on*, pages 1–4. IEEE, 2017.

[7] Nikita Zemtsov, Jaroslav Hlava, Galina Frantsuzova, Henrik Madsen, and John Bagterp Jørgensen. Economic nonlinear mpc for a population of ther-

mostatically controlled loads. *Computer Science-Research and Development*, 33(1-2):157–167, 2018.

[8] Nikita Zemtsov, Jaroslav Hlava, Galina Frantsuzova, Henrik Madsen, Rune Grønborg Junker, and John Bagterp Jørgensen. Economic mpc based on lpv model for thermostatically controlled loads. In *Control and Communications (SIBCON), 2017 International Siberian Conference on*, pages 1–5. IEEE, 2017.

Attachments

The attached CD contains the Matlab scripts, Simulink models, and R-scripts used to obtain the presented results as well as the electronic version of this document.

The content of the CD is organized as follows:

- **Doctoral_thesis_Zemtsov.pdf** is the electronic version of this document;
- the folder **EMPC-LPV** contains the R-Script that was used to obtain the simulation results presented in Chapter 3 as well as the Matlab script for plotting the results. The R-Script allows to change the simulation and model parameters; for more details refer to the script comments;
- the folder **ENMPC** contains the Simulink models and supporting Matlab scripts used to obtain the results presented in Chapters 4-6. The key items are:
  - the script **Run.m** was used to perform the simulations. This scripts controls the whole simulation process and allows to change some simulation parameters, for more details refer to the script comments;
  - the model **model_BIN.slx** is the Simulink model of the whole system;
  - the folder **results** contains the obtained simulation results with different simulation parameters and Matlab scrips for plotting them.

Curriculum Vitae

Nikita Zemtsov was born in Novosibirsk, Russian Federation, in 1992. He received his bachelor degree in Automation and Control at Novosibirsk State Technical University (NSTU) in 2012. During his master degree in Electrical Engineering and Informatics he was participating in double degree program at NSTU and Technical University of Liberec (TUL), Czech Republic. As a part of this program he also spent 1 semester at Zittau/Görlitz University, Germany, as an ERASMUS student. He received the master degree from both TUL and NSTU in 2014. In the same year he started double degree Ph.D. program at the same universities in Electrical Engineering and Informatics. The main focus of the studies was on predictive control in smart grids.

Nikita is author or co-author of more than 13 conference papers and journal articles in both Russian and English languages. Most of them are related to his Ph.D. studies and were presented at various international conferences. The final results were published in the Computer Science - Research and Development Springer journal and presented at the D-A-CH+ Energieinformatik 2017 conference in Lugano, Switzerland.

As a part of his Ph.D. program he attended an internship at Technical University of Denmark (DTU), where he worked for almost two semesters as a research assistant in 2016/17 academic year. During the internship he was developing Economic Model Predictive Controller for swimming pool heating system applying the results of his research. This work was done within the frameworks of the SmartNet and CITIES projects.